INCREMENTAL COLLAPSE OF REINFORCED CONCRETE FRAMES

INCREMENTAL COLLAPSE OF REINFORCED CONCRETE FRAMES

by

Jan Svihra, Dipl. Ing.

A THESIS

Submitted to the Faculty of Graduate Studies

in Partial Fulfillment of the Requirements

for the Degree

Master of Engineering

McMaster University

Hamilton, Ontario

1971

MASTER OF ENGINEERING (1971)

McMaster University
Hamilton, Ontario

TITLE: Incremental Collapse of Reinforced Concrete Frames

AUTHOR: Jan Svihra, Dipl. Ing. (Bratislava)

SUPERVISOR: Dr. R. M. Korol, Dr. R. G. Drysdale

NUMBER OF PAGES: viii, 163

SCOPE AND CONTENTS:

A research program is presented for assessing the plastic collapse load and incremental collapse load of reinforced concrete frames. This investigation attempts to establish a range of validity of simple plastic theory when applied to the under-reinforced concrete frames and to determine the sensitivity of such structures to variable repeated loading.

An experimental program was conducted on 4 reinforced concrete frames and two reinforced concrete columns. Deflections and strains of these models of nearly prototype size were measured and compared with predicted values at critical cross-sections.

Resulting conclusions and recommendations for further research are made.

ACKNOWLEDGEMENTS

The author would like to express his appreciation to Dr. R. M. Korol and Dr. R. G. Drysdale for their guidance and advice during the course of this investigation. The assistance provided by Mr. R. Danielsen is gratefully acknowledged.

The author also takes this opportunity to thank the following:

1. McMaster University for financial support during this research.
2. The staff of the Applied Dynamics Laboratory for their help in the experimental program.
3. The Steel Company of Canada for providing the reinforcing steel.

And finally, the author wishes to express his gratitude to his friends at McMaster University for their encouragement and help during the course.

TABLE OF CONTENTS

LIST OF TABLES

LIST OF FIGURES

Chapter 1

INTRODUCTION

The general task of science should be to make the discovery of unknown and help to understand and to solve the problems surrounding mankind. The applied scientist's aim, in fact, should be to push forward the boundary of knowledge in an unbroken line, surveying all the country as he goes, even though his observations and deductions cannot be, at the first attempt, as precise as those made by the pure scientist in dealing with more limited objectives. The task of engineers is to make connections between scientific discovery and everyday practical life, to make a practical use of knowledge developed by the scientist. Someone must deal with those difficult places before the designer can follow the new road.

While for structural steel, the method of plastic design has already found general use in reinforced concrete structure the plastic method of design revealed specific problems which became the subjects of recent research in many of the research centers.

The subject of this work was the behavior of reinforced concrete frames subjected to the repeated cyclic loading or proportionally increasing load when loads were causing plastic deformation finally resulting in collapse.

1.1 Historical Review

In tracing the first references to the plastic behavior of structural members one must go back as far as the end of the nineteenth century The need for the study of plastic behavior was appreciated by the elastician A.E.H. Love (1) who wrote in 1892 that the effect of materials strained beyond their elastic limit, which cannot be calculated exactly should be

taken into account in construction, and that elastic theory is at this time behind engineering practise.

In 1899 Ewing (2) in his work went on to discuss the influence of bending beyond the elastic limit on the distribution of stress. He went on to conclude that the bending moment which will "break the beam" cannot be calculated by the usual elastic stress formula because the distribution of stress assumed in that formula ceases to exist as soon as overstraining begins. Though it is unlikely that Eweng had ever carried out experiments by loading the beam until the full plastic moment was developed, the fact remains that the behavior he outlined over seventy years ago is the basis of the simple plastic theory.

The possibility of the development of plastic hinges was first suggested by G. Kazinczy (3) in 1914. He carried out some tests on fixed-ended beams and came to the conclusion that failure only took place when yielding had occurred at three cross sections, at which hinging action occurred. For his concept of the plastic hinge Kazinczy may claim to be the originator of plastic methods.

In the summer of 1936, Professor Maier-Leibnitz (4) officially expressed confidence in the possibility of basing design on plastic behavior. By his investigation and experiments (in 1928-29) on simple supported and continuous steel beams the plastic method for continuous beams was placed on a firm quantitative footing.

In the same decade works on plastic design of portal frames were published. Girkman (5) in 1931, published a paper on an approximate method for multi-bay rectangular frame design. In 1932 a review of plastic methods for beams and simple portal frames was published by F. Bleich (6).

Baker's (7) idea that the simple plastic theory could be a key to a simple and rational method of design of complex frames was fully developed and finally culminated in the Steel Skeleton published in 1956. His research started in 1938 by a series of tests on portal frames. In 1949 he described a method for calculating failure loads for multi-bay portal frames.

The proofs of the principles of plastic design were then independently published by Greenberg (8) and Prager (9) and by Horne (10) in the late nineteen-fifties.

The plastic method of design of steel structures became widely used in Great Britain and in the U.S.A. In the last decade a rash of publications became available on the topic of plastic design. The works of B.G. Neal (11) and Beedle (12) created further interest in plastic methods of structural analysis and design.

Plastic design theory for reinforced concrete - so-called "limit design" is relatively new. Though the concept of basing design on the failure load is almost as old as reinforced concrete itself the limit design theories were developed only in the last two decades.

In 1894 the French engineers, Coignet and deTedesco (13) attempted to calculate the strength of simple supported beams even though they made use of the assumption that concrete behaved as an elastic material up to failure in compression.

In 1897, the curvilinear nature of the stress strain relation was first recognized when R.M.V. Thullie (14) formulated what could be called the first true ultimate strength theory. Despite these earlier steps, the elastic theory of working stress design was used for another fifty years.

In the late 1940's A.L.L. Baker (15) published several papers on the plastic behavior of concrete, and in 1956 he published a book and gave recommendations for the plastic hinge design of reinforced concrete beams. The book included the expression for calculating the permissable hinge rotation. These expressions place severe limitations on the allowable hinge rotations and have subsequently been modified.

Many papers have been written about inelastic design of reinforced concrete within the last ten years. In 1964, A.H. Mattock(16) studied rotational capacity of hinging regions in reinforced concrete beams. His work was based on test results of more than thirty beams with different strengths of concrete, beam depths and yield points of reinforcement.

H.A. Sawyer (17) described a design method for concrete frames with two failure stages. His design method was based on a bilinear moment curvature relationship for reinforced concrete, and plasticity factors were used for the distributions of moments.

An outstanding work on the limit design of continuous beams and frames has been done by M.Z. Cohn (18). His optimum limit design procedures incorporated convenient serviceability criteria along with the limit equilibrium conditions, but left the compatibility problem to a seperate investigation. His paper included design tables and practical design recommendations.

The optimum limit design presented by Cohn is based on the following assumptions and requirements:

- reinforced concrete is an elasto-plastic material with limited ductility.
- the bending action prevails and therefore the effects of shear and axial forces are negligible.

- the frame resists any load combination of less intensity than the prescribed ultimate load.
- the critical sections remain within the elastic range for any combination of service loads.
- in the critical sections the plastic rotations remain within permissable limits.

The general solution of the problem stated above results in linear or non-linear programming techniques which require considerably complicated calculations. For practical purposes the author suggests a particular solution of less complexity, as frame with equal yield safety and partial elastic design. The determination of the plastic rotations developing in plastic hinges under various loading combinations is not treated.

Hiroyuki Aoyama (19) described moment-curvature characteristics of reinforced concrete members subjected to axial load and reversal of bending. Results of his tests and analysis were noted to have a significant effect of axial load on moment-curvature relationship.

F. Beaufait and R.R. Williams (20) presented results of an experimental study of reinforced concrete frames subjected to alternating sway forces. In the conclusion of a study in which seven frames were tested they noted that placement of reinforcement at the joints is critical and the manner in which continuity of the reinforcement is developed at the joints can and does have a very definite influence on the behavior of the structure. Also, from the test results there is an indication that a cyclic swaying of a frame, at a working load or overload condition, does have an effect on the ultimate load capacity of the structure.

Another study on reinforced concrete frames under cyclic loads was made by G.M. Sabins and R.N. White (21). In an experimental study 10 small scale models and two prototypes were tested. As declared by the authors small scale models can be successfully used for studying the detailed behavior of reinforced concrete frames.

K.H. Gerstle and L.G. Tulin (22) investigated the behavior of reinforced concrete beams subjected to cyclic bending loads. Tests showed that incremental collapse occurred under cyclic loading approaching the ultimate load in magnitude, the actual shakedown limit being considerably in excess of that computed by simple elastic-plastic theory.

The same authors (24) made an investigation of stress-strain relation for concrete subjected to cyclic loading. In the conclusion of this investigation is stated that the ultimate strength of concrete is decreasing with number of cycle of loading, while the permanent strain is incrementally increasing. This behavior of concrete seems to be of significant importance for shakedown analysis of reinforced concrete structures.

Though much has been done on this subject in the last decade, a general design method has not yet been developed and research on this subject is still in the progress in many laboratory and research centers all around the world.

1.2 Scope of Research

The topic of this investigation is shakedown of reinforced concrete frames. Shakedown theories are based on certain properties of material behavior to which the steel structure approximates closely. An investigation

was made into under-reinforced concrete frames to study the necessary ductility characteristics by the use of a detailed program.

Certain basic questions were: How such reinforced concrete frames behaved under repeated cyclic loading? What is the shakedown load as compared with plastic collapse load and how closely is the behavior of reinforced concrete frames to that predicted by plastic methods of structural analysis?

To answer these questions a suitable experimental program was necessary. The first essential decision was the choice of a test model, which would satisfy requirements of validity, and accuracy of test, which would be close to the real structure, behave in a manner sufficiently close to the theoretical structure and which could be fabricated under laboratory conditions.

By co-ordination with another experimental research program (23) in the same laboratory on reinforced concrete frames, a full-scale model frame was chosen. A structure with high degree of indeterminacy was preferable. Considering all the factors, the decision was made to select a single storey two bay frame with an approximate height of nine feet and a length of about eighteen feet. Two types of tests were performed on this test model. Firstly, proportionally increasing loads up to the plastic collapse of the frame and secondly repeated cyclic loading to investigate the shakedown characteristics were performed. Because of the essential importance of knowing the moment-curvature characteristics of a cross-section, cantilever column tests were performed.

Altogether four frames and two columns were tested. Two of the frames were tested under proportionally increasing loads and the other two were tested under repeated cyclic loading.

Attempts to measure reactive forces were made, but not very successfully. Deflections of the frame and deformations of the concrete were measured and used for evaluating the results. These were then compared with values predicted by the simple plastic theory and by a more complex solution of plastic collapse and shakedown.

This investigation, of course, does not answer many questions about the subject, but some interesting conclusions and recommendations for further research are made.

Chapter 2

ANALYTICAL FORMULATION

2.1 Method of Analysis and Limitation

There are several methods for solving for the plastic collapse or incremental collapse of frame structures. All these methods are based on certain assumptions and simplifications.

The first and most important assumption is that the moment-curvature relationship for a cross-section is such that the moment tends to a maximum value with large curvature under elastic-plastic action. As a consequence the curvature increases linearly with moment up to the so-called plastic moment and then can increase indefinitely with the moment value remaining constant. The concept of the plastic hinge is defined at a cross-section as being an indefinitely high rotation under the fully plastic bending moment. The existence of plastic hinges is the basic assumption for all methods of plastic analysis.

It is generally assumed that geometrical changes are negligible during loading and that the influence of axial and shear forces can be neglected.

A structure will collapse under proportionally increasing loads at that value known as the plastic collapse load. This value can be calculated by several methods described by B. G. Neal (11).

These methods are sufficiently simple and yet are accurate enough for estimates of the plastic collapse load. Compared with the practical conditions which occur during the life of a structure, there are some unrealistic assumptions which can seldom be satisfied, however.

The assumption about proportionally increasing loads is quite far away from the practical point of view. The loads usually are not applied

proportionally. During the life of a structure different combinations of loads can occur. The assumption about proportional loading is in this case on the unsafe side. The loads in practice are in certain ranges of values and different critical load combinations can occur many times during the life time of structures. Then even the most critical combination of loads would be not so dangerous to structures as different combinations of loads applied several times repeatedly.

An analysis which permits loads to vary within a prescribed range in any possible combination has a more rational basis in design and prescribes maximum permissable loads that are on the safe side.

During the life time of a structure some of the loads can be applied in opposite senses on a structure and bending in opposite directions can take place in some of the members. Yielding of particular cross-sections can occur alternately in tension and compression in the outer fibres. In such cases, the failure of the structure can occur even though the collapse mechanism was not developed and load value can be less than the maximum prescribed value. This case was described by J. F. Baker (7) as alternating plasticity.

If the loads vary in a prescribed value but in the same direction permanent plastic deformation can occur after each cycle of loading. There are two possibilities of behavior on such a case. The increment of permanent deflection can decrease after each cycle and after a sufficient number of cycles of loading the structure behaves purely elastically. Such a structure has shaken down. In the other case the increment of permanent deformation stays fixed after each cycle and the failure of the structure occurs as the consequence of secondary effects caused by high deflection. The secondary moments could reach values in the range of the

primary moments which lead to the earlier failure of the structure. This type of collapse is generally known as incremental collapse and was described by J. F. Baker (7) as well as by B. G. Neal (11).

The highest value for shakedown load which refers to an infinite number of cycles of loading is, at the same time, the lowest value for incremental collapse load. This critical value of load is calculated by analysis introduced by J. F. Baker (7) or by B. G. Neal (11).

It was generally assumed by the authors mentioned above that incremental collapse of a structure will occur if sufficient number of plastic hinges is developed in single cycle to transfor structure into collapse mechanism when applied simultaneously. This action is based on the assumption that plastic action of some cross-sections of the structure is taking place under any combination of loads and when these loads are removed a residual moment occurs at that section.

There are several methods to calculate shakedown. By using a step by step calculation shakedown can be evolved by tracing out the loading history but this is not convenient for predicting either the incremental or alternating plasticity load. For the problem considered here the incremental collapse is more critical than is alternating plasticity.

A reasonable method for calculating the incremental collapse load is similar to the method for calculating the plastic collapse load. Such a mechanism method was originally developed by Bleich (6). The first step is to assume the incremental collapse mechanism and then the value of load W_S corresponding to it can be found. At this value of W_S, a distribution of residual moment would be attained such that when the maximum and minimum elastic moments for this value of W_S were superposed on the residual moments the fully plastic moment would just be attained at each of the cross-sections at which the plastic hinges occur in the assumed incremental collapse mechanism.

If none of the extreme values of bending moments exceed the fully plastic moment, it follows from the uniqueness theorem (A1), that the correct incremental collapse mechanism has been chosen. Difficulties in checking the moments at critical points other than the plastic hinges arise if the incremental collapse mechanism is of the partial type, because of the statistica indeterminancy implicit in collapse.

The method of combined mechanisms as developed by B. G. Neal (11) fulfills the same role in the calculation of incremental collapse load as the corresponding method fulfilled in the calculation of the plastic collapse load. There are no additional difficulties when mechanisms of the partial type are encountered. The method differs from the method of combining mechanisms for calculating plastic collapse loads only in details of its application. The method is closely detailed in Section 2.4.

All the methods mentioned above are applicable to steel structures, and seem to be applicable to any structure possessing a moment-curvature relationship of elastic-plastic materials. Though the behavior of the reinforced concrete cross-section during the loading is much more complicated than is the behavior of a steel cross-section, the fulfillment of certain conditions on the reinforced concrete structure can be analyzed by a similar approach as that for the steel structure.

2.2 Plastic Collapse

The method of combining mechanisms was used for calculating the plastic collapse load for the frame shown in Figure 2.1. This method will now be illustrated on the example which symbolizes the frame model used in this study.

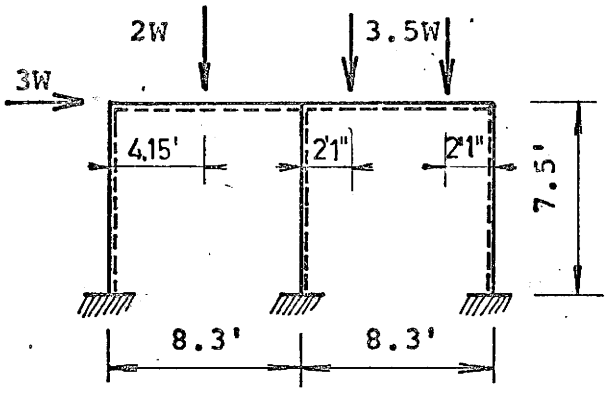

a, Size of frame and loading.

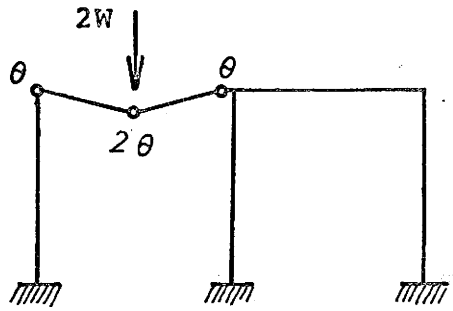

b, Left beam mechanism.

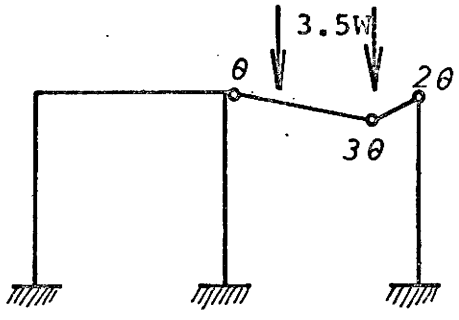

c, Right beam mechanism.

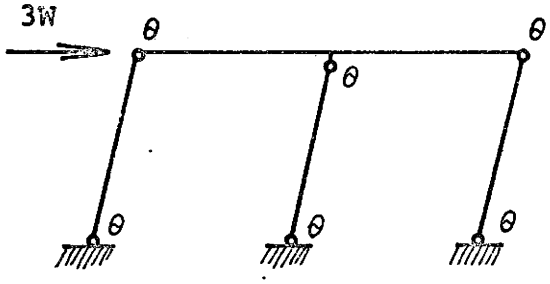

d, Sway mechanism.

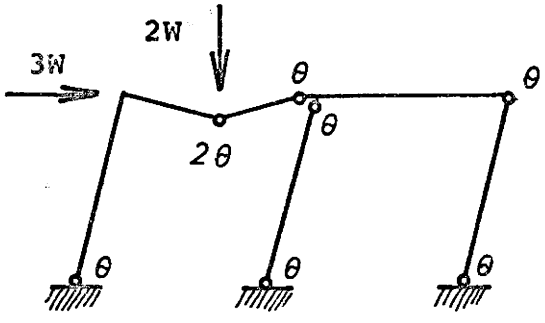

e, Combined mechanism.

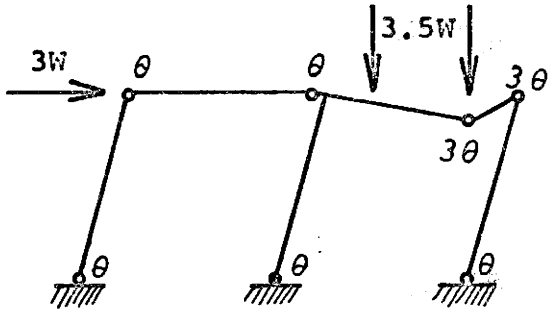

f, Combined mechanism.

Fig. 2.1. Frame loading and collapse mechanisms.

The dimensions of the frame and the relative values of the applied loads is shown in Figure 2.1, a. The positive moment and positive rotation of hinges is considered when the fibres on the side of the dotted line are under tension.

The first step is to find all independent collapse mechanisms. The computations associated with the combined and independent mechanisms are given below. The plastic collapse load was then calculated from the virtual work equations and the smallest value was taken as the correct one. The virtual work equations and calculation of load values corresponding to the mechanisms shown in Figure 2.1 are as follows:

Left beam mechanism Figure 2.1,b: $4 Mp \times \theta = 2 \times W \times 4.15 \times \theta$

$$W = 0.482 Mp$$

Right Beam mechanism Fig. 2.1,c: $6 \times Mp \times \theta = 7/4 \times W \times (6.225+2.075) \times \theta$

$$W = 0.413 Mp$$

Sway mechanism Figure 2.1, d: $6 \times Mp \times \theta = 3 \times W \times 7.5 \times \theta$

$$W = 0.266 Mp$$

Combined mechanism Fig. 2.1, e: $8 \times Mp \times \theta = W \times (3x7.5+2x4.15) \times \theta$

$$W = 0.2597 Mp$$

Combined mechanism Fig. 2.1, f: $11 \times Mp \times \theta = W \times (3x7.5+8.3x7/4) \times \theta$

$$W = 0.297 Mp$$

The correct collapse mechanism is the one shown in Figure 2.1e since it gives rise to the smallest value of plastic collapse load. For a plastic moment value of 312.0 inchkips the plastic collapse load would be 6.75 kips. The value of Mp relates to the experimental cross-section and is developed in Section 2.3.

The validity of this result was proven by tracing the loading history step by step until the same plastic collapse load and the same collapse mechanism were reached. In this loading increment approach the elastic solution is obtained. The cross-section with the highest moment value is assigned as the first plastic hinge and the elastic analysis is repeated while the structure is considered as having a natural hinge at that cross-section. The moment values are then multiplied by a coefficient such that when added to the previous moment distribution some other section just reaches the value of Mp with all other critical points less in magnitude than Mp. The procedure is then repeated until the collapse mechanism is developed. Though this method is not very practical for calculating the plastic collapse load, the deflection of the frame at any stage of loading can be easily determined. A computer program was written for this purpose so that the effect of load increments applied to almost any current state could be established. The sequence of hinge formation and the consequent load-deflection curve were obtained by this method for the frame model shown on Figure 2.2. The value of the plastic moment considered in calculation was 300.0 inch-kips taken for convenience.

For estimating the deflection at incipient collapse the method of plastic slope-deflection equations was used. This method had been proposed by Symonds and Neal (11) in which it is assumed that the moment-curvature is of the ideal type with the spreading of plastic zones along the members neglected. The method is similar to that for the elastic solution with the principal difference being that at each cross-section where a plastic hinge underwent rotation, the bending moment is known to have the plastic moment value but where the plastic hinge rotation remains unknown.

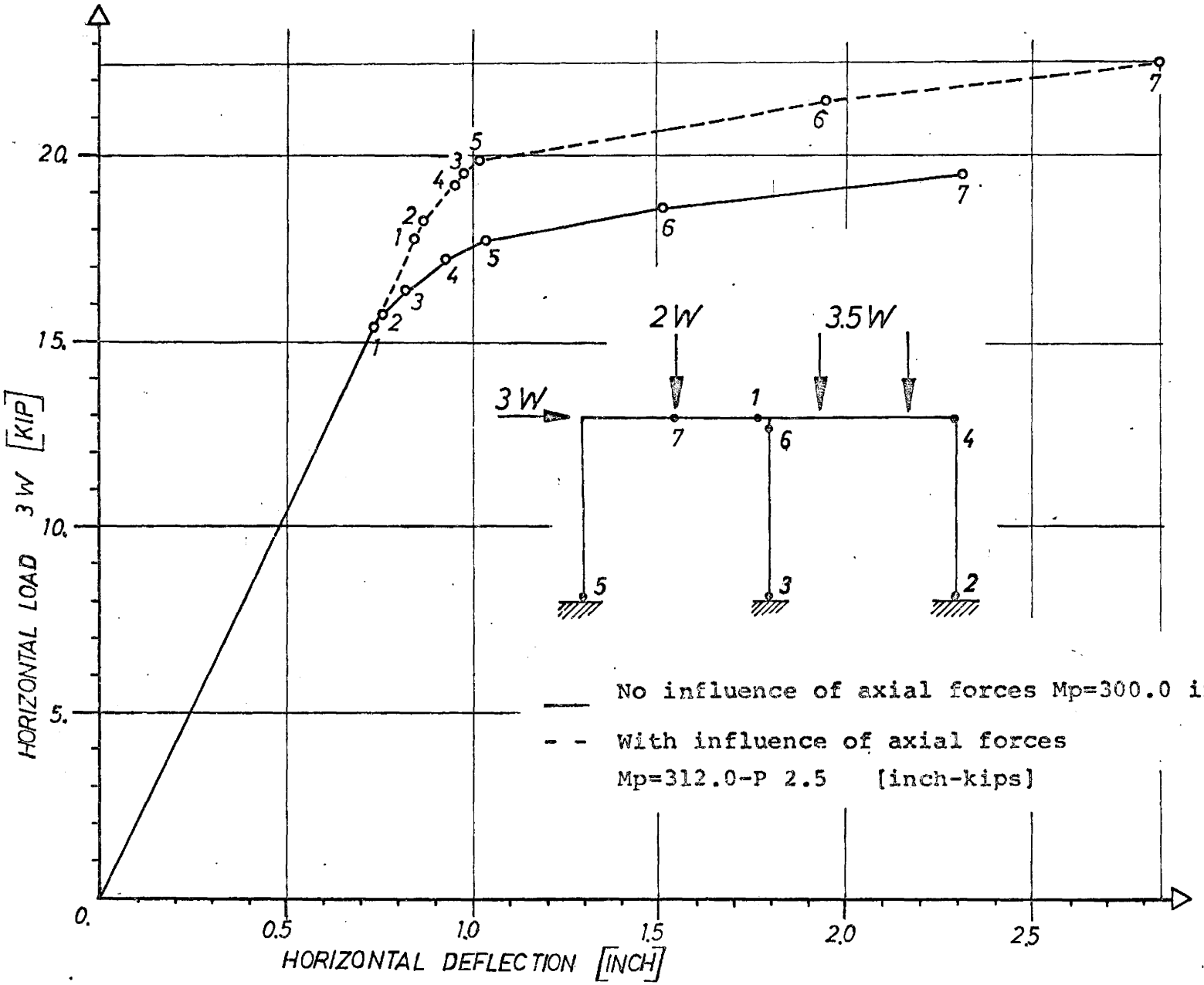

Fig. 2.2. Horizontal deflection-horizontal load relationship.

In the wholly elastic frame the bending moment at the cross-section would be unknown but the hinge rotation would be zero. For our case the prediction is based on the assumption that for the last hinge to form there is a rotation of zero at the point of collapse.

The method of plastic slope-deflection will now be demonstrated on the example which symbolizes the frame model used in this work. The positive moments and positive rotation at the ends of the member are shown on Figure 2.3,a. These rotations can be shown to be given by the slope-deflection equations:

$$\phi_{AB} = \frac{\delta}{L} + \frac{L}{6EI}\left[2(M_{AB} - M^F_{AB}) - (M_{BA} - M^F_{BA})\right]$$

$$\phi_{AB} = \frac{\delta}{L} + \frac{L}{6EI}\left[2(M_{BA} - M^F_{BA}) - (M_{AB} - M^F_{AB})\right]$$

where M^F_{AB} and M^F_{BA} are the fixed-end bending moments which would be produced at the ends of the member if it were subjected to the same loading but both ends were held clamped in position and direction. The plastic moment M_p was for the frame shown in Figure 2.3,a, considered to be 300 inch-kips throughout the frame. The value of moment of inertia I and modulus of elasticity E were taken from Section 3.4. The deformation of the frame during the collapse was assumed as is shown on Figure 2.3,c. The plastic slope-deflection equations for this frame could be written as follows:

$$\phi_{1,2} = \frac{\delta}{90} + \frac{90}{6EI}\left[2(M^F_{1,2} - M_{1,2}) - (M_{2,1} - M^F_{2,1})\right]$$

$$\phi_{2,1} = \frac{\delta}{90} + \frac{90}{6EI}\left[2(M_{2,1} - M^F_{2,1}) - (M_{1,2} - M^F_{1,2})\right]$$

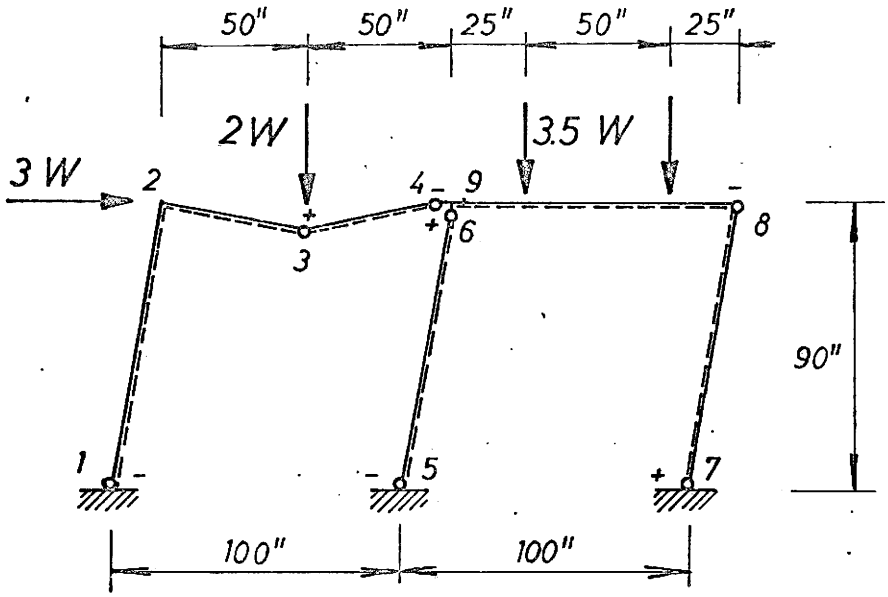

a, Dimension, loading and collapse mechanism.

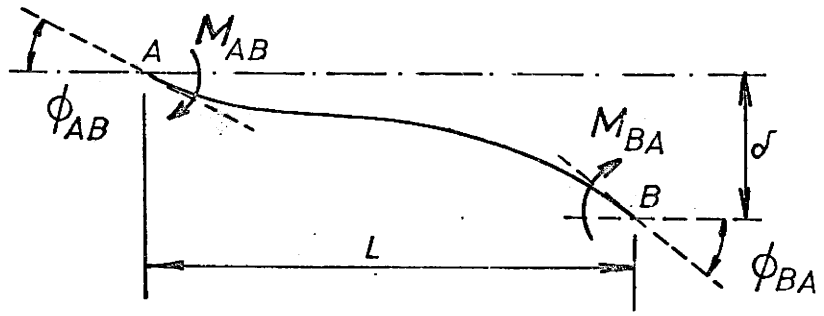

b, Definition of terms in slope-deflection equations.

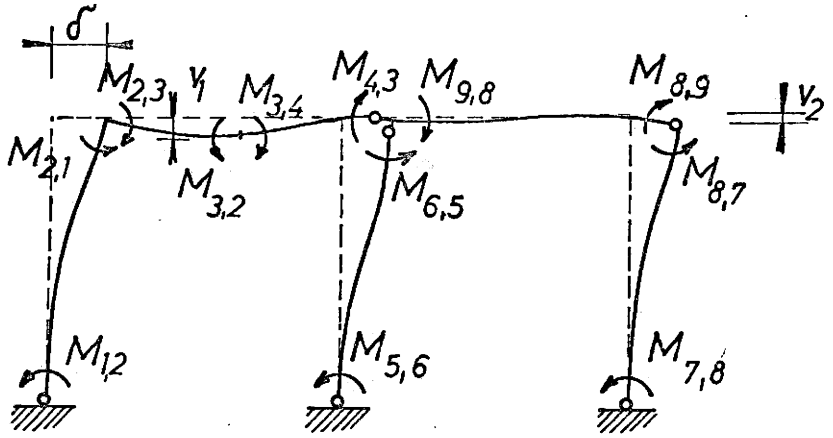

c, Deformations in the time of collapse.

Fig. 2.3. Rectangular two-bay portal frame.

$$\phi_{2,3} = \frac{v_1}{50} + \frac{50}{6EI}\left[2(M_{2,3} - M^F_{2,3}) - (M_{3,2} - M^F_{3,2})\right]$$

$$\phi_{3,2} = \frac{v_1}{50} + \frac{50}{6EI}\left[2(M_{3,2} - M^F_{3,2}) - (M_{2,3} - M^F_{2,3})\right]$$

$$\phi_{3,4} = \frac{v_1}{50} + \frac{50}{6EI}\left[2(M_{3,4} - M^F_{3,4}) - (M_{4,3} - M^F_{4,3})\right]$$

$$\phi_{4,3} = \frac{v_1}{50} + \frac{50}{6EI}\left[2(M_{4,3} - M^F_{4,3}) - (M_{3,4} - M^F_{3,4})\right]$$

$$\phi_{5,6} = \frac{\delta}{90} + \frac{90}{6EI}\left[2(M_{5,6} - M^F_{5,6}) - (M_{6,5} - M^F_{6,5})\right]$$

$$\phi_{6,5} = \frac{\delta}{90} + \frac{90}{6EI}\left[2(M_{6,5} - M^F_{6,5}) - (M_{5,6} - M^F_{5,6})\right]$$

$$\phi_{7,8} = \frac{\delta}{90} + \frac{90}{6EI}\left[2(M_{7,8} - M^F_{7,8}) - (M_{8,7} - M^F_{8,7})\right]$$

$$\phi_{8,7} = \frac{\delta}{90} + \frac{90}{6EI}\left[2(M_{8,7} - M^F_{8,7}) - (M_{7,8} - M^F_{7,8})\right]$$

$$\phi_{8,9} = \frac{v_2}{100} + \frac{100}{6EI}\left[2(M_{8,9} - M^F_{8,9}) - (M_{9,8} - M^F_{9,8})\right]$$

$$\phi_{9,8} = \frac{v_2}{100} + \frac{100}{6EI}\left[2(M_{9,8} - M^F_{9,8}) - (M_{8,9} - M^F_{8,9})\right]$$

The fixed-end moments for all members except the member between critical points 8 and 9 are zero. The value of fixed-ends moments for member 8-9 is calculated in Appendix A2 as well as slope-deflection equations being assessed numerical values.

The last plastic hinge to form was found to be at critical point 3. Consequently the rotation of joint 3 was considered equal to zero. The joint rotations in terms of member end rotations is given on the next page. The subscript refers to the joint location as shown in Figure 2.3 a.

$$\psi_1 = -\phi_{1,2} \quad \ldots\ldots (1)$$

$$\psi_2 = \phi_{2,1} - \phi_{2,3} = 0 \quad \ldots\ldots (2)$$

$$\psi_3 = \phi_{3,2} - \phi_{3,4} \quad \ldots\ldots (3)$$

$$\psi_4 = \phi_{4,3} \quad \ldots\ldots (4)$$

$$\psi_5 = \phi_{5,6} \quad \ldots\ldots (5)$$

$$\psi_6 = \phi_{6,5} \quad \ldots\ldots (6)$$

$$\psi_7 = \phi_{7,8} \quad \ldots\ldots (7)$$

$$\psi_8 = \phi_{8,7} + \phi_{8,6} \quad \ldots\ldots (8)$$

$$\psi_9 = \phi_{6,8} \quad \ldots\ldots (9)$$

By solving the equation (3) for zero joint rotation the deflection v_1 is obtained. By substituting this value in equation (2) the horizontal deflection is obtained. As shown in Appendix A2 the horizontal deflection thus obtained is 2.19 of an inch. By substituting already known values into the equations for joint rotation shown above a check of the sign of joint rotations can be made. If the signs agree with signs considered in the collapse mechanism the solution is correct. A check of signs for this case is shown in Appendix A2 and validates the assumed behavior.

2.3 Limit Analysis

In this section the necessary limitations of plastic analysis implicit in reinforced concrete behavior will be discussed. It is obvious that the most important characteristic of reinforced concrete in this case will be the moment-curvature relationship. As it is generally known from

ultimate strength theory of reinforced concrete the percentage of steel in the cross-section has a significant influence on the moment-curvature characteristic. The transition between under and over reinforced sections is a gradual one in terms of an increasing proportion of reinforcement. A convenient dividing line is that of the balanced reinforcement ratio which is defined in the ACI Building Code (26) as:

$$p_b = \frac{0.85\ k_1\ f'_c}{f_y} \quad \frac{87000}{87000 + f_y}$$

where coefficient k_1 is equal to 0.85 for f_c less than 4000 psi and is decreasing by 0.05 times the difference for f_c higher than 4000 where f_c is the compressive strength of concrete and f_y is the yield strength for reinforcement For this case when f_c is taken as 4850 psi and f_y=60,000 psi the balanced reinforcement ratio p_b is 3.28% when k_1 is:

$$k_1 = 0.85 - 0.05\ \frac{(f_c - 4000)}{1000} = 0.8075$$

The basis of limit analysis lies in the ability of a reinforced concrete section to sustain a given yield moment while permitting a considerable increase in local curvature. It follows that the moment curvature curve at the critical points in the frame should be close to the ideal type mentioned previously. Such characteristics are based on the under reinforced section which is generally recommended for limit design.

The percentage of reinforcement p is defined as:

$$p = \frac{A_s}{b \times d} = \frac{0.88}{8 \times 6.625} = 1.66\%$$

A_s = 0.88 si for two #6 bars

where A_s is the tension steel area, b is the width of the section and d is the distance from compression face of the section to the centroid of tension steel. The cross section is shown in Figure 3.6.

The moment-curvature curve for this section was calculated and was plotted in Figure 2.4. The curves shown dotted are the moment curvature curves of the same section with different axial force P. The basic curve is for axial force equal to zero. The hooks in the lower part of the curves are due to the instability condition at the point of the crack formation. The influence of axial force on the value of the plastic moment was so significant that it could not be neglected. Fortunately, the relationship between the plastic moment M_p and axial force P was very close to linear in the range of axial forces occurring on the frame during the loading. This relationship is plotted in Figure 2.5. If the lower part of the moment-curvature curve had not been considered, the moment-curvature relationship would have been fairly close to the ideal type. This behavior formed the basis for utilizing plastic methods where appropriate. The moments which caused cracking at the cross-section were low compared with the plastic moments and therefore the influence of cracking was neglected.

The method which was used for tracing behavior during loading history was adjusted to take into account the influence of axial force. This adjustment was provided by iterating the plastic moment value with the axial forces. Firstly, the forces were calculated due to the load at first hinge formation, while the plastic moment value was assumed equal to that for zero axial force. Then a set of new values of plastic moment were calculated due to the obtained axial forces and the procedure was repeated.

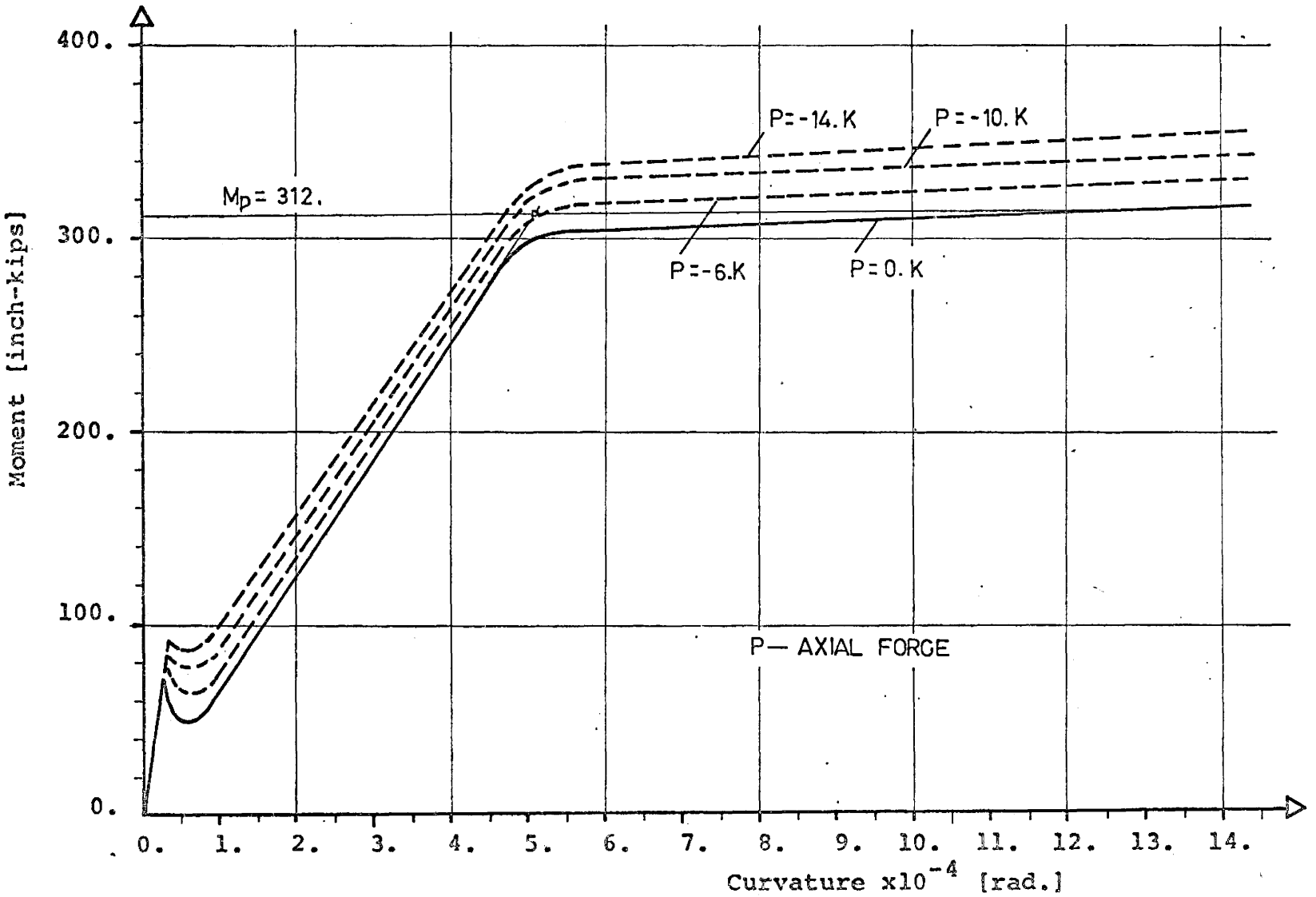

Fig. 2.4. Moment-curvature relationship of typical cross-section.

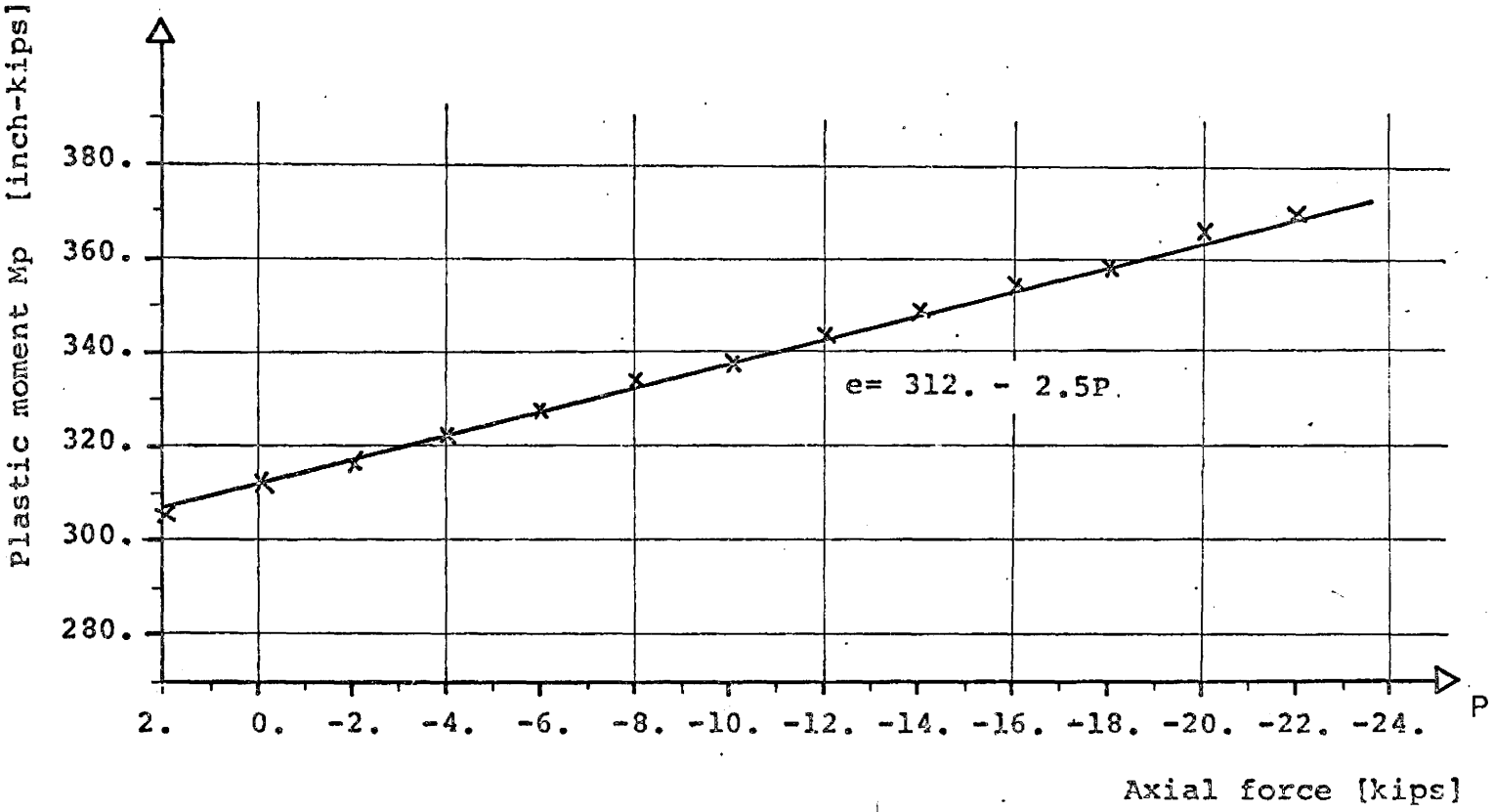

Fig. 2.5. Plastic moment-axial force relationship.

Iteration was quite rapid and in the calculation used in the computer program five cycles were performed. The following Table includes the plastic moment values M_p for columns and beams cross-sections of frame during the five iteration cycle when the first plastic hinge is forming.

Table 2.1

No. of Cycle of iteration	Plastic Moment Value Mp in Kips-Inch				
	First Column	First Beam	Sec. Column	Sec. Beam	Third Column
0	312.000	312.000	312.000	312.000	312.000
1	312.223	314.469	315.381	315.275	314.287
2	314.804	343.056	354.524	328.034	340.773
3	315.059	345.879	358.389	329.492	343.388
4	315.084	346.158	358.771	329.636	343.647
5	315.086	346.185	358.809	329.650	343.672

The load-deflection curve obtained by this method is shown in Figure 2.2 by the dotted curve. Comparing this curve with that for M_p independent of axial force P the importance of influence of axial forces on the behavior of the whole frame is obvious. The obtained plastic collapse load was at least 11% higher than that obtained by the method of combined mechanism. Also the plastic hinges formed in different sequences.

The computer method for a step by step calculation is described in Chapter VII.

2.4 Incremental Collapse and Shakedown

In the previous section, the behavior of the frame structure under proportionally increasing load was described. The failure of the frame was caused at the plastic collapse load and is called plastic collapse.

Another type of failure may occur when frames are subjected to variable repeated loading. If during loading a number of critical combinations of loads follow one another in fairly definite cycles the structure may either shake down or else fail by incremental collapse.

If the increments which occur in the rotation at plastic hinges during subsequent cycles of loading become progressively smaller as the number of cycles of loading increases, the structure is said to be shaking down.

If, on the other hand, the increments of rotations taking place at plastic hinges during subsequent cycles of loading tend to be constant and a sufficient number of cycles of loading takes place, unacceptably large deflections will be built up; the structure will then accelerate to collapse (27)

A value of W above the critical shakedown value W_s will give rise to incremental collapse and the lowest such value is referred to as the incremental collapse load. It follows then that the incremental collapse load and the shakedown load are virtually identical.

The uniqueness theorem of incremental collapse as presented by B. G. Neal (11) is included in Appendix (A1). According to this theorem equilibrium at each critical cross-section can be expressed by the equation:

$$\begin{aligned} m_j + \mathcal{M}_j^{max} &= (M_p)_j \text{ if rotation } \theta_j > 0 \\ m_j + \mathcal{M}_j^{min} &= -(M_p)_j \qquad\qquad \theta_j < 0 \end{aligned} \tag{2.4.1}$$

where m_j are the residual moments at critical point j, $\mathcal{M}_j$ are the elastic moments and M_p is the plastic moment value for cross-section at critical point j. The moments are considered of the same signs as the rotation θ.

The incremental collapse load W_s was calculated by using the method of combining mechanisms. Since the m_j are in equilibrium with zero external load, and the Θ_j represent a set of hinge rotations for a mechanism, it follows from the Principle of Virtual Work that:

$$\Sigma \; m_j \; \Theta_j = 0 \qquad (2.4.2)$$

$$\Sigma \left\{ \begin{array}{ll} (M_p)_j & -\mathcal{M}_j^{max} \\ -(M_p)_j & -\mathcal{M}_j^{min} \end{array} \right\} \; \Theta_j = 0 \qquad (2.4.3)$$

Since the m_j are known from the equation (2.4.1) and the $\mathcal{M}_j^{max}$ and $\mathcal{M}_j^{min}$ are all known in terms of W, the equation (2.4.3) will determine the value W_s of W above which incremental collapse would occur.

Since the approach is similar to that described in the previous section for combined mechanisms the method of plastic collapse defines the smallest value of W as the incremental collapse load W_s and the corresponding mechanism as the incremental collapse mechanism

The elastic moments can be obtained by any of the elastic methods. In this case the matrix method was used. Table 2.2 includes the elastic moments for critical points of the frame model. The maximum and minimum value of the moments apart from the case of zero load were obtained and are entered in Table 2.2. Positive moments

LOAD W = 1 [KIPS]	MOMENT IN CRITICAL POINT [IN-KIPS]										
	1	2	4	5	6	7	8	9	10	12	13
3 W →	-4.067	2.782	0.336	-2.110	2.088	4.198	0.883	-1.531	-2.735	3.987	-4.734
2 W ↓	0.513	-1.226	2.614	-1.846	-0.694	1.151	-0.491	-0.084	0.119	0.036	-0.671
3.5 W ↓ ↓	0.048	0.153	-0.375	-0.904	-2.413	-1.509	1.410	1.813	-1.608	0.608	0.878
M^{max}	0.561	2.935	2.950	0.	2.088	5.349	2.293	1.813	0.119	4.631	0.878
M^{min}	-4.063	-1.226	-0.375	-4.860	-3.107	-1.509	-0.491	-1.615	-4.343	0.	-5.405

Table 2.2 Elastic Moments in Critical Points for Given Load as a Function of Load W.

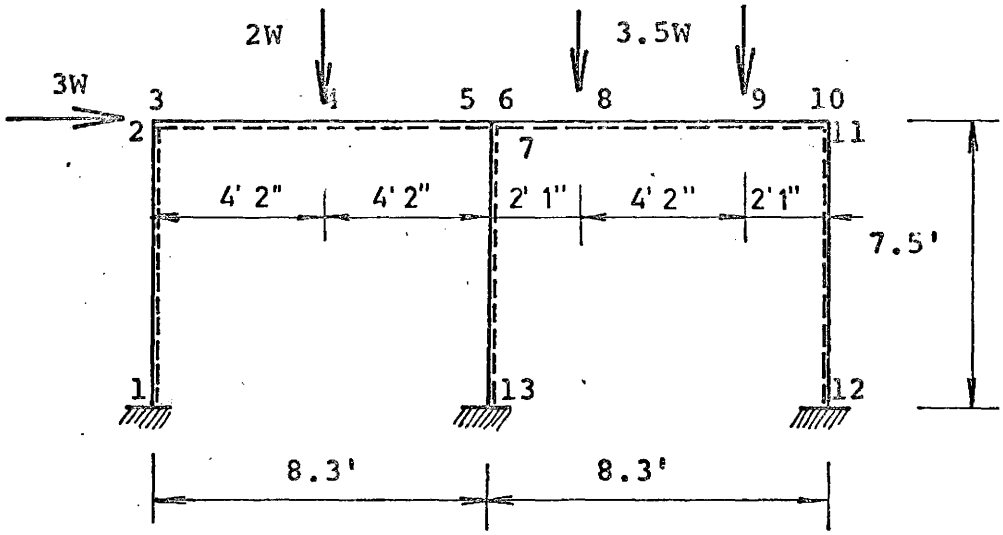

a, Dimension of frame.

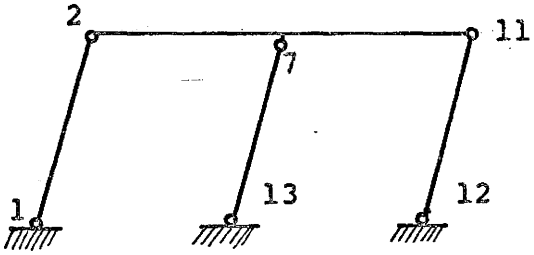

b, Sway mechanism.

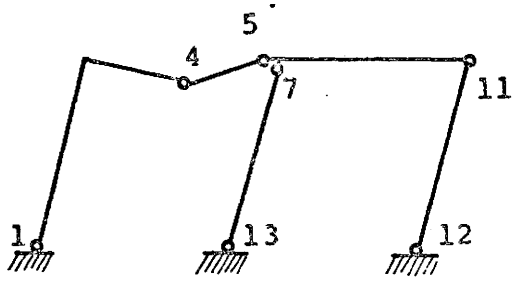

c, Combined mechanism.

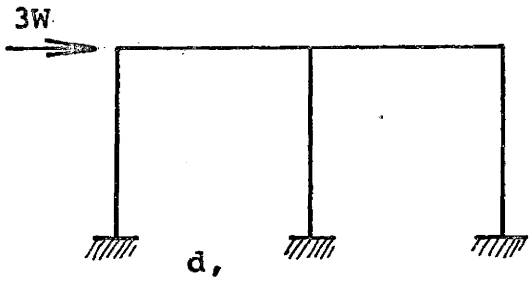

d,

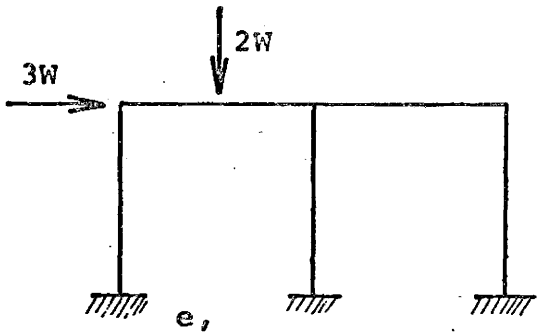

e,

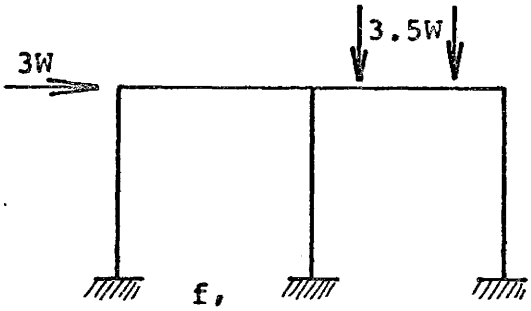

f,

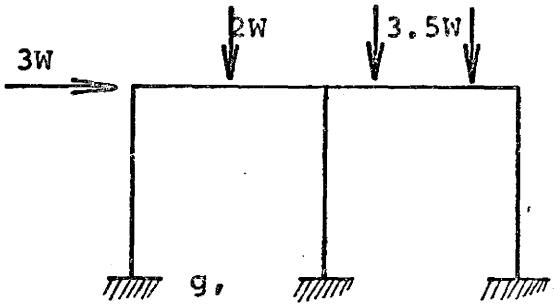

g,

Fig. 2.6. Dimension, mechanisms and load combinations for incremental collapse of frame.

were considered which caused tension in the outside fibres of the cross-section on the side of the dotted line as marked in Figure 2.6,a.

Considered incremental collapse mechanisms are shown in Figure 2.6, b, c. These two mechanisms give the most critical value of W. Therefore, the other mechanisms are not included. From the sway mechanism on Figure 2.6, b the equilibrium of the residual moments on the frame can be expressed.

$$-m_1 + m_2 + m_7 - m_{11} + m_{12} - m_{13} = 0$$

Referring to the equations (2.4.2) and (2.4.3) the equation above can be written as:

$$-\mathcal{M}_1^{\min} + \mathcal{M}_2^{\max} + \mathcal{M}_7^{\max} - \mathcal{M}_{11}^{\min} + \mathcal{M}_{12}^{\max} - \mathcal{M}_{13}^{\min} = 6M_p$$

In numerical values:

$$W\ (4.063 + 2.935 + 5.405 + 4.343 + 4.631 + 5.349) = 6\ M_p$$

for which the load $W = 0.2245\ M_p$. Similarly for the combined mechanism of Figure 6,c the following equation can be written:

$$-m_1 + 2m_4 - m_5 + m_7 - m_{11} + m_{12} - m_{13} = 0$$

W is then equal to $0.229\ M_p$.

Because of a lower value of W for the sway collapse mechanism the incremental collapse load was assumed as 0.2245 M_p and this mechanism was therefore the incremental collapse mechanism.

The step-by-step calculation as described in the previous section was used also for calculation of incremental collapse. In this case it was necessary to estimate a load combination forming a typical cycle of loading. Due to the method described above the incremental collapse mechanism was known. With respect to this collapse mechanism the most efficient load combination was chosen after determining which combination had to be incorporated in a cycle. Since the sway governs, the critical points to be considered are 1, 2 (or 3), 7, 13, 12, and 11 (or 10). Peak elastic moments need to be considered at critical points 2 (or 3), 7 and 12, while minimum values are associated with critical points 1, 13 and 11 (or 10). Then, for example, the load combination on Figure 2.6 e, associated with critical point 7 for peak moment 5.349 W and for minimum moment with critical point 13 where the minimum moment is -5.405 W as can be seen from the Table 2.2. The load combination which is considered in the step by step calculation is shown on Figure 2.6, d, e, f, and g.

The calculation for each loading was similar to the proportional loading case except that actual plastic moments and load values were considered. When loads reached then prescribed values, some of the critical cross-sections developed plastic hinges. The calculation procedure for unloading was then followed. The unloading was considered as pure elastic changes to existing bending moment distributions due to the same loads but of opposite signs being applied on the frame. The resulting moments were residual moments and they were considered in the following load calculation procedure. The

calculation procedure of loading and unloading was repeated and incremental collapse was determined in the cycle in which all plastic hinges forming the incremental collapse mechanism were developed.

Table 2.3 includes moment values of critical points obtained by a step-by-step calculation for the frame shown in Figure 2.6,a. The plastic moment value was considered to be 300.0 inch-kips. The Table includes the maximum value which occurred at critical sections during a cycle and the residual moment at critical points after the cycle was completed. The table refers only to the critical points involved in the incremental collapse mechanism. The most interesting critical point is 2 where the maximum moment is increasing by every cycle until the plastic moment is reached. The incremental collapse calculated by this method occurred in the 21st cycle when all plastic hinges associated with the incremental collapse mechanism occurred during this cycle. The incremental collapse load W considered in this calculation is 0.2245 Mp, which is the same as the load obtained by the method of combined mechanisms.

By considering the same plastic moment value several different values of load W were considered and an interesting relationship between the load value W for incremental collapse and number of cycles necessary for incremental collapse was obtained. The curve of load W - number of cycle relationship, is plotted in Figure 2.7 and the horizontal deflection - number of cycle curves for different values of load W - are shown in Figure 2.8. Table 2.4 includes theoretical hinge formation for W_s = 5.6 kips.

CYCLE	MOMENT IN CRITICAL POINTS (IN-KIPS)											
	1		2		13		7		12		11	
	MAX	R	MAX	R	MAX	R	MAX	R	MAX	R	MAX	R
1	-300.0	-33.8	229.7	31.0	-300.0	+23.6	300.0	-37.2	300.0	-15.8	-300.0	-11.8
2	-300.0	-31.8	244.2	47.0	-300.0	31.9	300.0	-39.7	300.0	-15.8	-300.0	- 8.7
3	-300.0	-31.3	256.6	59.7	-300.0	39.5	300.0	-43.6	300.0	-15.8	-300.0	- 7.9
4	-300.0	-31.1	266.4	69.5	-300.0	45.3	300.0	-47.2	300.0	-15.8	-300.0	- 7.7
5	-300.0	-31.1	279.8	83.0	-300.0	53.2	300.0	-52.6	300.0	-15.8	-300.0	- 7.6
10	-300.0	-31.0	292.5	95.8	-300.0	60.7	300.0	-57.8	300.0	-15.8	-300.0	- 7.5
15	-300.0	-28.8	297.8	100.9	-300.0	62.5	300.0	-59.0	300.0	-15.8	-300.0	- 7.7
20	-300.0	-27.6	299.9	102.7	-300.0	63.0	300.0	-59.3	300.0	-15.8	-300.0	- 7.8
21	-300.0	-27.5	300.0	102.8	-300.0	63.0	300.0	-59.3	300.0	-15.8	-300.0	- 7.9

MAX Is the maximum moment which occurred at critical point during the cycle.

R Is the residual moment in the critical point at the end of loading cycle.

TABLE 2.3 MAXIMUM AND RESIDUAL MOMENTS DURING THE CYCLIC LOADING FOR Mp = 300.0 IN-K.

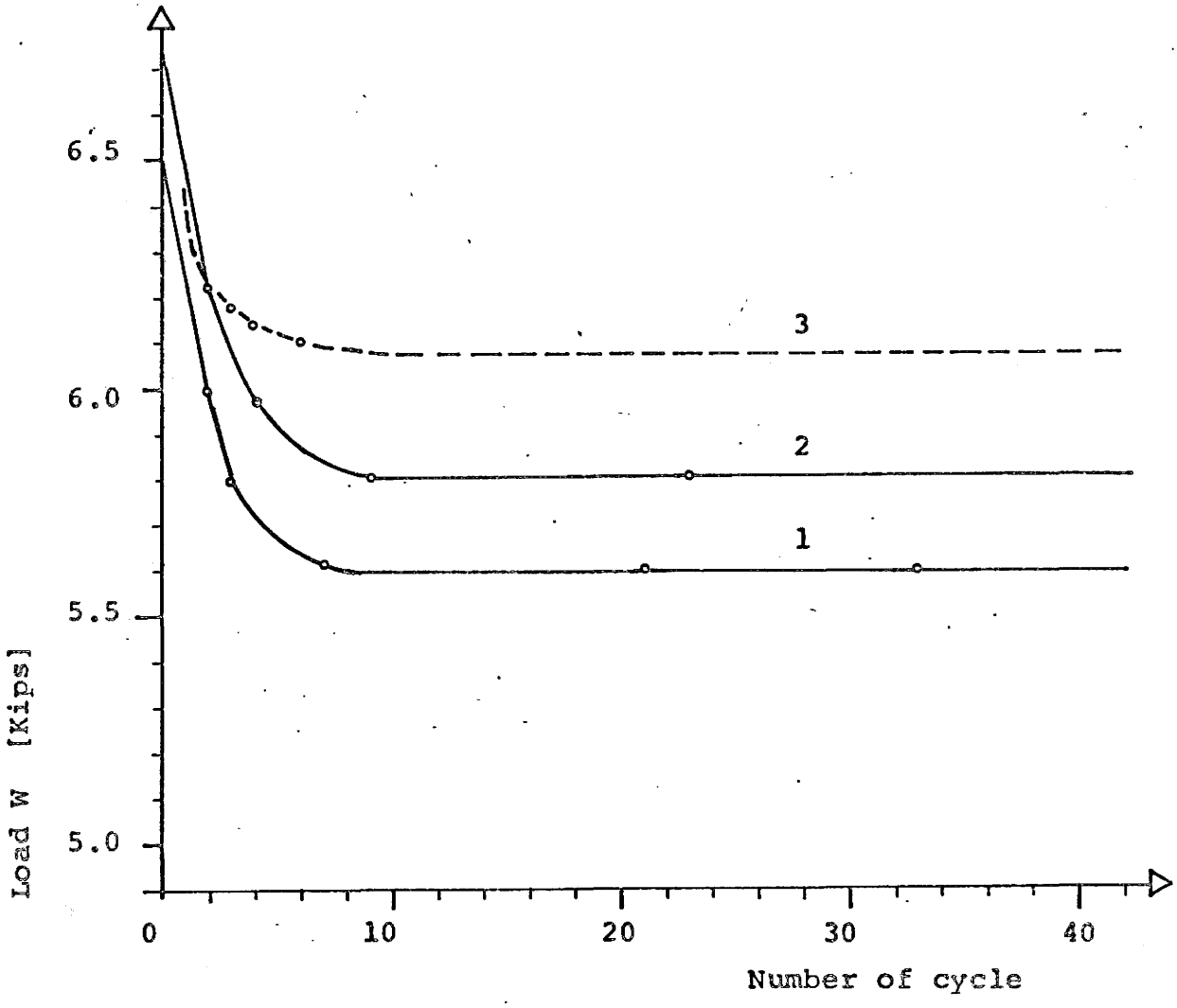

Curve	1	2	3
Plastic moment [inch-kips]	300.0	312.0	312.0 - 25 P
Load Ws [Kips]	5.6125	5.837	6.07

P = AXIAL FORCE

Fig. 2.7. Incremental collapse load-number of cycle relationship.

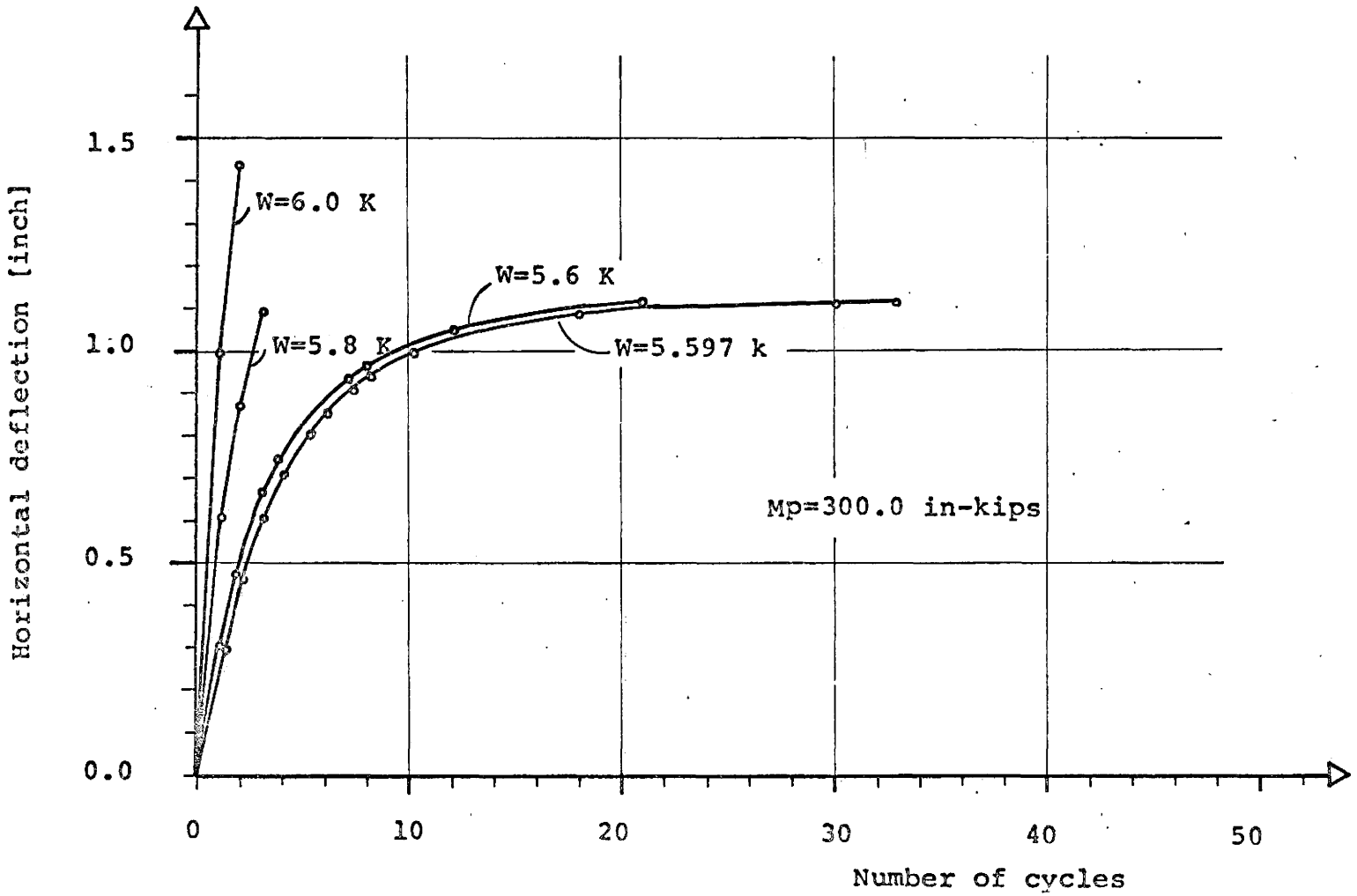

Fig. 2.8. Number of cycles-horizontal deflection relationship.

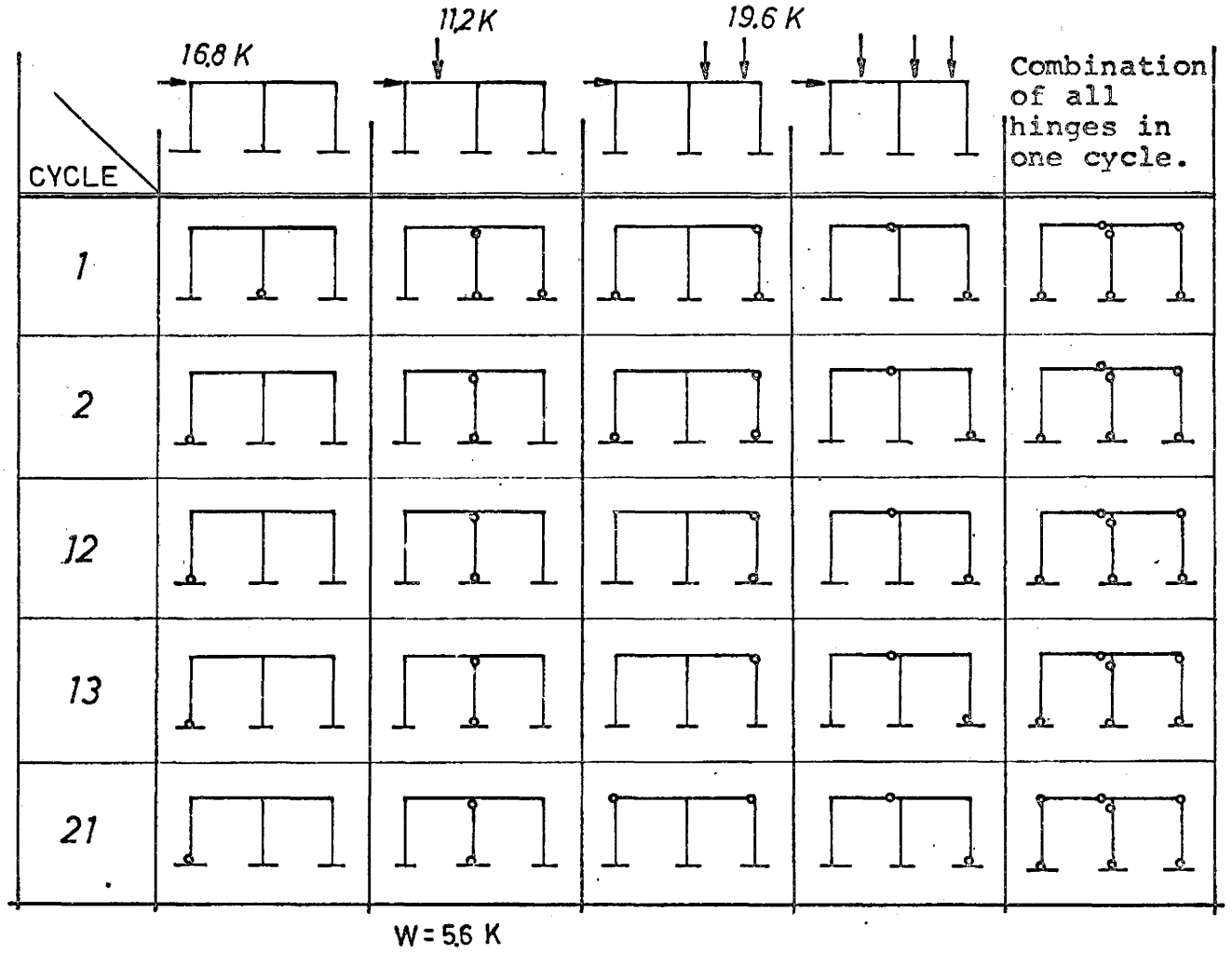

Table 2.4. Theoretical hinge formation during the cyclic loading for Mp=300.0 inch-kips.

2.5 Shakedown of Reinforced Concrete Frame

In order to analyze the shakedown of a reinforced concrete frame it is necessary to investigate the moment-curvature characteristic of the cross-section under repeated loading. The repeatability of the moment-curvature curves would be the basic requirement for analysing for the shakedown in a conventional way. An experimental and analytical investigation of moment-curvature relationships for repeated loading as done by Hiroyuki Aoyama (18) predicted the moment-curvature curves for different reinforced concrete cross-sections subjected to repeated reversed bending and axial force. The Bauschinger effect of reinforcing steel and the tension in the concrete were neglected. The results show quite good agreement between the theory and the test results. The moment-curvature curves were more or less spindle-shaped with the same slope in the elastic part of the curves. This requirement was met in the test program described in this work and therefore the frame is suitable for shakedown analysis.

The assumed moment-curvature relationship as finally considered is shown on Figure 2.4. Complete reversal of bending moment did not occur in any of the critical cross-sections, although in the middle column small reversed bending moments were expected.

The step by step calculation as described in the previous section but including the influence of axial forces was performed for the prediction of the incremental collapse load and for analysing shakedown. It is obvious that the value of the incremental collapse load obtained by this method of calculation was considerably higher than that obtained by the method of combining mechanisms. The difference was about 5%. The influence of axial force in the calculation was of the same

manner as in the step by step calculation for plastic collapse as described in section 2.3 and shown in Figure 2.4.

The theoretical curve for the number of cycle-incremental collapse load is shown in Figure 2.7 as marked by the dotted curve No. 3.

An attempt to trace the deformation in the frame during a cycle was made by the method based on the moment-curvature relationship under repeated loading. Moment values obtained by step by step calculations were used for the calculation of corresponding deformations. Three types of curves were used in this calculation dependent on the stage of loading The first type was for the uncracked section as shown in Figure 2.4. and was used only for the first load application. The second type was for unloading and was actually the moment-curvature relationship obtained by the method of transformed area. It was assumed that unloading was provided by only elastic linear changes. The third type was the curve corresponding to the already cracked section in which the influence of tension in the concrete was neglected. This curve was of a similar shape as the curves in Figure 2.4 except for the lower part of the curve which was in this case smooth. All of these types of curves are shown in Figure 7.2 in Chapter VII. The calculation procedure consisted of determining the corresponding curvature for a given moment and the strain distribution over the section. In the case of unloading the corresponding strain distribution to the moment change was calculated and then subtracted from the previous strain distribution. The strain distribution was added or substracted as a consequence of loading or unloading. The computer technique was used for this calculation and the computer program is described in Chapter VII.

A very important factor for describing the behavior of the reinforced concrete frame was the effect of joint stiffness due to the addition of stirrups and the placing of longitudinal reinforcement. This effect is described in Section 6.6 and in Chapter VIII, but could not be included in the analysis because of implicit complications arising there from.

Chapter III

TEST FRAMES AND COLUMNS

This chapter includes the description of the test specimen selection of the test specimens in detail. The modifications resulting from the test procedures are also described in this chapter, while the details are described in Chapter VI.

3.1. General Characteristic

In the selection of the test specimens several aspects were considered. An important one relates to the theory of plastic analysis in terms of hinge formations and consequent mechanisms. A 2nd criterion which pertains to concrete structures generally concerns the reinforcement. To justify plastic methods of analysis to reinforced concrete frames the cross sections at the critical points must be under reinforced.

Another important aspect was the limitation imposed by laboratory facilities and the endeavour to minimize errors caused by inaccuracies.

Referring to the theory of plastic analysis three aspects influenced the selection of the structural model.

Firstly, structures with a higher degree of indeterminancy were preferred for the structural model because of more plastic hinges required to form the collapse mechanism. Such a structure would give a better opportunity to study plastic hinge formation and collapse mechanism formation.

Secondly, the ratio between the plastic collapse load and incremental collapse load had to be considered. A structure with a high ratio was preferred since it could better be used for the demonstration of shake down.

Thirdly, the structure for which the plastic collapse load mechanism is different from the incremental collapse load mechanism would be preferable to distinguish between the two modes of collapse.

In order to simplify the analysis the same cross-section was chosen for beams and columns. Regarding the ultimate load design, a reinforced ratio of 1.66% was selected. The section had a moment curvature characteristic close to that for ideal elastic-plastic material at initial loading.

To justify a simplified shakedown solution to reinforced concrete structures it was imperative that repeated load tests be conducted on a cross-section to trace out the moment-curvature history. The basic assumption governing the conventional shakedown approach assumes that the same moment limits for positive or negative curvature apply and are presumed to be independent of the number of loading cycles. The proximity of this assumption with actual behaviour was studied. A column with a fixed end base and the same cross-section as the test frame was chosen for studying moment-curvature characteristic for chosen sections. The theoretical moment-curvature characteristic for the chosen section was discussed in sections 2.3 and 2.5 and is plotted in Fig. 2.4.

The availability of sufficient laboratory space and equipment provided a good opportunity for fabricating and testing full sized models, to reduce dimensional errors. The spacing of holes for anchor bolts in the test floor is 3 feet, center to center distance and this fact suggested a nine foot span distance per bay.

For simplicity of geometrical form the one story two bay frame was chosen with equal length of beams and columns.

The loads applied were considered to act as point loads. These included a horizontal load at the top of the left hand column and vertical loads, one in the middle of the first beam (first bay is the one closer to the horizontal load and the second bay is the one under two points load) and two at the symmetrical quarter points of the span of the second beam.

The two point loads in the second bay were chosen to approximate uniformly distributed load.

Rational limits to the independent loads were calculated by performing simple shakedown and plastic analyses to cause different collapse mechanisms. At the same time cognizance was taken of realistic values to be found in practice. Upper limits to the coefficients of some parameter W for the individual components of load were 3 for the horizontal, 2 for the vertical in the first bay and 3.5 (2 x 1.75) for the two point vertical loading in the second bay.

For the purpose of initial calculation the column bases were considered fixed. From a practical point of view the stiffness of the column bases was made as large as possible in the experiments in order to justify neglecting the influence of rotation of the bases on the frame moments.

3.2. Geometrical Properties

The scheme of frame and column models are shown in Figure 3.1 and 3.2. Inaccuracies in length were ±1/8 of an inch. The cross-section of a typical column or beam is shown in Figure 3.3,a. Four number six bars comprised the longitudinal reinforcement and was placed symmetrically in the section. The concrete cover over longitudinal reinforcement was one inch.

Number two bars were used for stirrups and they were placed at three inch centres in the beams and at six inch centres in the columns.

The theoretical lengths of members was considered as clear distance between columns for beam length and distance between the end of the wideflange base and the inside face of beam for the length of the column.

On this basis the height of the frame was 90 inches and the bay width was 100 inches.

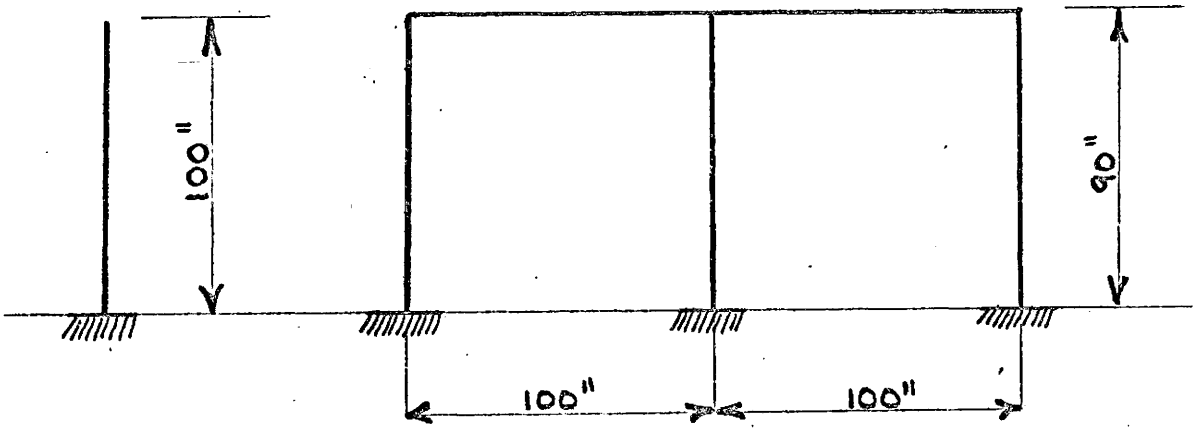

FIGURE 3.1 SCHEME OF TEST MODELS

3.3 Material Properties

The concrete mix used, as shown in Table 4.1 was identical to that used in University of Toronto column test series and on other concrete work in McMaster University (23).

Cylinder test results are included in Appendix A3. Twelve cylindrical prisms were cast with each frame. A slump of 2.2" to 3.5" was sought.

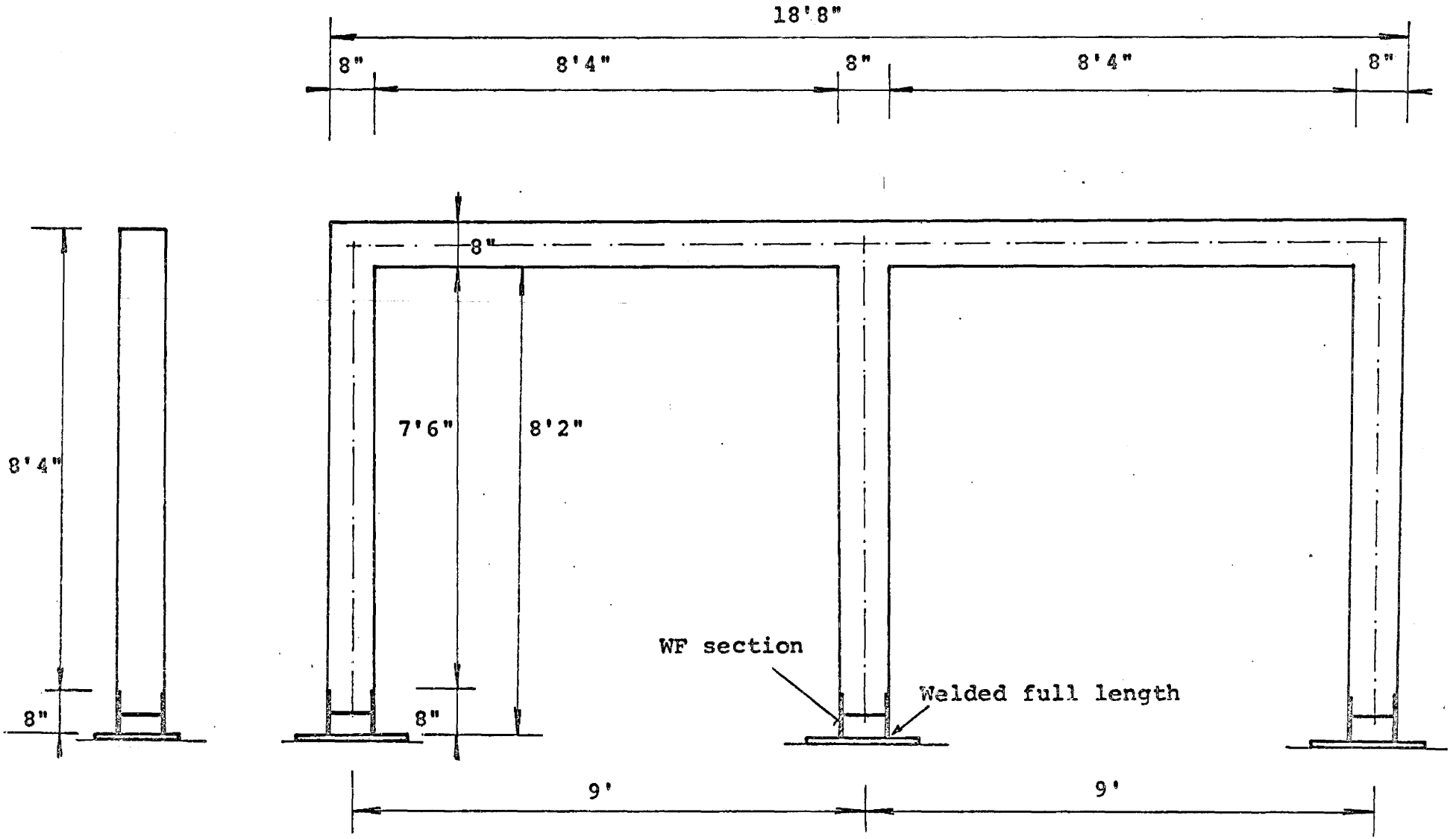

a, Column.

b, Two-bay frame.

Fig. 3.2. Reinforced concrete test models.

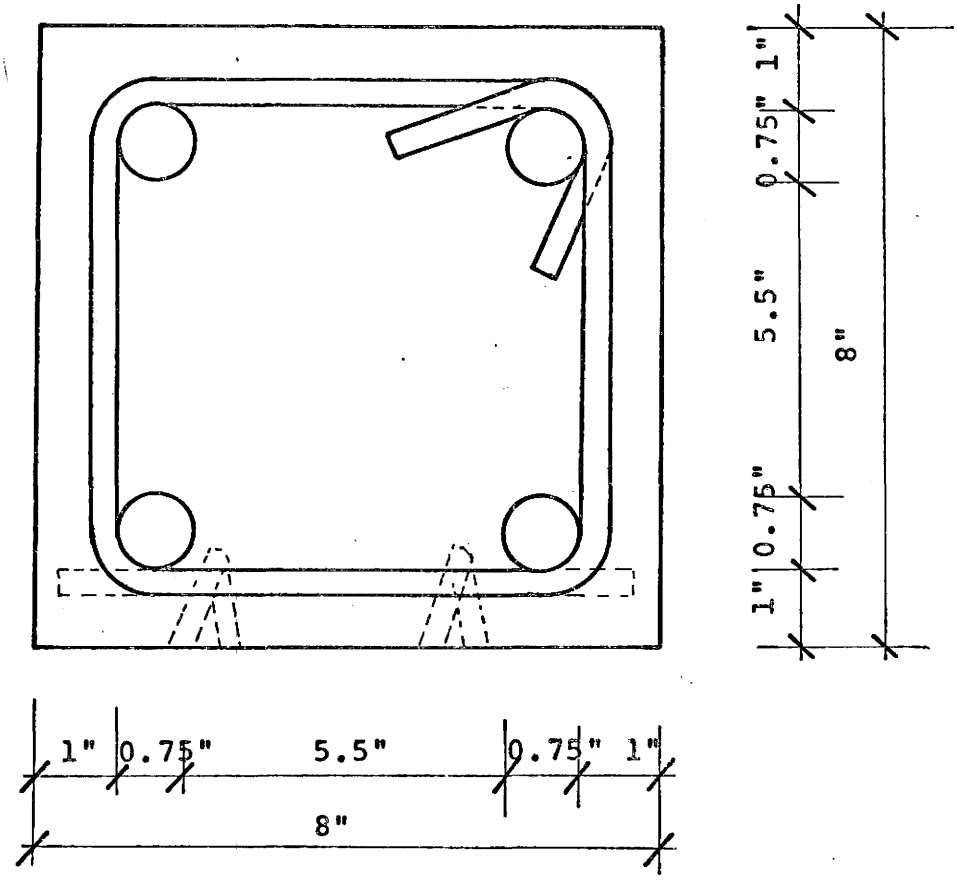

a, Typical cross-section.

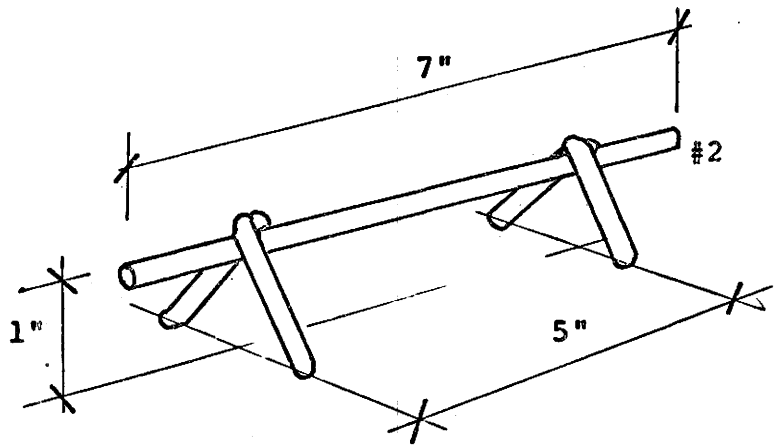

b, Spacing chair.

Fig. 3.3. Reinforcing steel details.

In the case of frame model BF-1, two shrinkage prisms were cast to obtain approximately the value of shrinkage.

Cylinder tests were performed at seven, fourteen and twenty-eight days and at the conclusion of testing for shakedown load test, which lasted several days. Concrete stress-strain relationships obtained from cylinder tests are shown in Figure 3.4.

The behavior of the reinforcing steel under uniaxial tension was ideally elastic-plastic up to a strain of 0.005. Subsequent strain hardening caused the stress to increase with strain. The stress-strain relationship obtained from tensile tests of reinforcing bars is shown in Figure 3.5.

Local heating with an acetylene torch was used in bending the longitudinal steel for the first case (frame model BF-1). This process was accomplished by gripping a section with two pipe wrenches and then turning one wrench relative to the other to produce a 90 degree corner. Because of a brittle failure of the reinforcement during the first frame test, a number of tensile tests on the reinforcement subjected to various degrees of heat treatment were performed.

It was concluded that the heat treatment used in bending the bars for the cage did not likely affect the strength of the steel or its behavior alone. The deformation caused by bending around a small radius in combination with the heating process could have produced micro-cracks on the tension side of the corner. This condition was probably the cause of the failure in the first test frame.

From the heat treated tensile specimen the yield strength of the reinforcing steel was found to be 59,800 ± 500 psi and the ultimate tensile strength was found 109,500 ± 700 psi. A series of bars

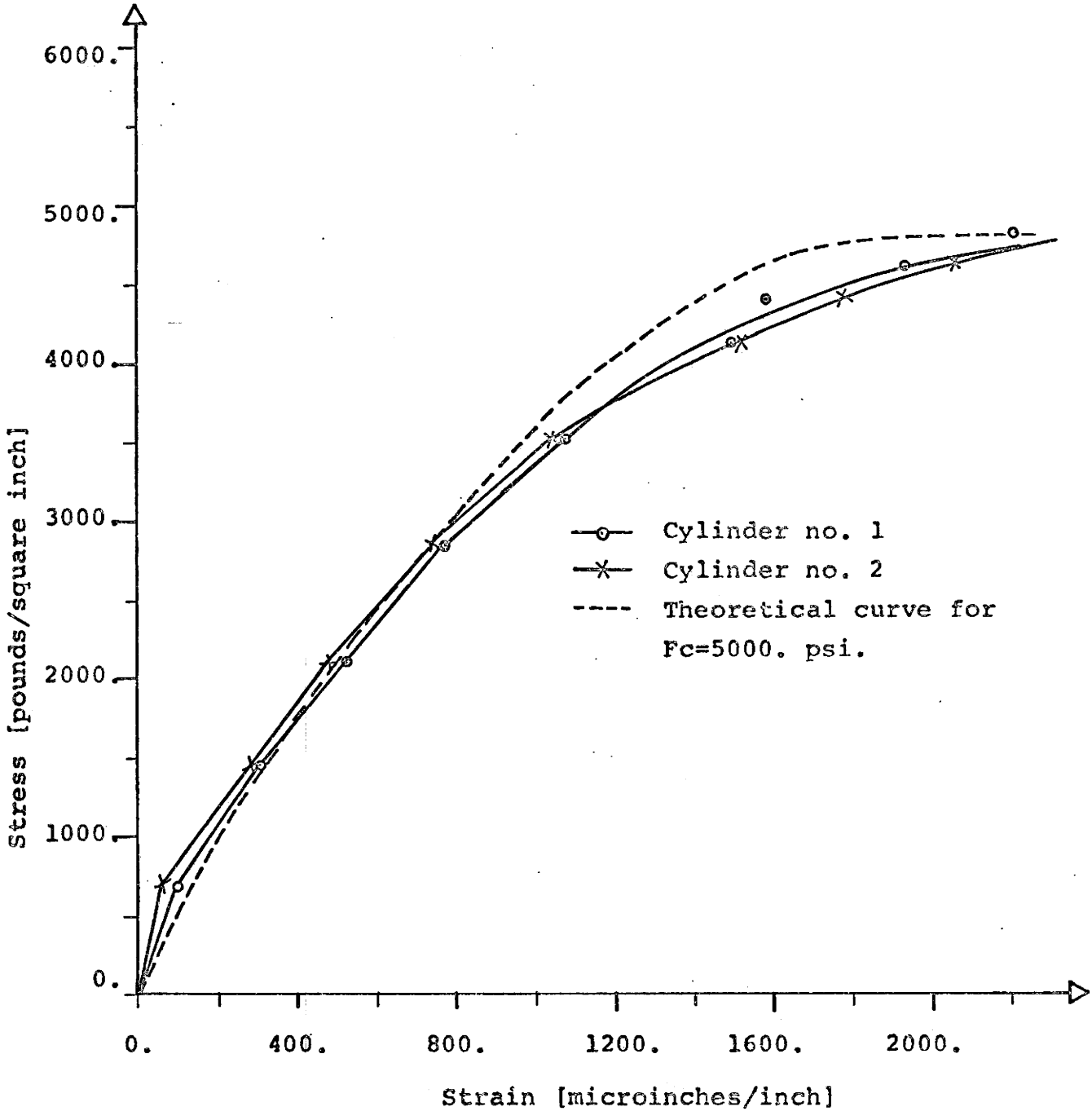

Fig. 3.4. Concrete stress-strain relationship.

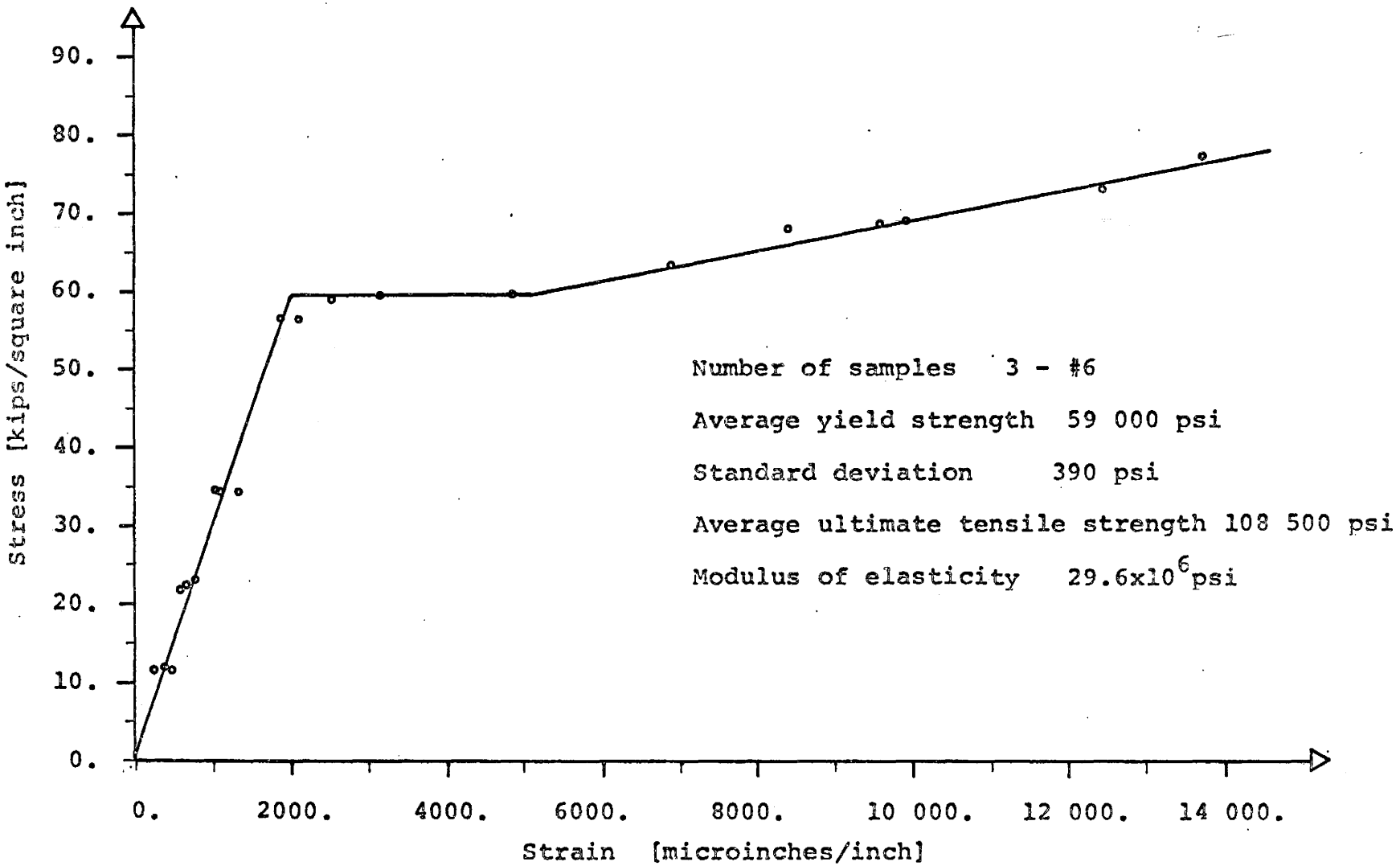

Fig. 3.5. Stress-strain relationship for reinforcing steel.

were bent to a radius of about 2" and then straightened by heat treatment by procedure similar to that mentioned for longitudinal reinforcement. Tensile tests on some of these produce strengths close to those above, while others fractured at considerably lower stress levels. By observation of the bent part of the specimen the presence of a crack was observed which led to the conclusion mentioned above.

Further, tensile tests were performed in order to determine the yield strength, ultimate strength, and modulus of elasticity of non heat-treated number six bars. Testing procedure as well as test results were described by R. Danielsen (23) in his thesis. Thus, obtained value of yield strength were 59,000 ± 500. psi, ultimate strength 108,500 ± 1700 psi and modulus of elasticity (29.6 ± 0.6) x 10^6 psi.

3.4 Gross Behavior

The cross-section, which was the same for columns and for the beams, is shown in Figure 3.3,a. The size 8 x 8 inches was the same for all test models. The symmetrical four number six bars were covered by one inch concrete and were placed in the same position in cross-sections throughout the whole model.

With 1.66 percentage of reinforcement this cross-section was under reinforced as recommended by limit analysis.

By using the method of ultimate strength design (25) the ultimate moment of this cross-section could be calculated as follows:

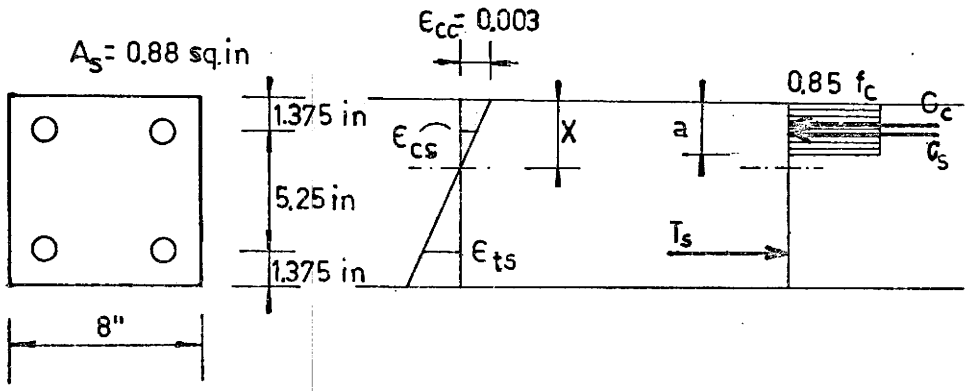

Fig. 3.6. ULTIMATE STRENGTH CONDITION FOR CROSS-SECTION

$k_1 = 0.85 - 0.05 \frac{(f'_c - 4000)}{1000} = 0.8075$ for $f_c = 4850$ psi

$a = k_1 X$

$C_c = 26.6 X - 4.26$

$C_s = 7.8 - \frac{10.75}{X}$

$T_s = 52.7$ KIPS for $f_s = 60$ ksi

$T_s = C_s + C_c$

$X = \begin{cases} 2.043 \text{ in} \\ -0.197 \text{ in} \end{cases}$

THEN

$C_s = 2.54$ KIPS $C_c = 49.94$ KIPS

ULTIMATE MOMENT CALCULATED TO POINT "A"

$M_u = 303.9$ (IN-KIPS). The reader is referred to Fig. 3.6.

Even this preliminary calculation gave fairly accurate results of plastic moment values. A morerealistic approach for obtaining the plastic moment value is when the stress distribution is considered as a function of strain. This approach is mentioned in Section 2.3 and a computer method of calculation is described in Chapter VII.

As the plastic moment, the value of moment transferred by the cross-section when compression strain reached the ultimate strain 0.003 was assumed. The effect of strain hardening was not considered and was not investigated.

Due to the present ACI code the modulus of elasticity for concrete was assumed as follows:

$Ec = W^{1.5} \times 33 \sqrt{f'_c}$ for W = 145 lb/sq.ft.

and f_c = 4850 lb/sq.in.

$Ec = 145^{1.5} \times 33 \sqrt{4850}$ = 4000 kips / sq. in.

The moment of inertia of section was calculated for a cracked section, as follows:

$$m = \frac{Es}{Ec} = \frac{29.0 \times 10^6}{4.0 \times 10^6} = 7.24$$

A_c = 2.043 x 8 = 16.35 sq. in.

A_{cs} = 0.88 (m - 1) = 5.49 sq. in.

Ats = 0.88 x m = 6.37 sq. in.

$A_{w.s}$ = 28.21 sq. in.

$$X = \frac{16.35\ (6.625 - 1.0215) + 5.25 \times 5.49}{28.21} = 4.26 \text{ in.}$$

$$I = \frac{1}{12} \times 8 \times 2.043^3 + 16.35 \times 1.3435^2 + 5.49 \times 0.99^2 + 6.37 \times 4.26^2 = 150.63 \text{ in.}^4$$

Ec is modulus of elasticity for concrete

W is the density of concrete

f'_c is the ultimate stress of concrete

Es is modulus of elasticity for reinforcing steel

A_c is area of compression part of concrete

A_{cs} is transform area of compression steel

Ats is transform area of tension steel

X is the distance between centroid of cracked cross-section and centroid of tension steel

A_{ws} is transformed area of whole cracked cross-section

I is moment of inertia of cracked cross-section

Chapter 4

FABRICATION

In this chapter the test frame and test column specimen are described in detail including the method of fabrication.

4.1 Test Frame and Test Column Details.

The full scale models as shown in Figure 3.2 were fabricated in the laboratory by using available laboratory equipment.

Longitudinal reinforcement consisted of four number six bars bent in the corners to a radius of 5.5 inches and welded to steel end bases. The number two bars were used as stirrups and were tied to the longitudinal reinforcement to hold reinforcing bars in the correct position in the section. A typical cross-section is shown in Figure 3.3,a.

In order to stiffen the corners, additional reinforcement was placed in the corners as shown in Figure 4.1. Number four bars were used for this purpose and they were placed in the plane of the longitudinal reinforcement in the case of frame BF-1 as shown in Figs. 4.1, a, b, c and Figure 4.2 and 4.3, For the remaining frames the corner reinforcement was placed approximately the same way as shown in Figure 4.1, d, e and f. These bars were tied by wires to the longitudinal reinforcement and formed an integral unit with the cage.

The end bases were made of eight inch deep wideflange steel sections. In the case of test column C-1 the end base used is shown in Figure 16a. This type of end base was redesigned and additional reinforcement was welded onto the flanges and to the wall of the wideflange section as

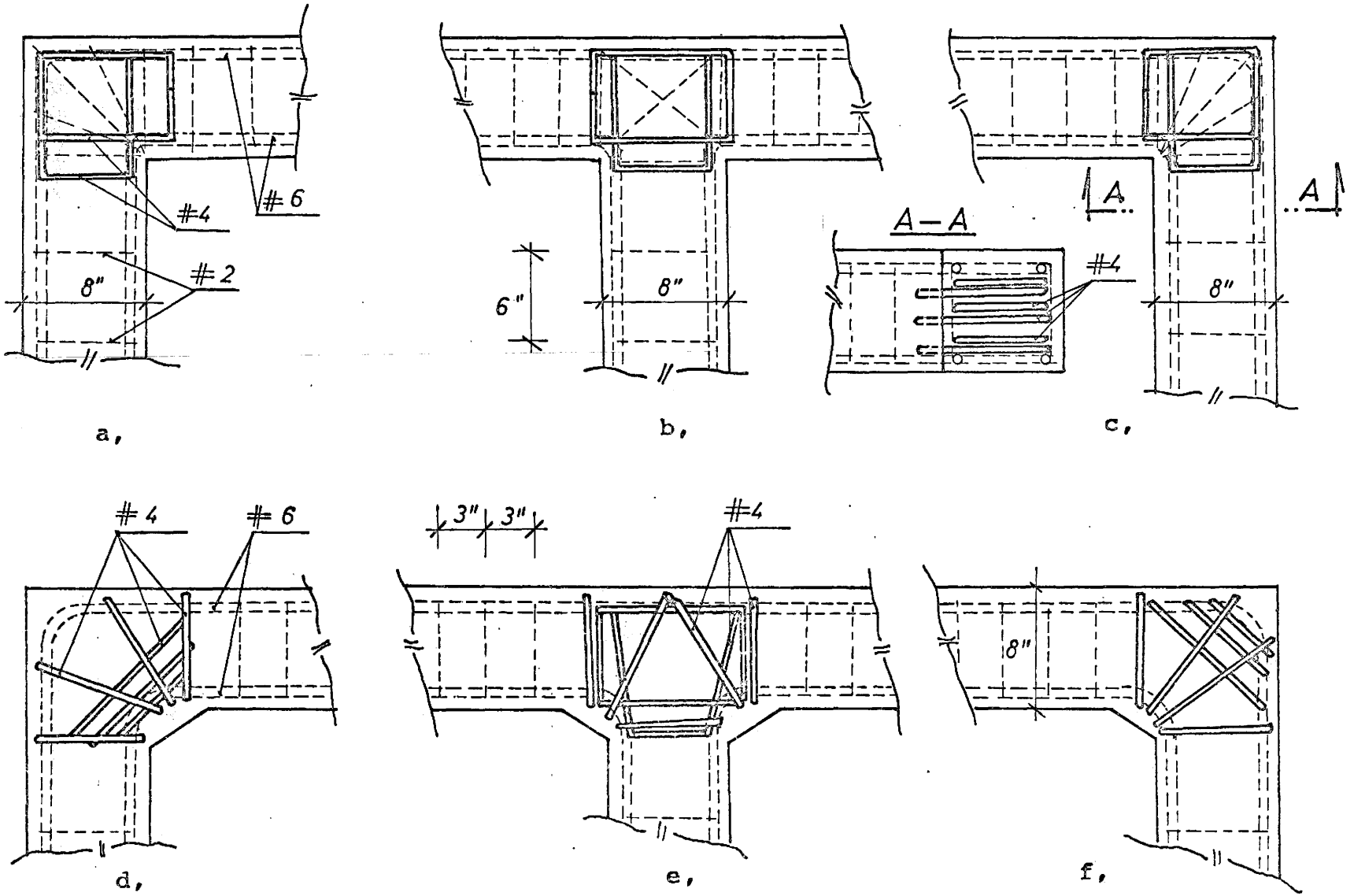

Fig. 4.1. Additional reinforcement of frame corners.

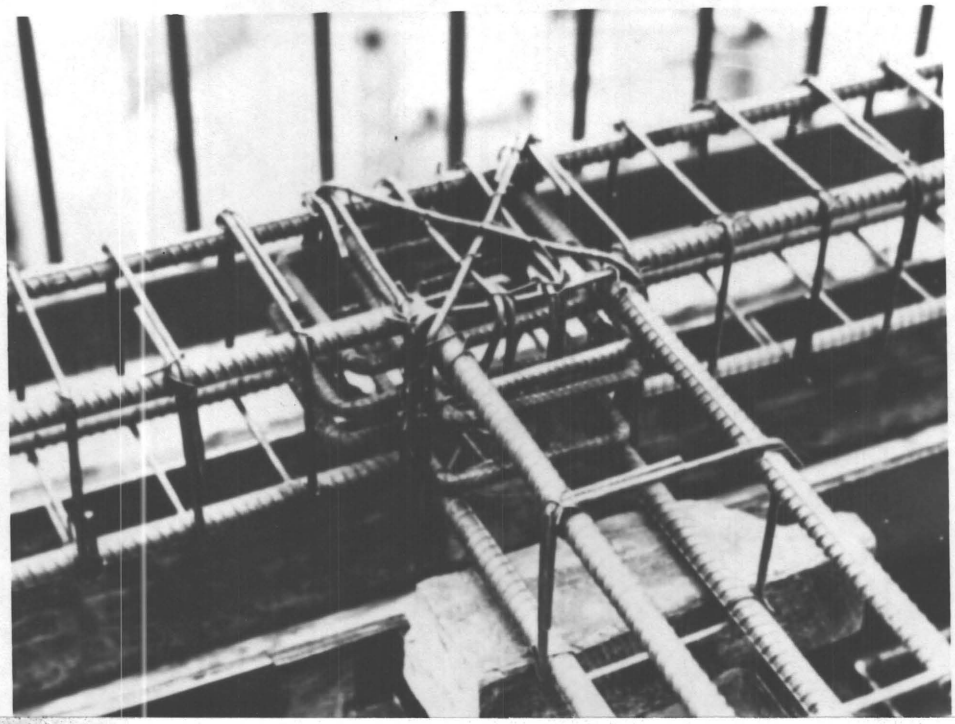

Fig. 4.2 Cage of Frame BF-1, Middle Joint.

Fig. 4.3 Cage of Frame BF-1, Right-hand Corner.

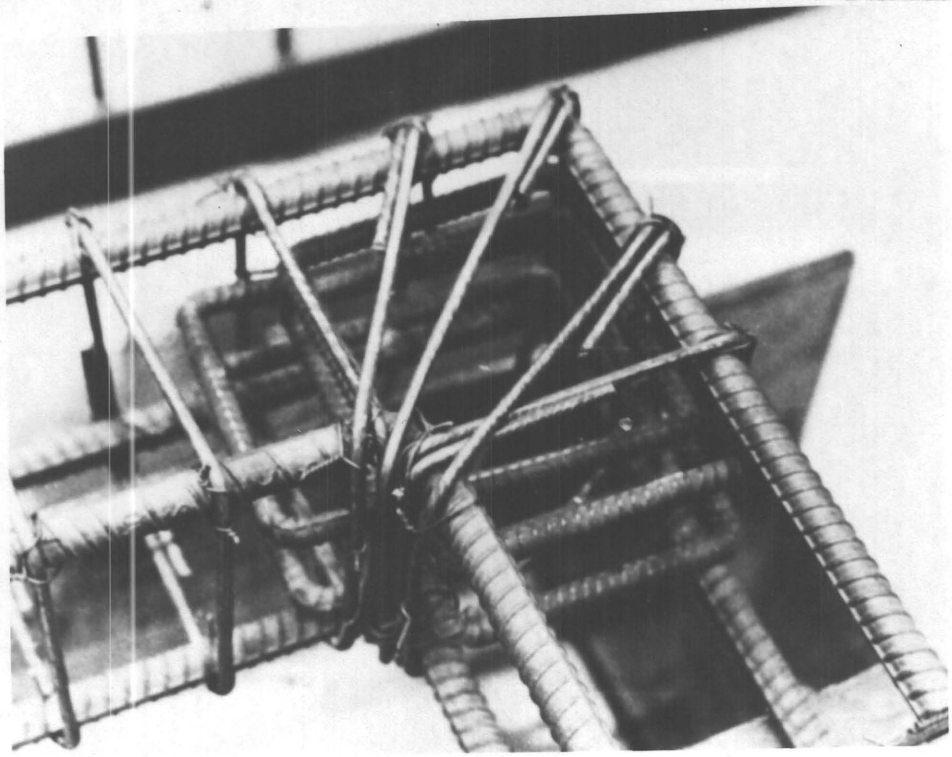

illustrated in Figure 4.4 and 4.5. Also, the longitudinal reinforcement connection with the end base was improved by welding it to both sides of the wall of the wideflange section. In the case of frame BF-4 the longitudinal reinforcing bars were welded also to the thick steel plate of lower base as shown by the dotted line in Figure 4.4,b.

For the test column the same type of reinforcement and the same end bases were used as for the test frame.

4.2 Form Details

The forms for casting were constructed of 9 x 4 x 1/2 inch angles bolted to a 24 x 1/2 inch plate below. Numerous hole regimes were drilled in the plate to allow casting of frames of different cross-sections. The sections could vary from four to sixteen inches in depth with increments of 1/2 inch. The width of the section could vary continuously up to nine inches and independent of the depth.

The steel form also provided durability, strength and accuracy. The allowable dimensional tolerance was 1/8 inch.

Each part of the form was light enough that it could be handled by two men. It could be easily cleaned and produced a smooth surface on the concrete. The shape of the form and cage is shown in Figure 4.6 and in Figure 4.7.

4.3 Cage Assembly

The cage fabrication and setting it into the form for pouring concrete involved approximately the work of two men for one week. The procedure of fabrication was, in general, that described below.

The longitudinal reinforcing number six bars were cold bent around five inch diameter pipe to the required shape. The stirrups,

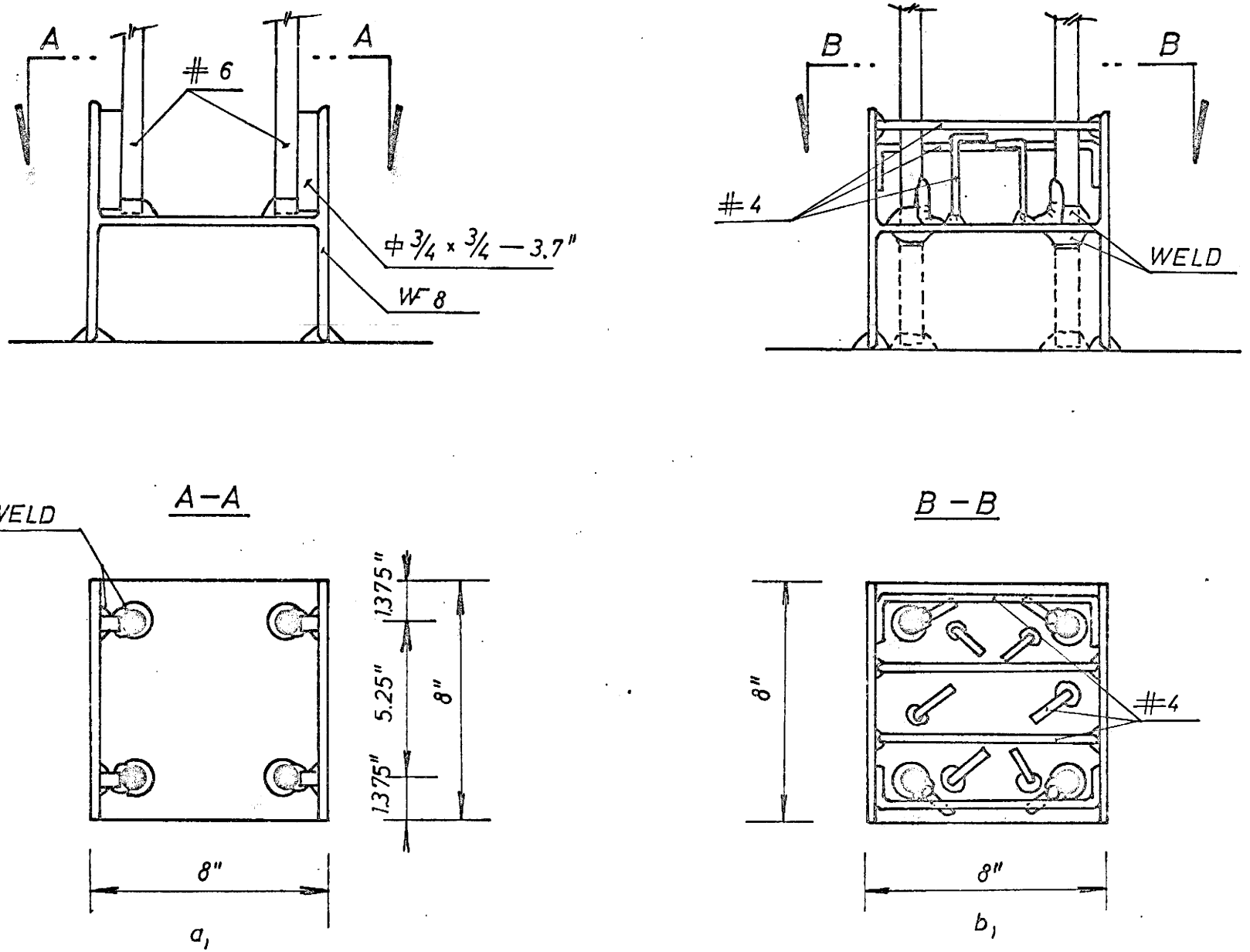

Fig. 4.4. Steel bases of the frame columns.

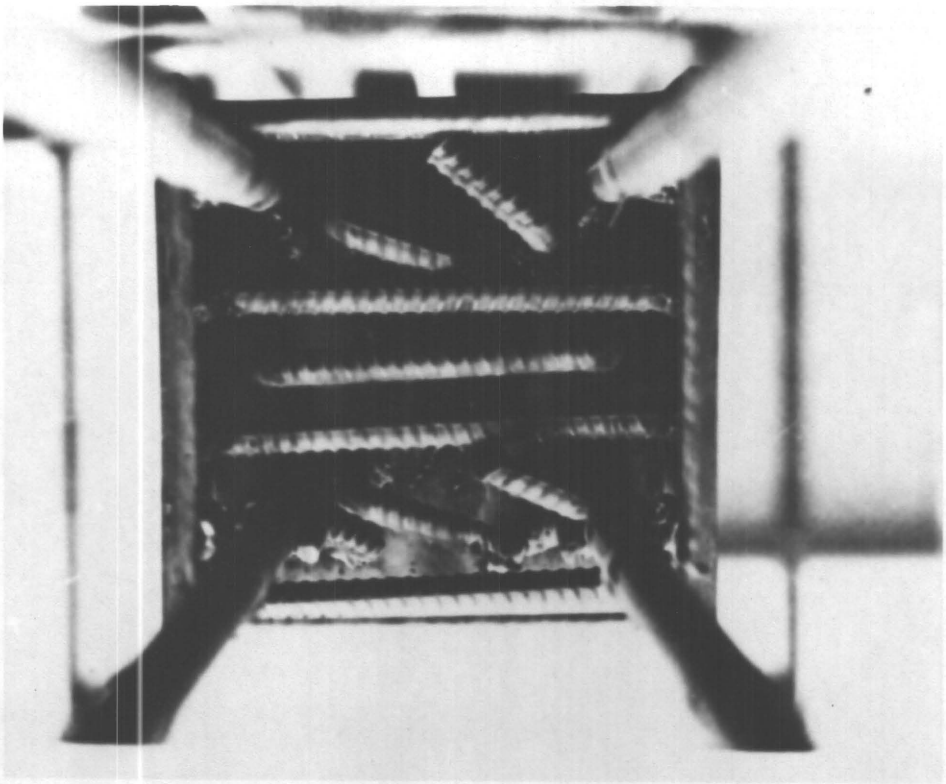

Fig. 4.5 Inside and Side View at Base Reinforcement.

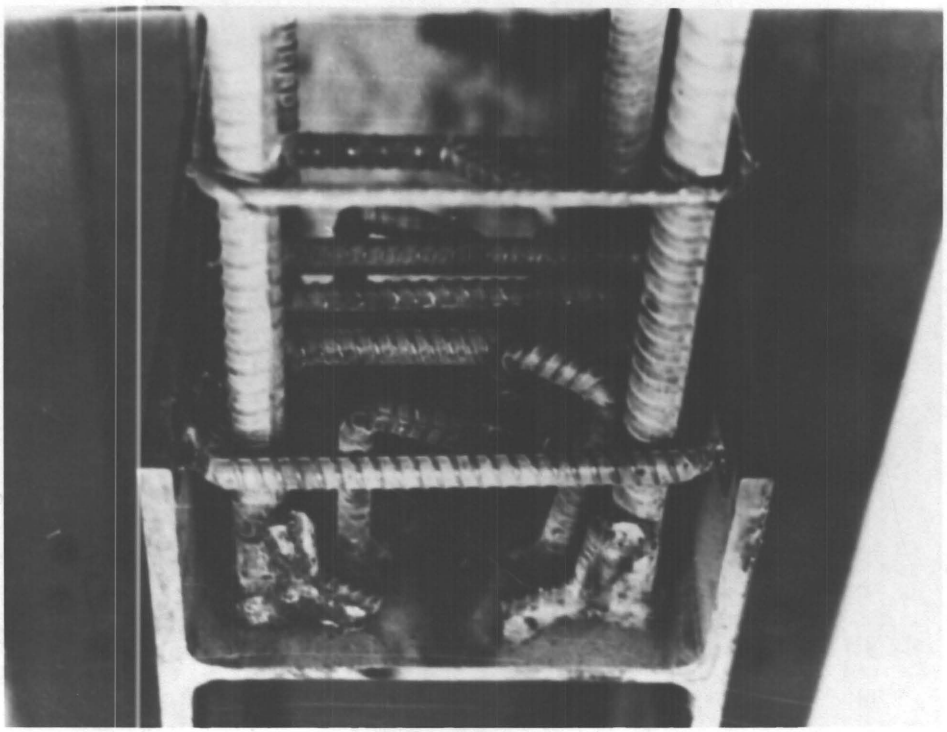

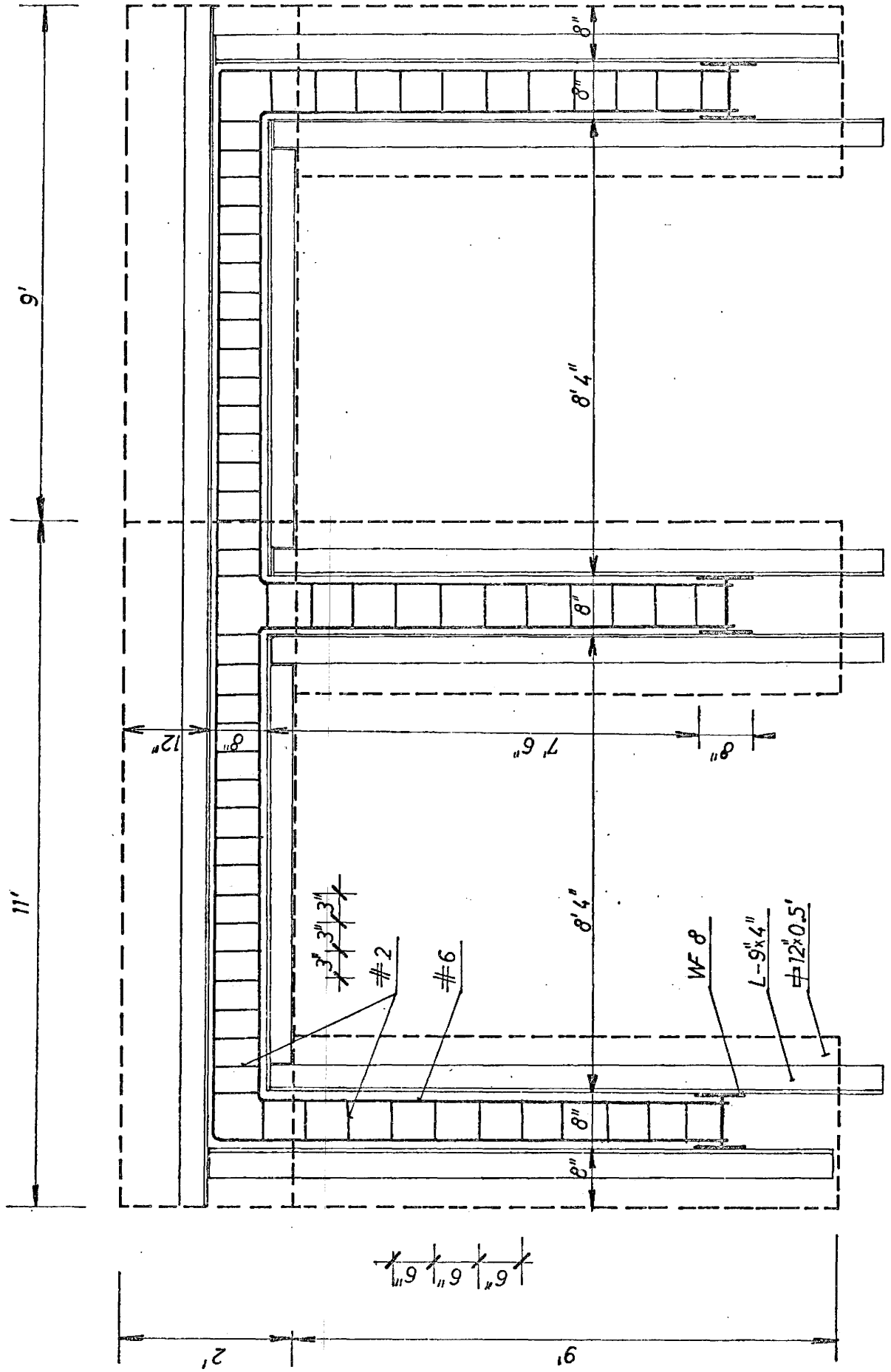

Fig. 4.6. Form and cage.

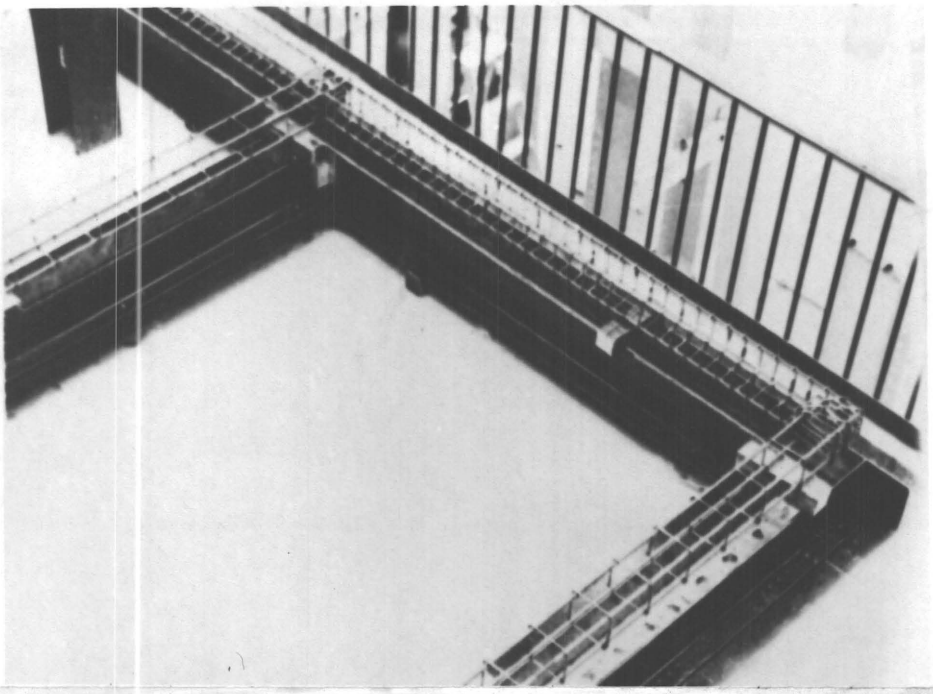

Fig. 4.7 Cage (Frame BF-1) and the Form.

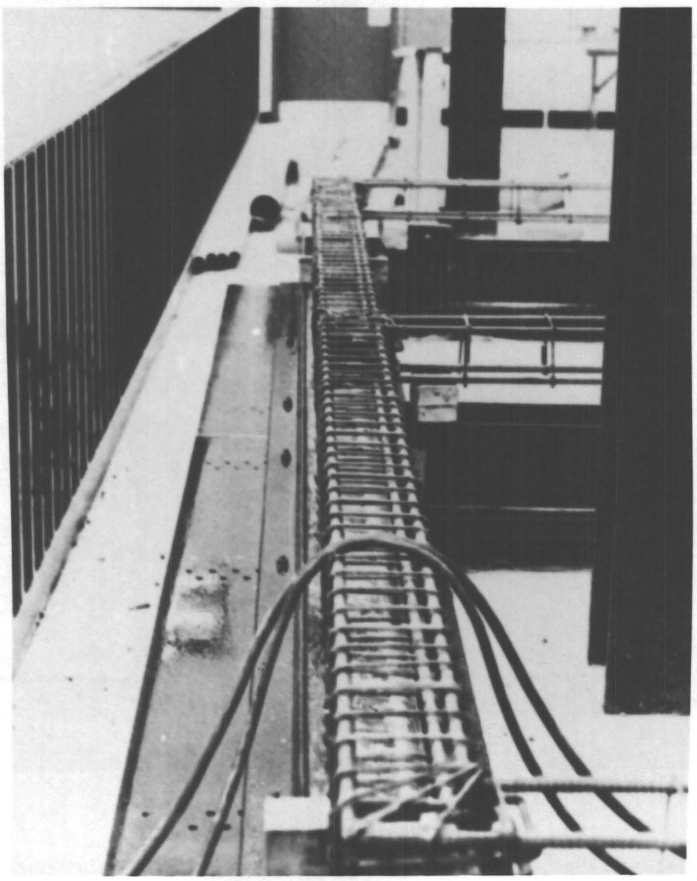

made of 30 inches long number two bars were bent on special bar bending rig designed for this purpose. With the help of plywood templates inserted inside the longitudinal bars the shape of the cross-section was held. Wire ties were used to fasten the stirrups to the longitudinal reinforcement. The additional reinforcement of corners was made and ties to the proper position in the corners.

The cage was strong enough to be handled as a unit and could be carried by the laboratory crane to the form.

Special spacing chairs shown on Figure 2.4,b were used for holding the cage in the proper position in the form.

After correcting the position of the cage in the form the end bases were situated in the correct position and welded onto the longitudinal reinforcing bars. When this was done, the cage was ready for pouring the concrete.

4.4 Concrete Requirement

For making a smooth surface of concrete the form was treated with oil which also made it easier to take the form apart.

The concrete components were prepared by weight and mixed in a horizontal drum mixer in batches of six cubic feet. The concrete mix was used as shown in Table 4.1. A slump of 2.5 to 3.5 inches was sought.

By using the horizontal crane in the laboratory the concrete mix was carried to the form and transferred by shovel. By using an electric vibrating machine concrete was vibrated by the usual procedure. The concrete was allowed to set in the form for one hour before surface finishing. The sides of the form were removed after about twenty-four

hours after pouring. The concrete frame or column and cylinders were then moist cured on the casting bed using damp burlap for seven days before being moved to the test areas.

Twelve cylinders were cast with each frame and they were performed after seven, fourteen and twenty-eight days.

TABLE 4.1: CONCRETE MIX DATA

COMPONENT	PERCENT BY WT.	WT. PER BATCH (LB)
Portland Cement Type I	14.0	127.4
Water	9.1	82.6
Fine aggregate (washed pit run sand, fineness modulus - 2.51)	46.6	424.0
Course aggregate (3/8 inch maximum size crushed limestone)	30.3	275.5
	100.0	909.5

Slump for standard 12 inch high slump cone - 2½"

Volume per batch - 6.0 cubic feet (approx.)

Chapter 5

INSTRUMENTATION AND PROCEDURE OF TESTS

5.1 Instrumentation of Tests

Various types of instrumentation were used in performing the tests. Load cells were used for measuring loads, dial gauges for measuring deflection and demac point gauges for measuring strain data across concrete sections. To obtain reaction forces a special type of base was designed. Similar test equipment was used for all tests. The components are described in more detail in this section.

The rigid bases were originally designed so that the reactions could be measured using electric resistance strain gauges. These bases were stiff enough to resist significant motion of the concrete column bases while undergoing adequate straining so that the reactions could be determined to a reasonable degree of accuracy. This type of base is shown in Figure 5.1. Horizontal strain was registered by a cantilevered section held rigidly at one end and supported on rollers along its length. A hollow steel cross-section was used for this purpose with electric resistance strain gauges having been mounted on the outside face of section as shown. Vertical strain was registered by electric resistance strain gauges mounted on outside of flanges of column steel end bases. Because of problems which occured during the test of frame BF-1, as described in Section 6.2.1, the strain measuring part of bases were omitted in subsequent tests. The concrete column end bases were welded directly to the one inch thick plate of lower bases as shown in Figure 5.2 and Figure 5.4. The lower base plate was stiffened with eight inch channel sections. The entire assembly was bolted to the test floor using 2 5/8 inch

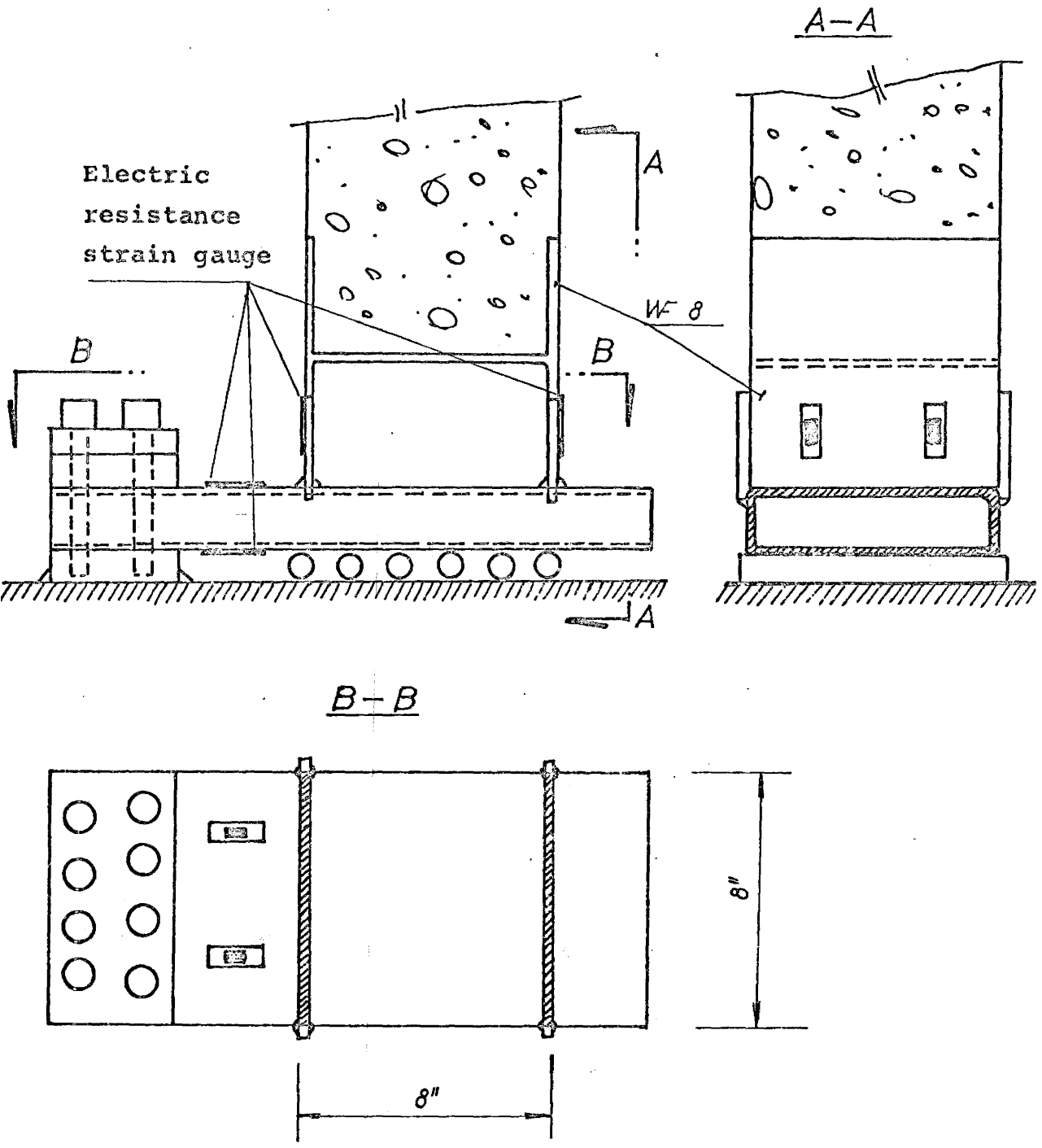

Fig. 5.1. Base of column with electric resistance strain gauges for measuring reactions of frame bases.

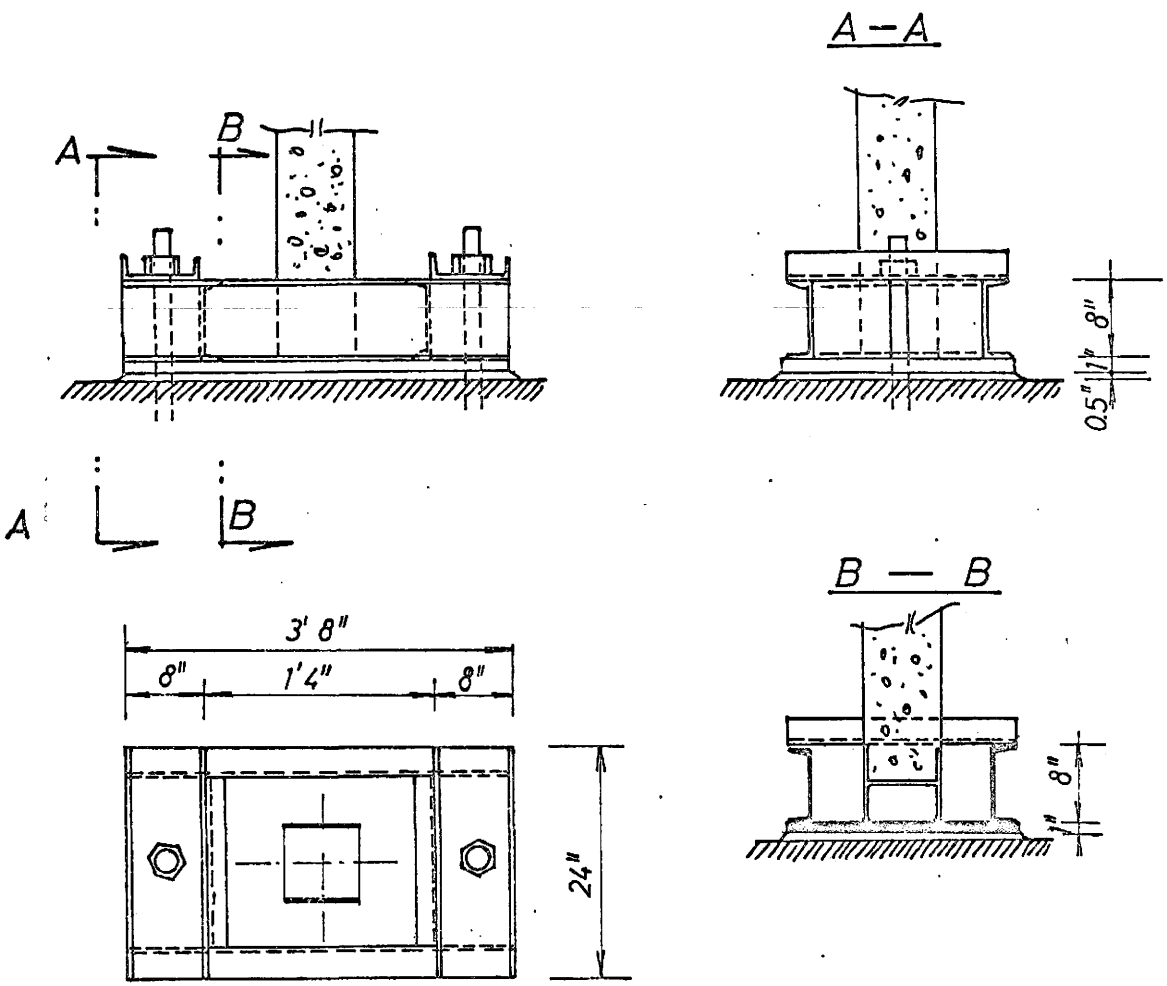

Fig. 5.2. Base of the column.

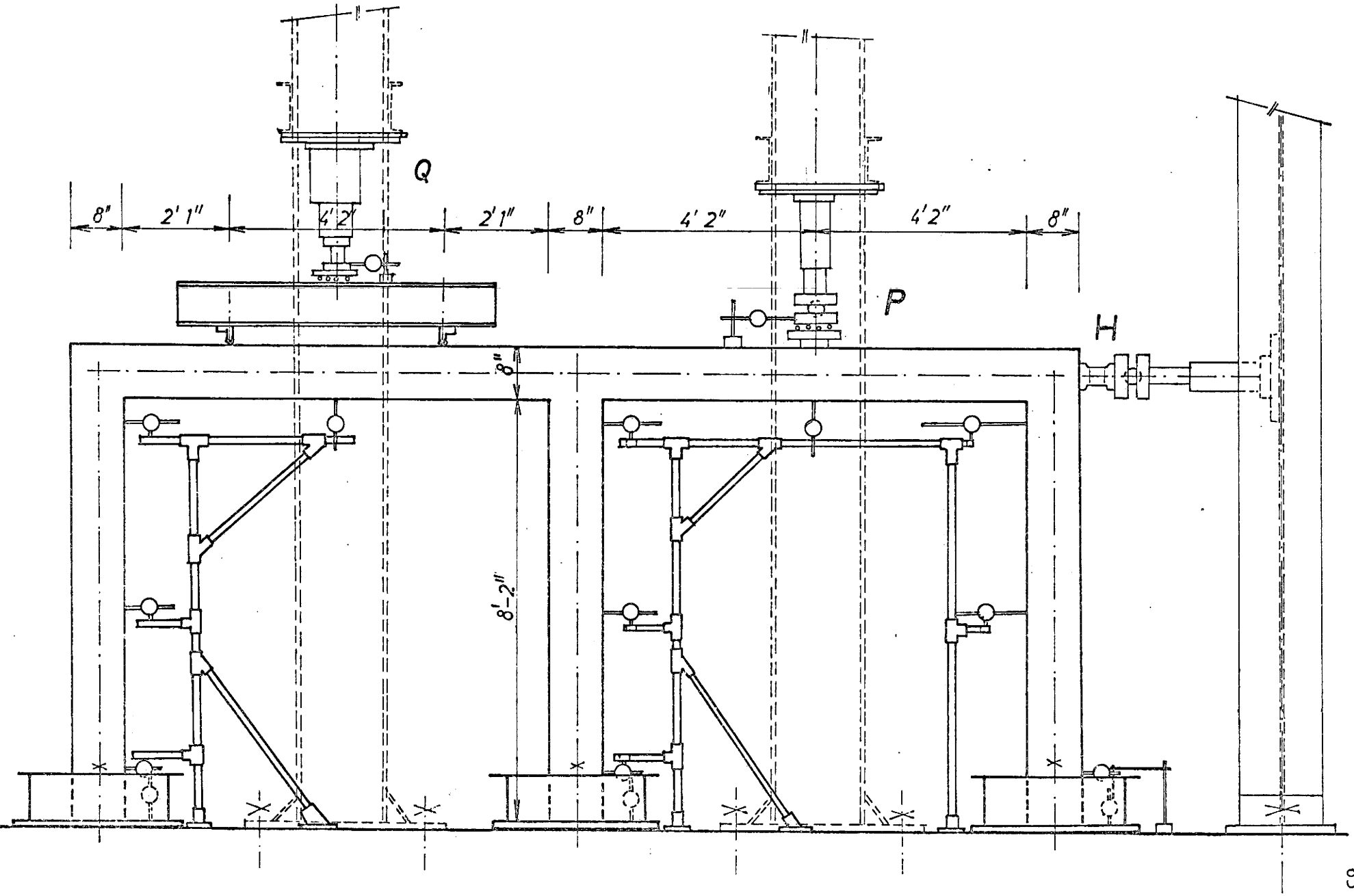

Fig. 5.3. Loading system and dial gauge positions

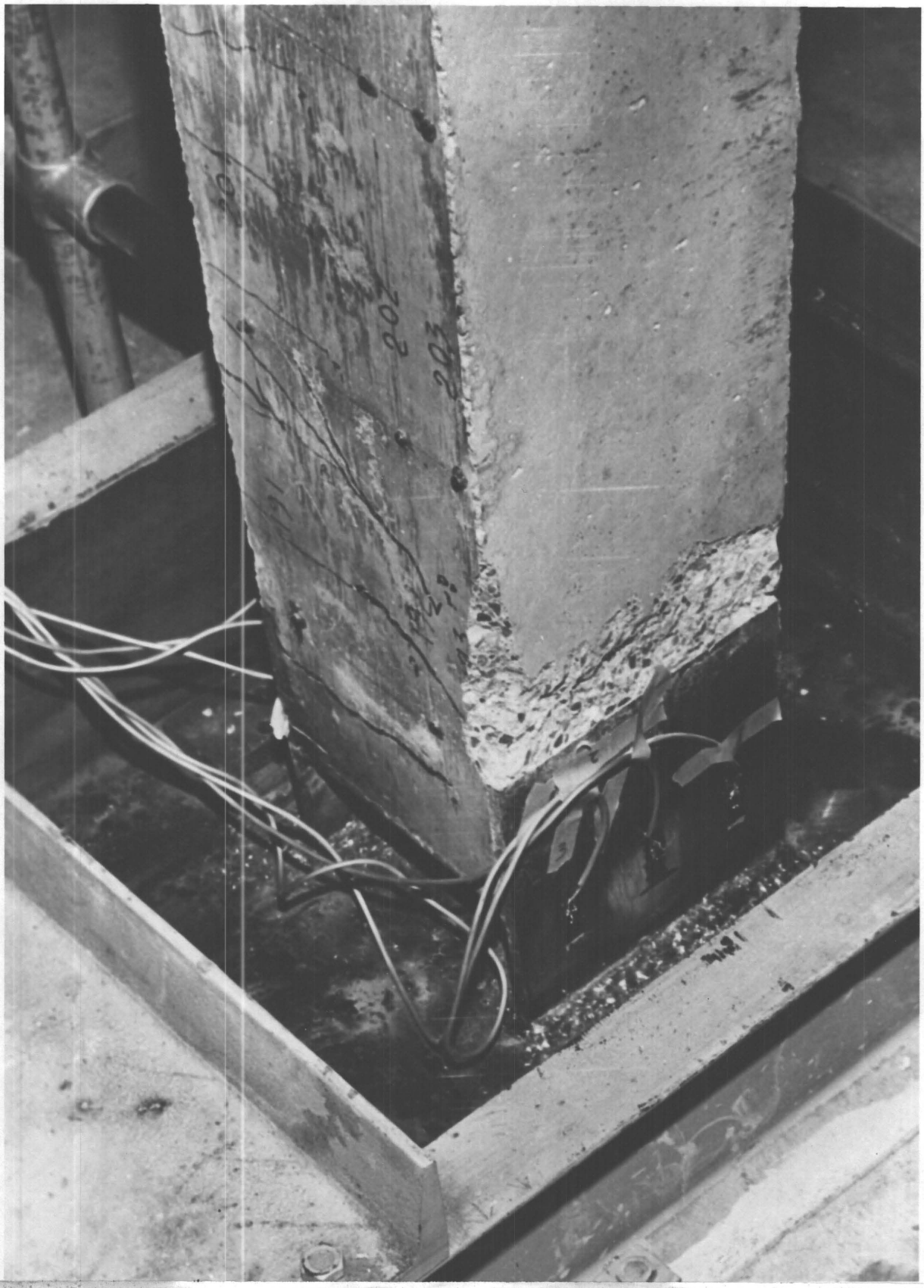

Fig. 5.4 Typical Base Connection

diameter anchor bolts which were prestressed up to sixty kips.

A common type of dial gauge was used for measuring deflection during the tests. The dial gauges with scale divisions of 0.001" and extensions varying from two to four inches were used for recording deflections of columns or beams. For deflection of the bases the dial gauges which could be read to within 0.0001" and extensions varying from 0.4" to one inch were used. The position of the dial gauges is shown in Figure 5.3. As is shown an auxiliary frame of pipes was built for supporting the dial gauges. Bases of this frame were glued on the test floor.

For measuring strain in concrete a demac point gauge was used. The length of the demac point gauge was eight inches with an accuracy of reading about 5 microinches which is one-half a division. The gauge points were made of ¼ inch diameter brass discs drilled with a number 60 centre hole. Using epoxy cement the gauge points were placed for two gauge zone on each place where the peak moments were expected. A typical position of gauge points is shown in Figure 6.6.

Several types of load cell were used for measuring loads. A spool-shaped steel cylinder was used for this purpose by measuring strain changes under different loads. Four electric resistance strain gauges, two horizontal and two vertical, were mounted on the outside surface of the load cells and were wired to a full Wheatstone bridge circuit. Readings of strain were made through a switch and balance unit and Budd Model B-350 strain indicator. The strain gauges were protected by a wax coating. The size of load cells was such to provide full required loads in the elastic strain range. The strain readings were usually in range from 300

to 800 microinches. The type of load cell is shown in Figure 5.5. The piston of the hydraulic jack used to apply load acted in one case as the load cell. Electric resistance strain gauges were mounted directly to its surface. This load cell is shown in Figure 5.6.

Before and after each test and even sometimes during a test the load cells were calibrated in a Tinius-Olsen universal testing machine. Calibration consisted of recording a strain reading under certain increments of loads. After obtaining several agreeable readings for the same load, the load cells were ready for use. After calibration the wires were not disconnected until after a test and recalibration was over. This gave a satisfactory check for values of loads.

Manually operated jacks were used for applying loads. By using a mechanical slide system the position of the vertical loads could be easily corrected during the loading accordingly to the deflection. Photographs pictures of vertical jacks are shown in Figure 5.5 and Figure 5.6. The jacks with a mechanical slide system were mounted on fourteen inch wideflange steel columns placed around the test frame. Column bases were fixed to the test floor by two 2 5/8 inch diameter anchor bolts prestressed up to sixty kips. Ball joints and roller bearings were used for transferring forces from the jacks into the test specimen and therefore no additional forces caused by movement of the structure were involved. An overall test set up is shown in Figure 5.7.

5.2 Proportional Loading Case

Two test frames were tested under proportionally increasing loads. The relative values of the loads and their positions were determined by plastic analysis as mentioned in Chapter II. When W is a plastic

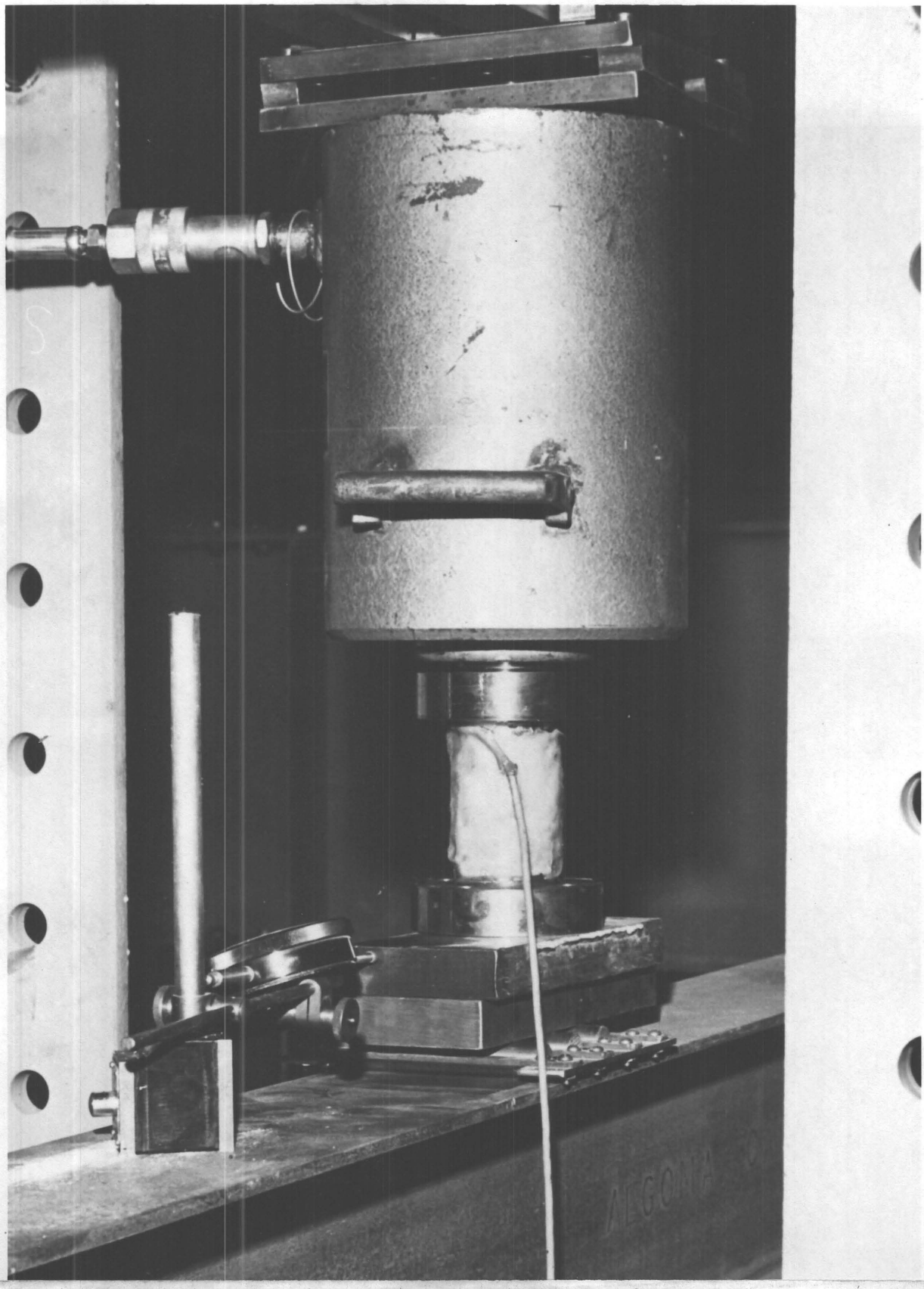

Fig. 5.5 Loading System for Two-point Load.

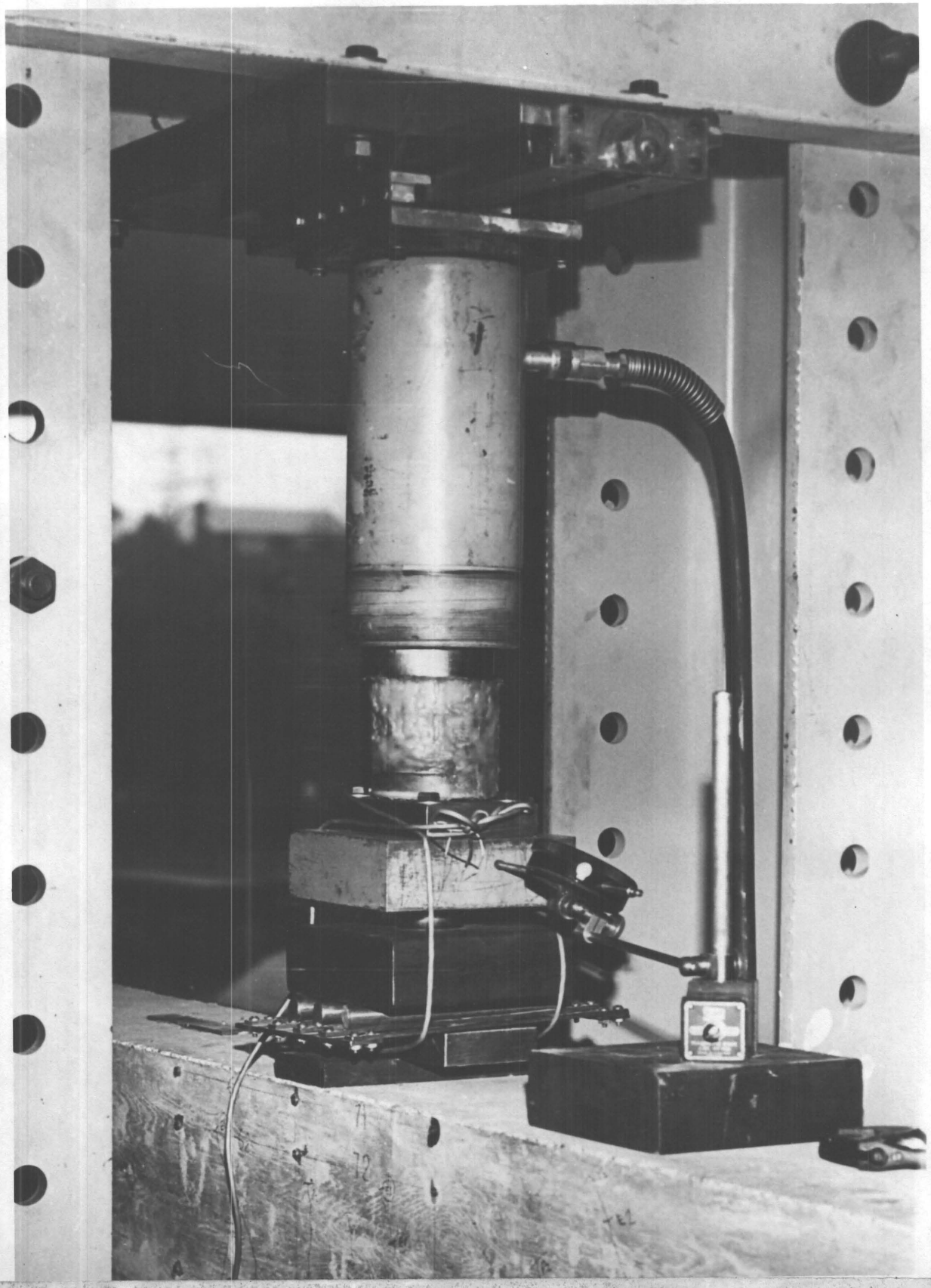

Fig. 5.6 Loading System for One-point Load.

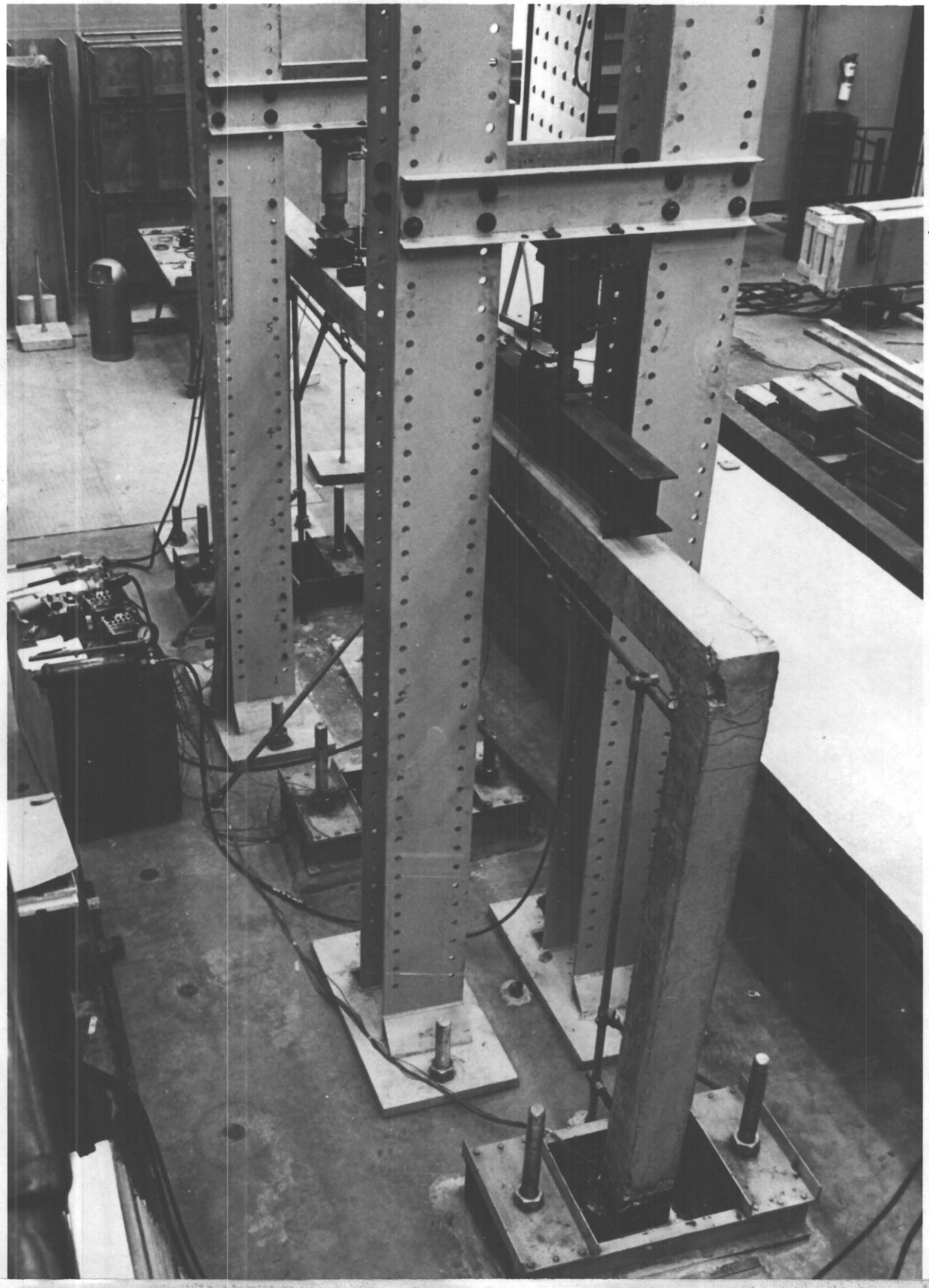

Fig. 5.7 Overall Test Set-up.

collapse load parameter of the frame the relative values of loads are 3W for horizontal load, 2W for vertical load in the middle of the first beam and 3.5W for vertical two point loading on the second beam.

In general, preparations for testing involved several necessary operations which were performed as follows:

a) the frame was moved into the test area by crane and was positioned onto bases. After the frame was correctly positioned it was fixed between the steel columns projecting above the laboratory floor and welding took place.

b) During welding of the bases the demac point gauges were glued onto and the loading system was mounted.

c) An auxilliary frame for carrying the dial gauges was built. The dial gauges were then positioned and after marking gauge zones the specimen was ready for testing.

A plastic collapse load test of the frame was performed by proportionally increasing loads up to the stage when the frame collapsed. Collapse was defined as inability to carry applied loads while the deflection was increasing disproportionally.

All demac and dial gauge readings were recorded after each load increment. The load increments were chosen in advance so that several readings were made in the elastic range of behavior to obtain data for moment distribution. The remaining readings were made in the range of load values when plastic moment redistribution was taking place.

The position of the vertical loads was corrected simultaneously with deflection by turning the bolts of the mechanical slide system. The crack formation was recorded and marked on the frame as well as other general observations.

5.3 Program of Loading for Incremental Collapse Case

According to incremental collapse theory the relative values of maximum and minimum loads applied to a structure must be specified. In terms of parameter W, these were as follows:

a) horizontal load $3W \geq H \geq 0$

b) vertical load $2W \geq P \geq 0$

c) vertical load $3.5W \geq Q \geq 0$

Any sequence of loading or any combination of loads is permitted since all three loads H, P and Q are assumed to be independent (see Section 2.4).

With respect to one load cycle the program of loading chosen was one which minimized the number of load combinations in one cycle. Such a combination of loads was considered if the corresponding moment distribution tended to activate hinges of the incremental collapse mechanism yielding the lowest value of W.

In Figure 2.6 all combinations of load

for elastic frame are shown. The numerical value of elastic moment distribution for these load combinations are in Table 2.2.

The anticipated incremental collapse mechanism for the test frame was the sway mechanism with hinges forming at the top and bottom of each column. The sequence of loads which initiate the sway mechanism is given in Figure 2.6. It follows that one cycle of loading was the application of four different loading regimes each of which of is preceded by a zero loading state.

The unloading step in a cycle was assumed to be performed by loads with opposite sign under conditions of purely elastic behavior.

The following steps were involved for one cycle of the test:

1. Horizontal load was applied up to the prescribed value and was then removed.
2. Horizontal and vertical loadings in the first beam were applied proportionally up to prescribed values and were then removed.
3. Horizontal and vertical loads in the second beam were applied proportionally up to prescribed values followed by their unloading.
4. Combinations of all loads proportionally increasing was applied up to prescribed values and the loads were again removed.

The test procedure was similar to that for the proportional loading case described in Section 5.2. Also, the preparation of the test frame and the test apparatus for conducting the experiment was the same as in Section 5.2 and is therefore not described here.

At the beginning of the test each of the loads was applied to the test frame separately by half of the full value to obtain data for the elastic moment distribution. This part of the test was called elastic loading because of the behavior of the frame.

After completing this phase, the cyclic type of loading was performed with full maximum values of the loads.

Readings of dial gauges and demac point gauges were recorded during the most important times.

Chapter 6

TEST PROCEDURE AND TEST RESULTS

6.1.1 Test of Column C-1 and C-2

Two columns were tested with the purpose of obtaining information on the moment-curvature characteristic under repeated loading. The knowledge obtained therefrom could then be used to assess plastic hinge formation for a given cross-section.

The same type of instrumentation as employed in the frame tests was used as described in Section 5.1 including bases and loading system. The test set up is shown in Figure 6.1. Demac point gauges were placed along the length of the column to provide the strain value for different values of moment under the same load.

The horizontal load acting at an eight foot long lever arm was repeatedly applied to various load levels to simulate a typical loading history of the test frame cross-sections.

In case of column test C-1 collapse occurred before the anticipated ultimate load was reached. This was caused by failure of longitudinal reinforcing bars in the tension side of the section close to the connection with the column end base. The photograph of Figure 6.2 was taken after the test following removal of part of the concrete from the critical section. As shown on this picture, the longitudinal bars broke where the welded connection with the end base started which was the place of highest stress concentration. This detail of connection was redesigned and no further failure of this type occurred in the following tests.

The test of column C-2 was more successful and gave valuable information about the moment-curvature characteristic and carrying capacity of the section.

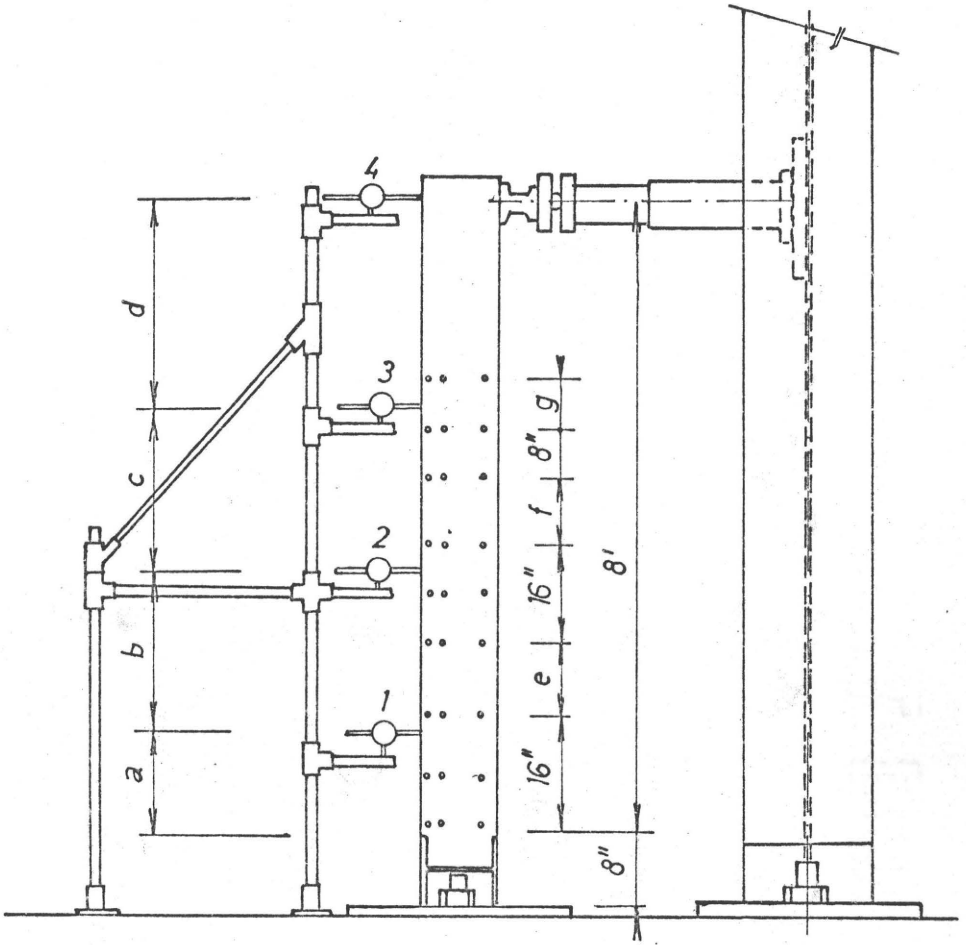

DISTAN. (inch)	COLUMN	
	C-1	C-2
a	31.375	16.0
b	17.0	16.0
c	21.125	36.0
d	21.0	28.0
e	24.0	12.0
f	20.0	12.0
g	0.0	8.0

Fig. 6.1. Test set up for column C-1 and C-2.

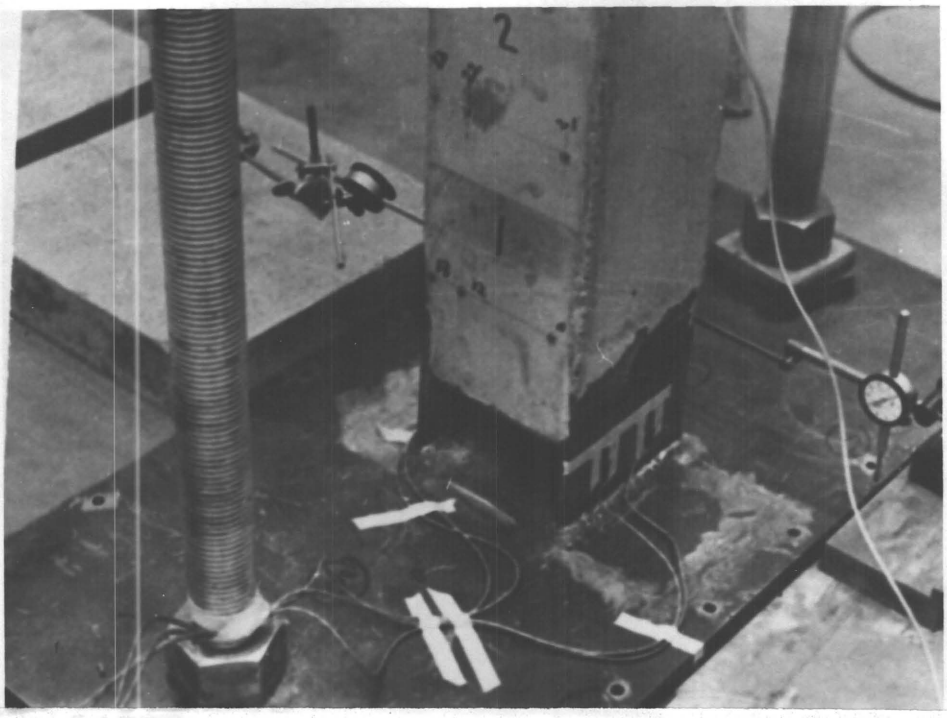

Fig. 6.3 Typical Base Connection of Column Tests.

Fig. 6.2 Broken Longitudinal Reinforcing Bar of Column C-1.

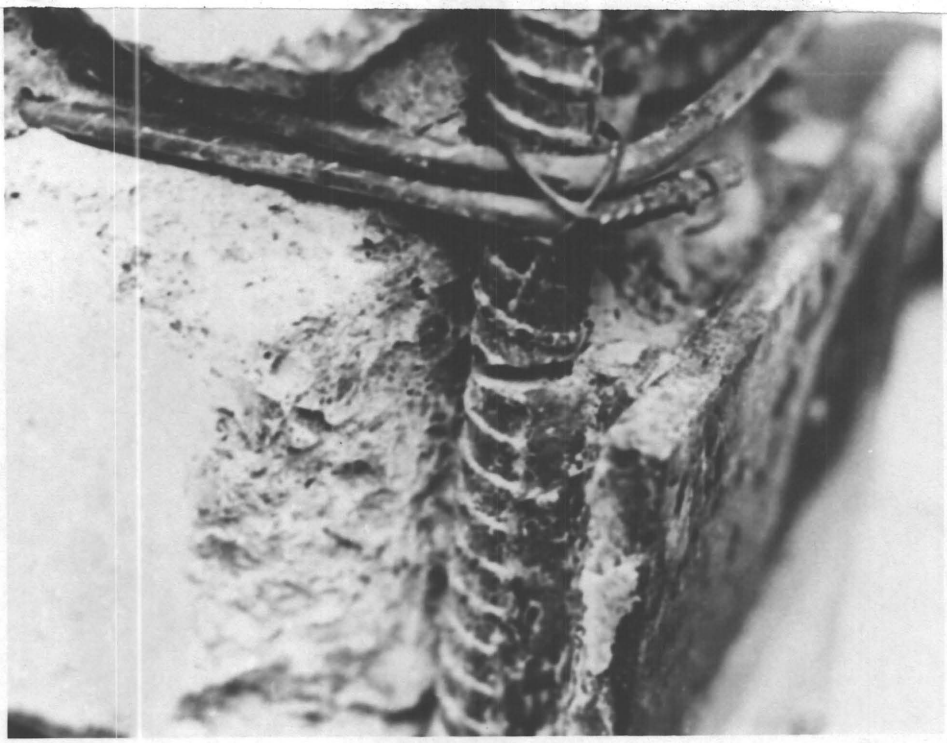

In both cases (column C-1 and C-2) the electric resistance strain gauges were mounted on the outside faces of steel bases. Although the structure is statically determined with known reactions, the strain gauges were mounted with the purpose of checking the method of measuring reaction for the frame tests. The column base with electric resistance strain gauges is shown in the photograph denoted by Figure 6.3. The results of electric resistance strain gauge readings did not satisfy accuracy requirements and were not used for analysis.

6.1.2 Test Results of Column C-2

The results of the test of column C-2 were used for determining the moment-curvature relationship under repeated loading (see Figure 6.4.) for comparison of actual to theoretical moments (see Figure 6.7) and for plotting deflection curves of the column under various loads (see Figures 6.8 and 6.9).

The curvature in the section was calculated due to the strain data obtained from demac gauge readings. The typical gauge zone and a strain distribution is shown on Figure 6.6. The demac points were placed so that in the compression side two strain readings were available while the third reading was in the position of tension steel. Two readings in the compression side (denoted as X_1 and X_2 on Figure 6.6) determined the strain distribution in the section while the strain reading on the tension side (denoted as X_3 on Figure 6.6) due to cracking was neglected. The measured strains were in general attributed for the section in the middle of the gauge zone. The curvature can be then expressed as:

$$\Phi = \frac{X_1 - X_2}{e}$$

where X_1 and X_2 are the strain readings as shown on Figure 6.6 and e is the distance between these two readings. For a typical gauge zone e is 1.625 of an inch.

Because the structure is statically determined the moment values are known and the moment-curvature can be plotted. In Figure 6.4 the curvature versus moment is plotted for gauge zone "0". The plastic hinge formation was observed during the test in the 16th reading (see Table 6.1) that refers to the moment value 307.0 inch-kip at the considered fixed end of the column (96 inch lever arm). However, the exact value of plastic moment can't be determined very accurately because of loading by a hydraulic jack where any increment of deflection is causing a change in the load value. Because of plastic action on the fixed end of the column starting by loading no. 16 the moment in gauge zone "0" was assumed the same as moment at point of fixation. This assumption gives more realistic values for moment-curvature curve due to the fact that strain readings in gauge zone "0" are highly influenced by plastic hinge formation at the bottom of the gauge zone.

The section was able to carry a higher moment than the assumed plastic moment. The highest value of moment transferred by the section was about 400.0 inch-kips in loading 22. In Figure 6.4 the theoretical moment-curvature relationship for the same section is shown by the dotted line. In the prediction for the moment-curvature curve the effect of strain hardening in steel was not considered which is likely the reason of lower moment capacity of the section.

From the strain readings the moments were calculated at each gauge zone by balancing forces in the section as shown on the free body diagram

TABLE 6.1: TEST OF COLUMN C-2.

NO. OF LOADING	HOR. LOAD H (KIP)	HORIZONTAL DEFL. h (INCH)	CURVATURE * $\phi * 10^{-4}$ (inch^{-1})
1	0.64	0.124	0.096
2	0.96	0.259	0.173
3	1.60	1.131	0.267
4	0.64	0.555	0.192
5	0.96	0.698	0.241
6	2.24	1.386	0.489
7	0.00	0.155	0.211
8	0.96	0.897	0.343
9	2.56	2.037	0.712
10	0.00	0.272	0.264
11	0.96	0.954	0.423
12	2.88	2.492	0.787
13	0.00	0.292	0.296
14	2.56	2.109	0.768
15	2.88	2.523	0.825
16	3.20	3.647	1.722
17	0.00	1.026	0.945
18	3.20	3.694	1.726
19	0.00	1.172	0.949
20	3.88	4.578	2.318
21	0.00	1.698	1.444
22	4.175	5.550	2.871
23	0.00	2.243	1.997

* Curvature at gauge zone "0", at fixed end.

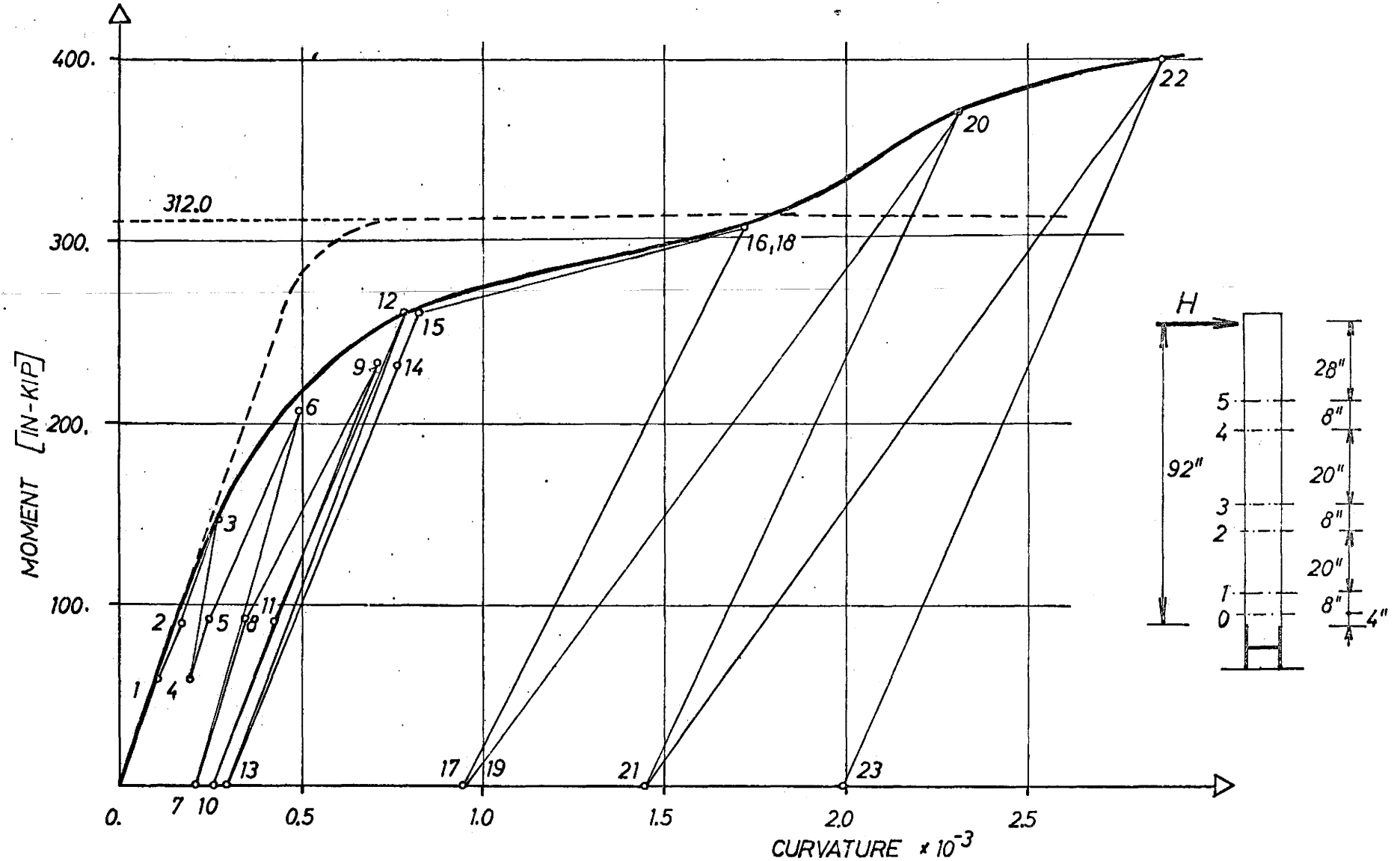

Fig. 6.4. Moment-curvature relationship from test of column C-2 for gauge zone 0 at the bottom of the column.

of Figure 6.5. Because the strain distribution in the section is known the moment and axial force should satisfy equilibrium. In this case when no axial force is applied on the section, the calculated value of axial force represents an error of strain readings. The computer program described in Chapter VII was used for this calculation and resulting moments are shown in Figure 6.7, where a theoretical moment distribution is marked by the dotted line. The full lines of obtained moment distribution is the connection of moment values calculated for each gauge zone.

The method of calculation for these moment values did not consider the influence of repeated loading on strain history and effect of steel strain hardening; this could be one of the main reasons for disagreement of some moment values compared with the theoretical values.

The deflected shape of the column under increasing load is shown in Figure 6.8. Horizontal load versus horizontal deflection is plotted in Figure 6.9 and for the better illustration the horizontal deflection versus number of loading is shown in Figure 6.10.

The results of this test show the repeatability of the moment-curvature curve under repeated loading and also that the moment capacity of the section obtained from the test was greater than the predicted value.

6.2.1 Test of Frame BF-1

The frame BF-1 was tested under proportionally increasing loads with the purpose of obtaining the plastic collapse load of the frame.

This frame was the only one of the four in which the longitudinal reinforcing bars were heated prior to bending. The additional reinforcement

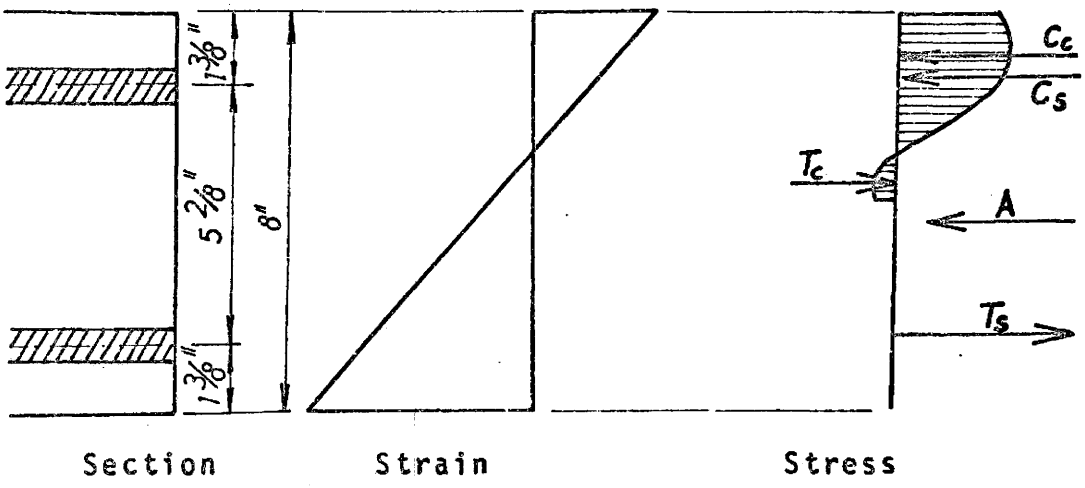

Fig. 6.5. Free Body Diagram for Cross-section

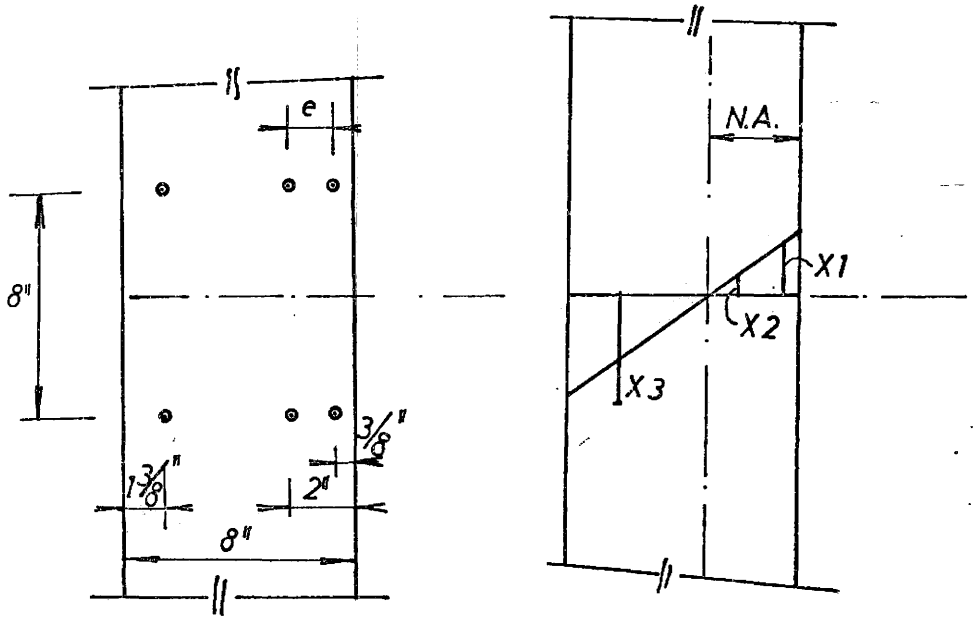

Fig. 6.6. Demac Gauge Zone and Strain Readings

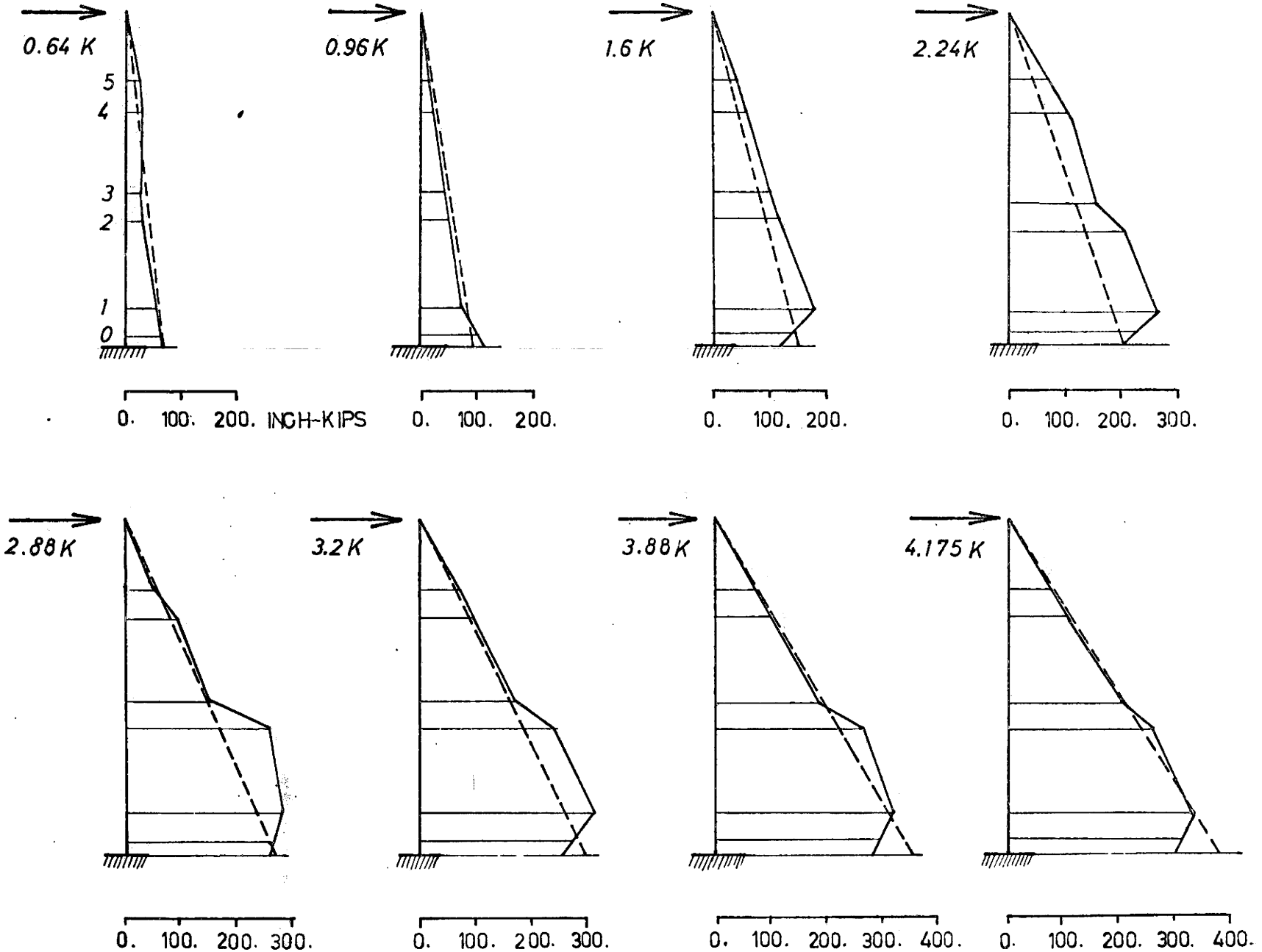

Fig. 6.7. Moments on Column C-2 from Demac Points

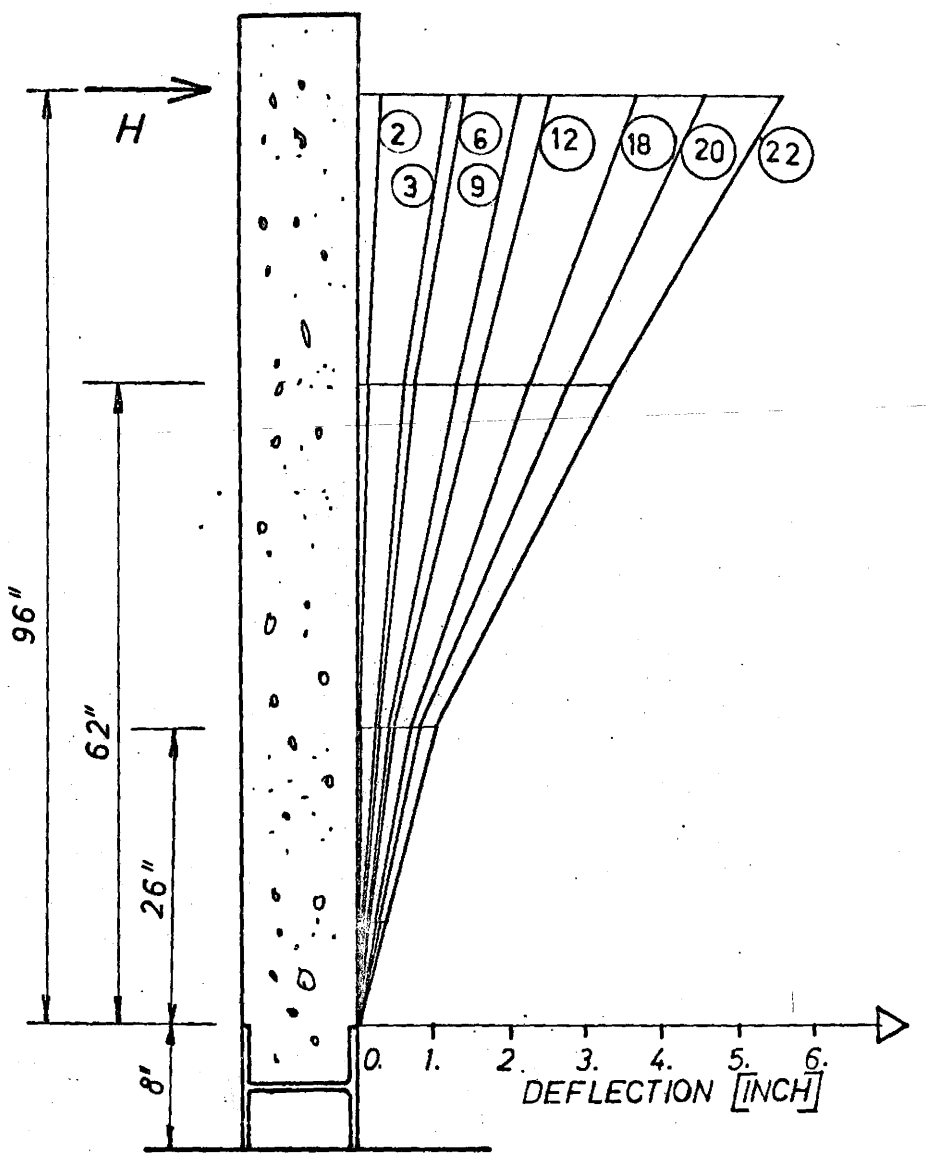

a, Under Load

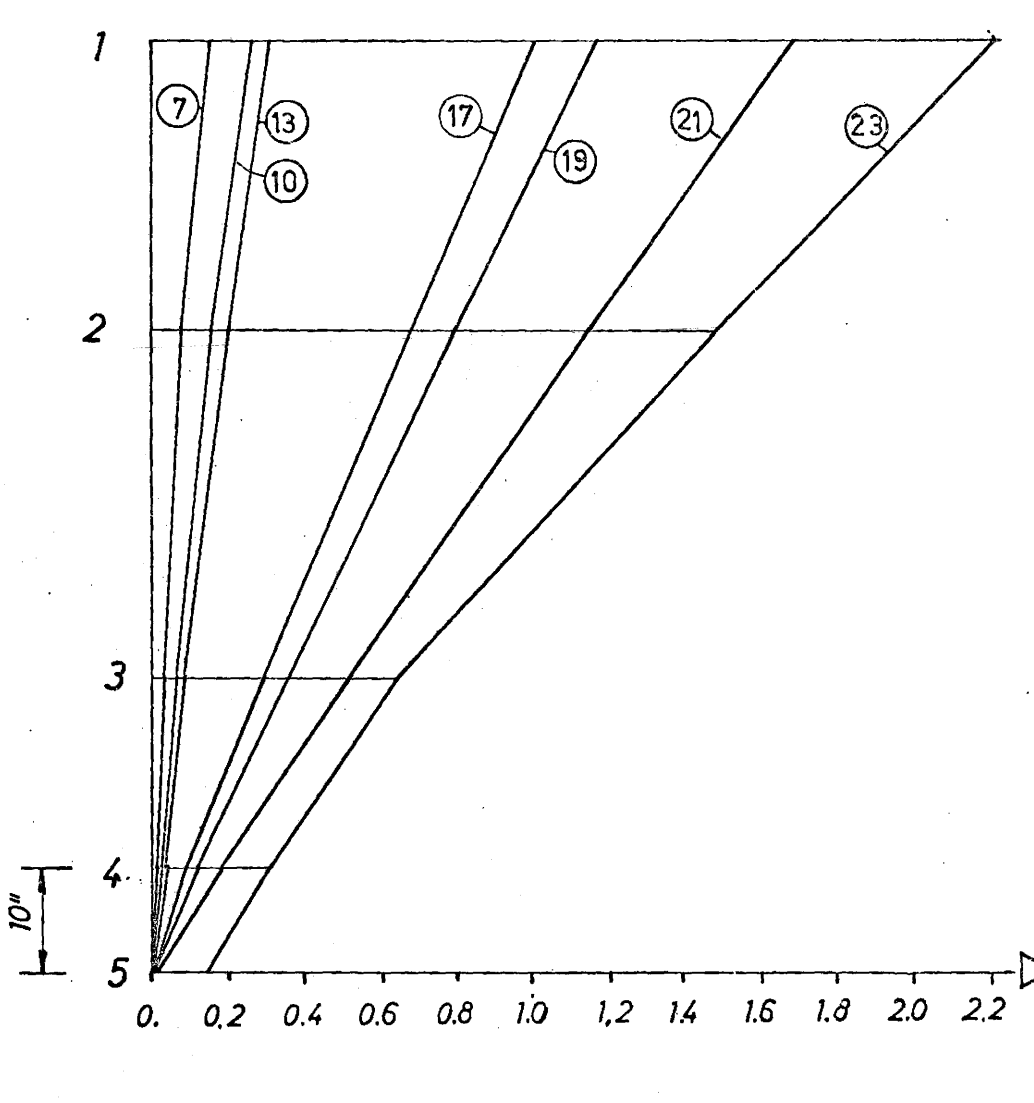

b, Permanent Deflection

Fig. 6.8. Column C-2 , Deflection under Increasing Load

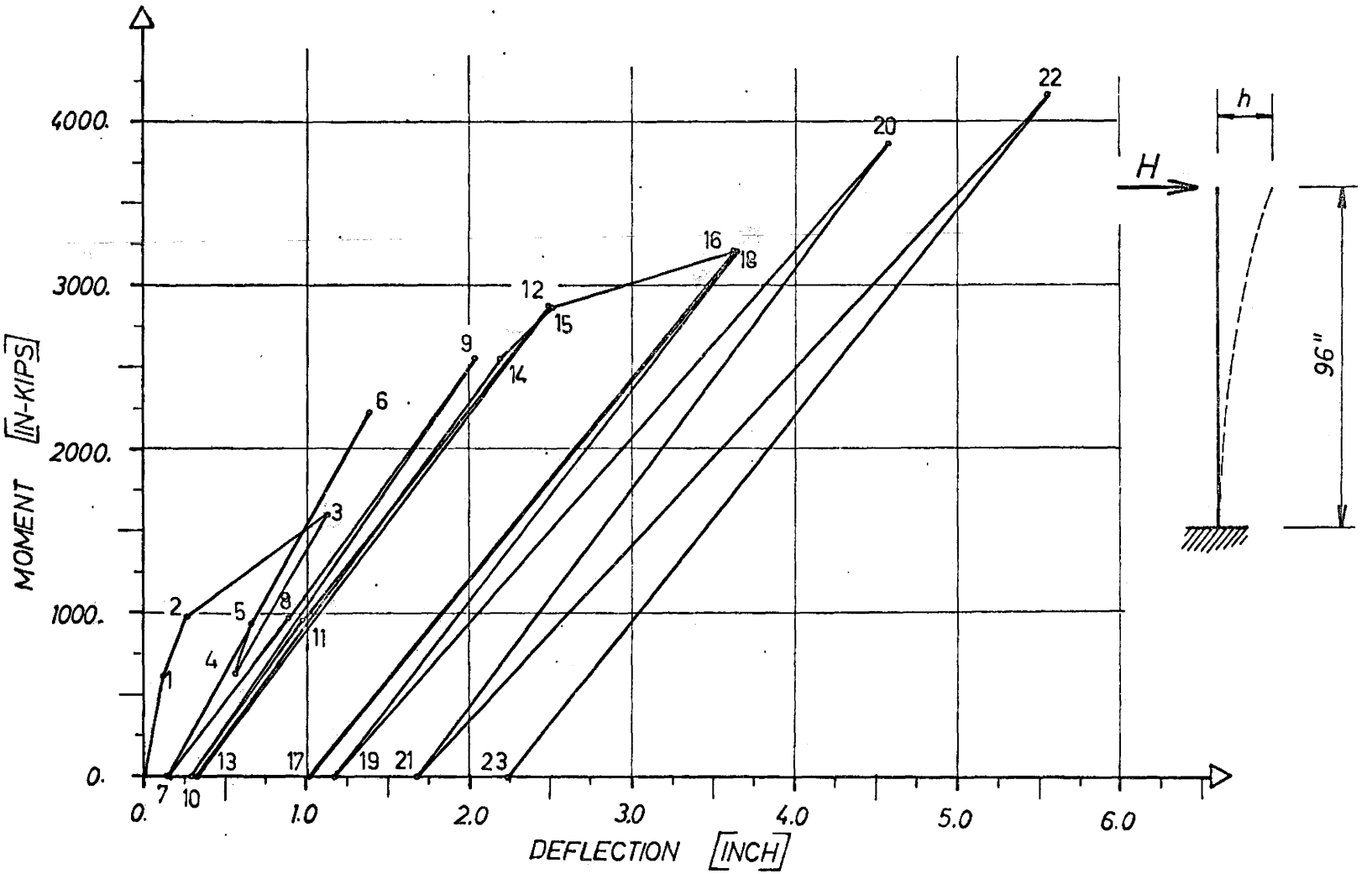

Fig. 6.9. Horizontal Deflection (h)-Horizontal Load (H) Relation for C-2

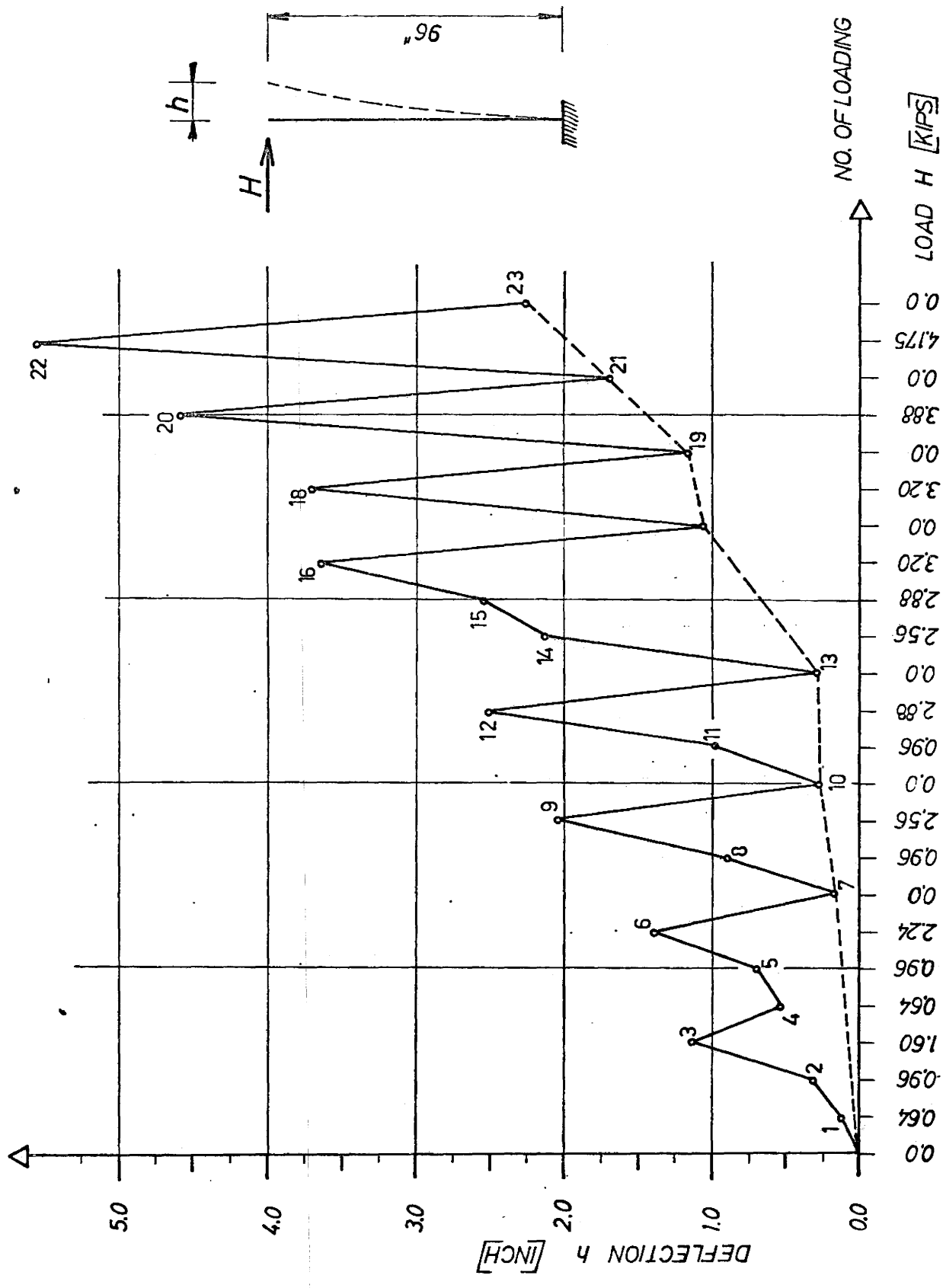

Fig. 6.10. Horizontal Deflection of Column C-2

of the corners for BF-1 is shown in Figure 4.1a. The bases of the frame being described in Section 5.1 and shown in Figure 5.1 were equipped with electric resistance strain gauges for measuring reactive forces of the columns.

The test procedure as described in section 5.2 consisted of incrementing all three loads proportionally at which time readings of demac gauges, dial gauges and electric resistance strain gauges were recorded prior to the next increment of loads. Procedure of loading is shown in Figure 6.11.

During the test an unexpected high rotation of bases were observed. Simultaneously the horizontal deflection of the frame increased rapidly, more than was predicted by the elastic solution.

Upon reaching the value of W=5.0 kips (for values of load see Figure 6.11) the horizontal deflection was significant and culminated in a loud crack with a sudden increase in horizontal deflection of the frame until collapse.

It was observed that collapse was caused by breaking the longitudinal reinforcing bars in the tension face of the section in the third corner marked in Figure 6.11 as critical corner. This corner is shown with the pictures of Figure 6.12.

The investigation of problems mentioned above led to several resulting modifications and changes in fabrication of the frames and test procedures. Undesirable rotation of the bases was caused by an error made in prestressing the base anchor bolts.

By an investigation of the effect of heating longitudinal reinforcing bars used in bending as described in Section 3.3 it was

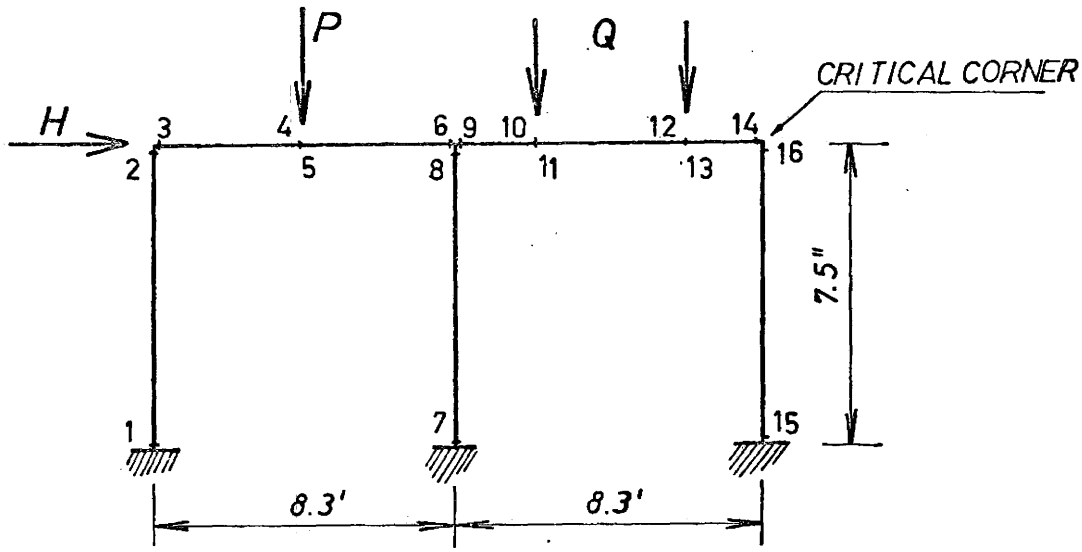

a, Notation of Frame

b, Table of Loading of Frame BF-1

LOADING	0	1	2	3	4	5	6	7
W [KIPS]	0.	3.285	0.	3.285	3.835	4.400	4.790	5.000
H = 3 W	0.	9.735	0.	9.735	11.500	13.200	14.360	15.000
P = 2W	0.	6.490	0.	6.490	7.670	8.800	9.580	10.000
Q 3 5 W	0.	11.360	0.	11.360	13.420	15.400	16.780	17.500

Fig. 6.11. Loading of Frame BF-1

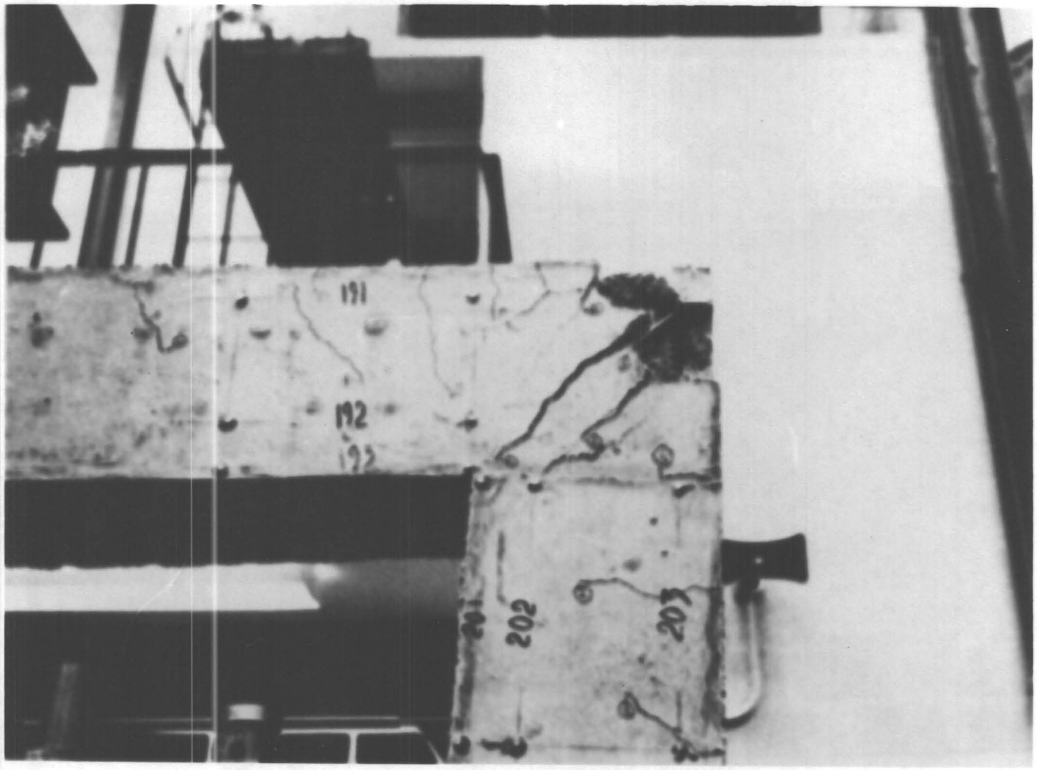

Fig. 6.12 Critical Corner of Frame BF-1.

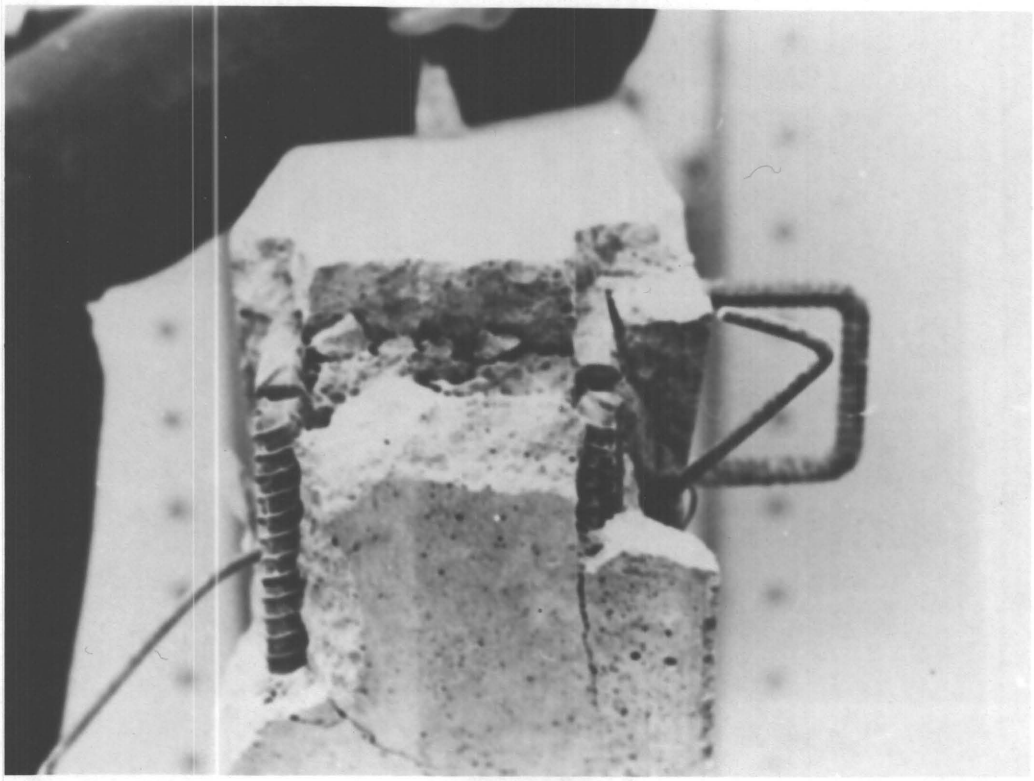

concluded that this procedure was responsible for the failure of the corner reinforcement of frame BF-1. The procedure of bending of longitudinal reinforcing bars was changed and heating was no longer used. Also the stiffness of the corners did not seem to be high enough and some redesigning was done (see Figure 4.1d).

Base equipment for measuring reactive forces of the frame's columns did not satisfy expectations and was not used for the following tests. Wideflange steel end bases of the column were welded directly to the one inch thick steel plate of the lower bases in subsequent frames.

6.2.2. Test Results of Frame BF-1

As described in the previous section some technical difficulty caused premature collapse of the frame. These difficulties were considered in the calculation of theoretical frame deflection and comparisons were made.

The computer program for analysing planar frames as described in Chapter VII was used for calculating the deflection of the frame & moment distributions. A spring connection of joints and bases was considered in the calculation to give the opportunity for considering different stiffness of base connections. Calculation was based on the assumption that frames behave elastically until in some of the critical points the plastic moment value was reached. At this time the stiffness of the joint connection was changed to provide plastic hinge action. In other words, the joints were able to transfer maximum moment equal to the plastic moment value. For more detail, the reader is recommended to see Chapter VII where the computer programs are described.

By trying several different stiffnesses of constants of the bases the deflection versus horizontal load curve was found to have a similar shape to the one obtained from the test results. Some of the curves of horizontal deflection versus horizontal load for different base stiffnesses were plotted in Figure 6.14. The corresponding base stiffness and the sequence of hinge formation is shown in Table 6.2. For best similarity with curve obtained from the tests, the curve denoted in Figure 6.14 by no. 5 was selected. This curve is compared with the curve obtained from tests in Figure 6.15.

Moments calculated from strain measurements are plotted in Figure 6.16 and 6.17. As can be observed from moment distributions in columns I and II the bases were transferring from the beginning of the test a smaller moment value than did the upper joints. This result is due to the fact that small base stiffness, caused by unproper procedure of pre-stressing of the anchor bolts, after reaching a certain limit of rotation was increased. Another interesting observation from the moment distribution can be made due to the high moment concentration in the critical corner (as denoted in Figure 6.11). Due to these high moments it is quite natural that the frame collapsed in this particular corner.

In terms of plastic hinge formation from the test results and from theoretical calculations (sequence of hinge formation is presented in Table 6.2) the first hinge formed at the top of the middle column. For determining a plastic hinge from test data the critical curvature was a boundary which divided elastic action from plastic action in the section. From the theoretical moment-curvature curve as plotted in Figure 2.4 for axial force equal to zero the critical curvature is close to

Table 6.2. Base Stiffness (Curves of Fig. 6.14)

CURVE NO.	STIFFNESS OF BASES [IN-K/RAD.]	PLASTIC COLLAP. LOAD W [KIPS]	SEQUENCE OF PLASTIC HINGE FORMATION
1	1.0×10^{10}	7.5	6,15,14,7,1,8,4
2	5.0×10^{4}	7.5	6,14,15,7,1,8,4
3	1.0×10^{4}	6.7	6,14,8,2,1,4
4	5.0×10^{3}	5.8	8,14,6,2,1,4
5	2.0×10^{3}	5.0	8,14,6,2,1,4

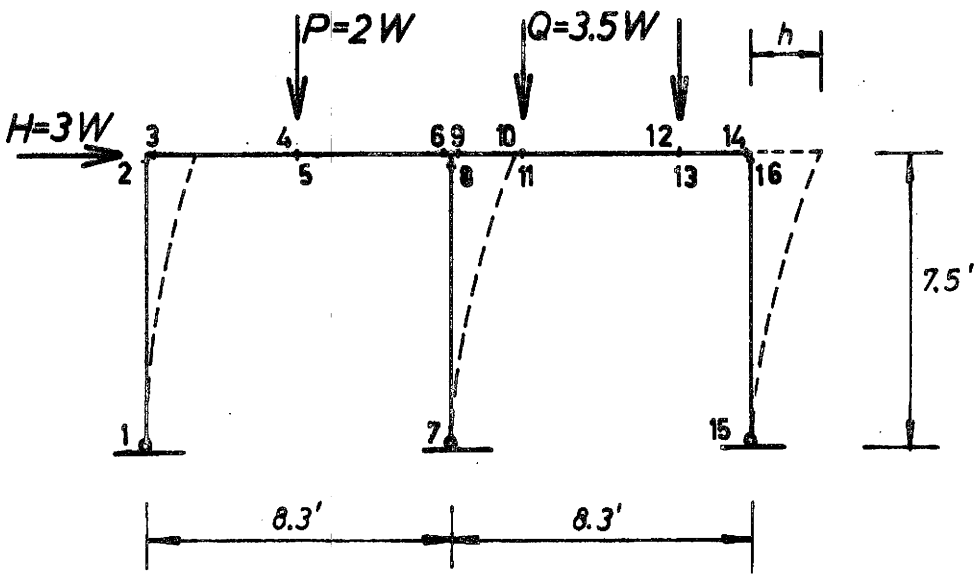

Fig. 6.13. Notation and Size of Frame Corresponding to Table 6.2

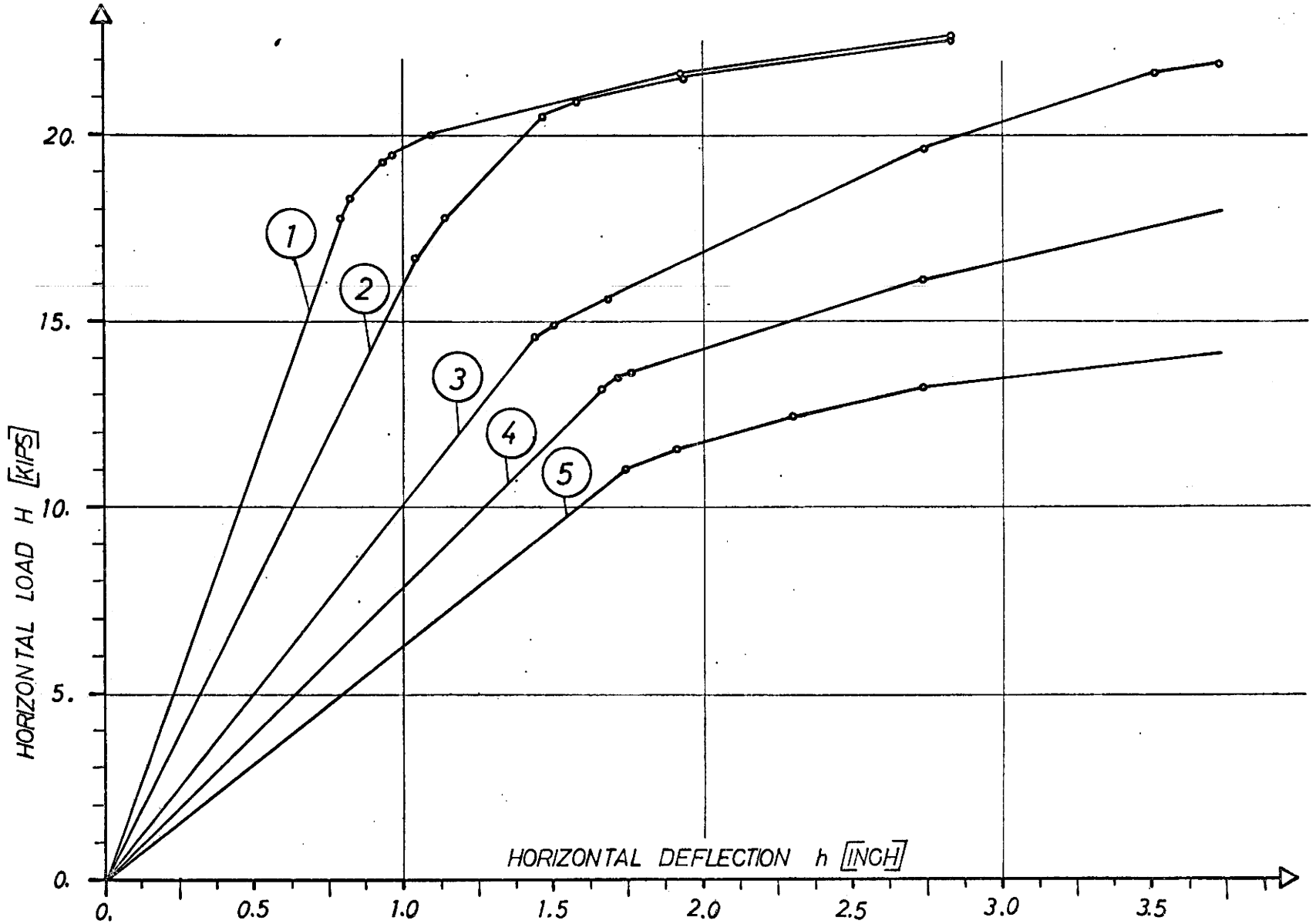

Fig. 6.14 Horizontal Load-Horizontal Deflection Curves: for Base Description see Table 6.2

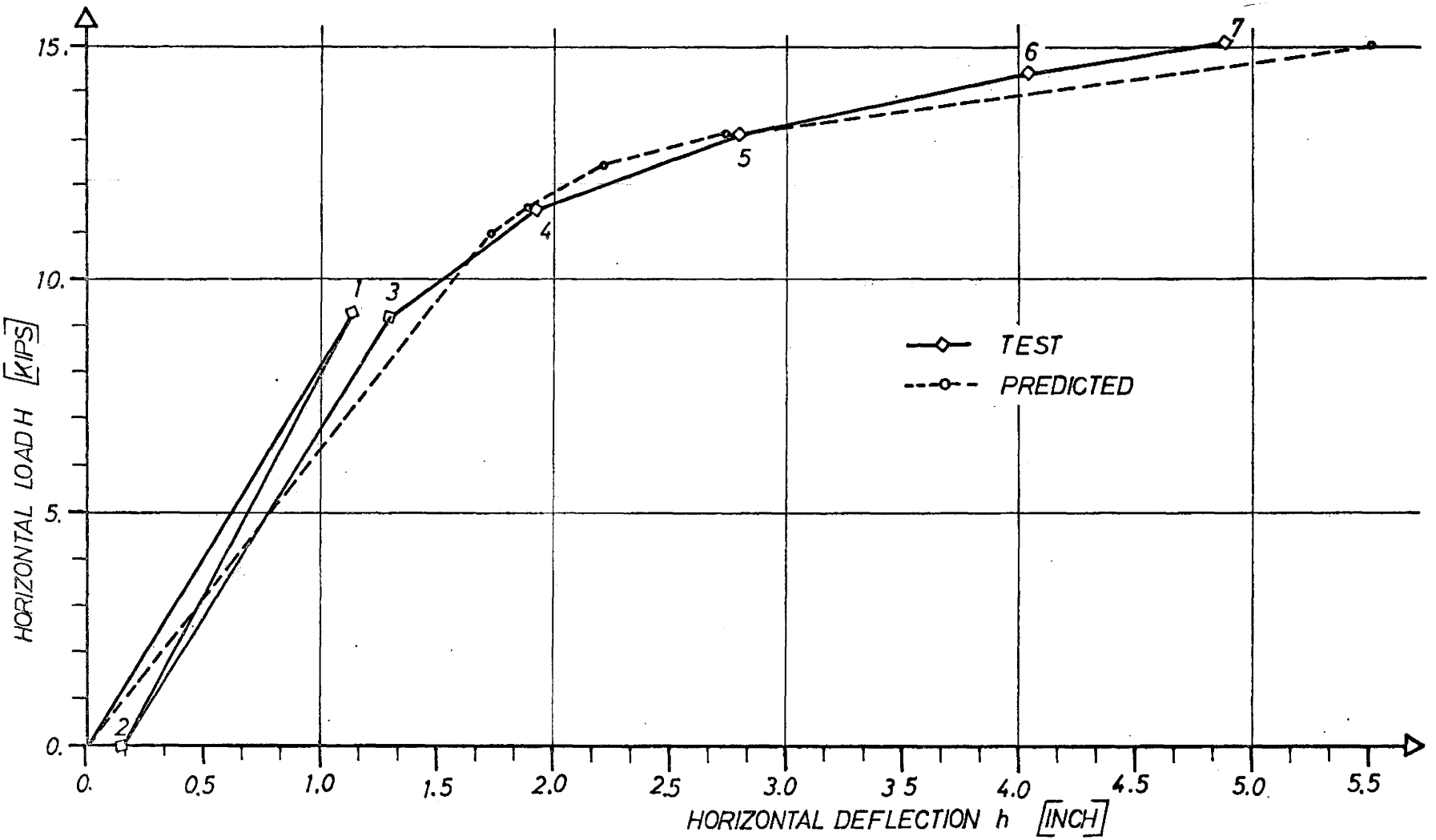

Figure 6.15 Horizontal Load Versus Horizontal Deflection of Frame BF-1

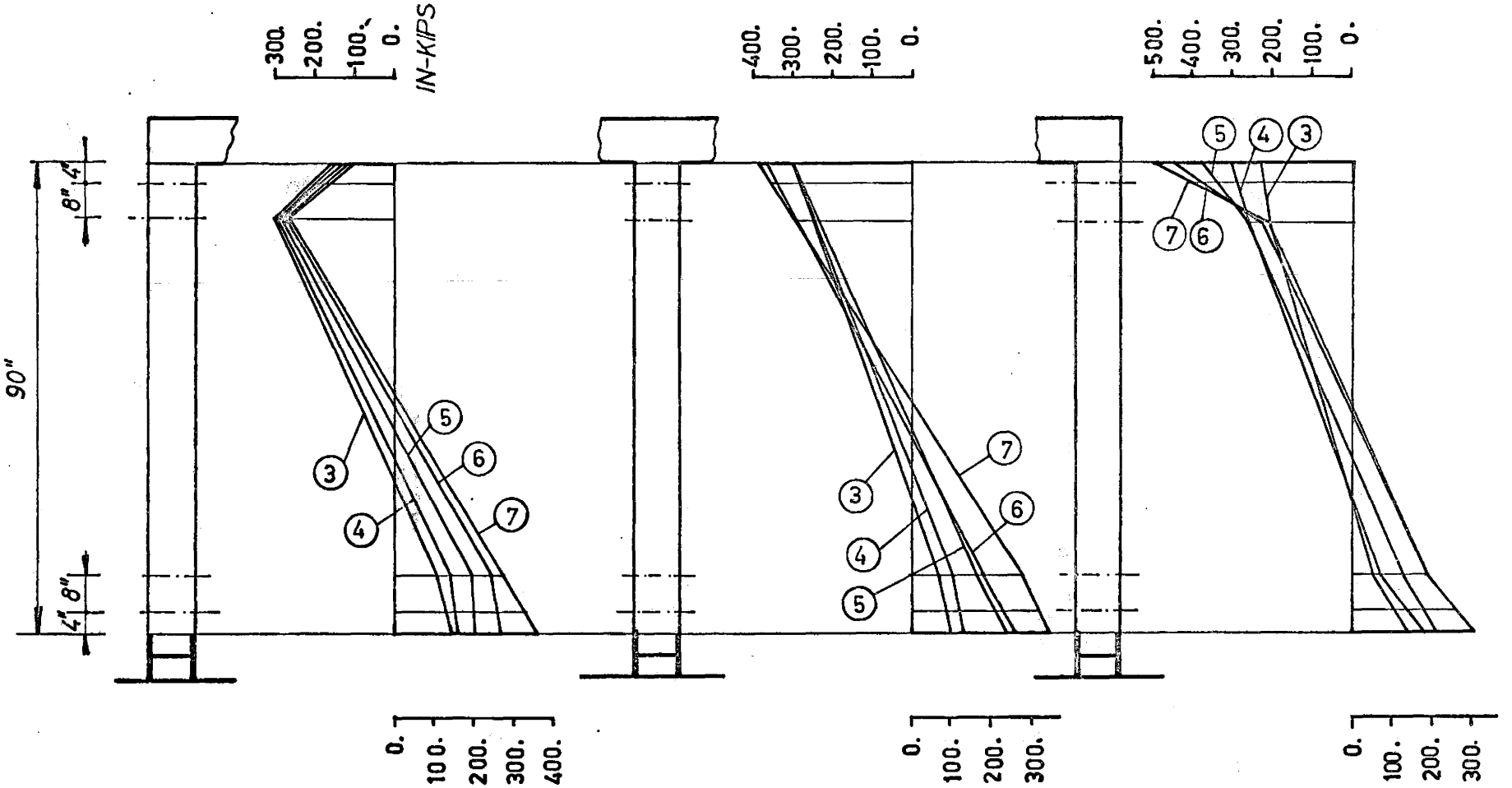

Figure 6.16 Moments in Columns of Frame BF-1 under Increasing Loads. Numbering of lines relates to the loading table of Figure 16.

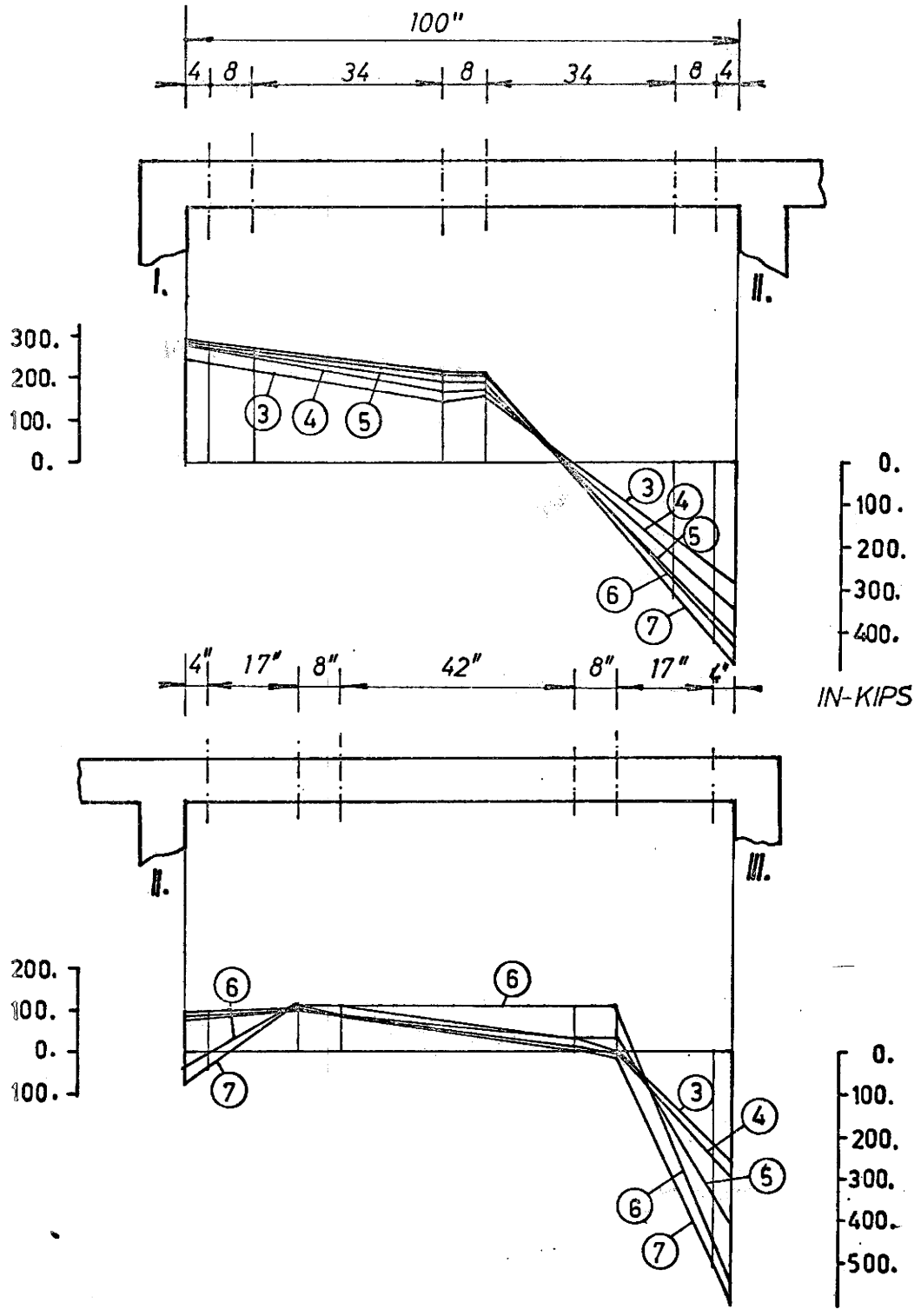

Figure 6.17 Moments in Beams of Frame BF-1 under Increasing Loads.

Curve's Numbers Relates to Loading Table of Figure 6.11.

5.0×10^{-4} 1/inch and is slightly higher for larger axial forces. It was assumed that when the measured curvature exceeded the critical curvature mentioned above the particular cross-section is under plastic action. This assumption is not valid for the repeated loading case where the residual strains could increase the critical curvature

The sequence of hinge formation from both the theoretical approach and test results is shown in Figure 6.18. The hinges at the bases of the test frame developed due to the already mentioned stiffening of the bases by reaching their rotation capacity. Also, the influence of the secondary moment due to deflection was in the final stage of the test significant and helped in the formation of plastic hinges in the bases. In the theoretical approach, where the influence of secondary moments was not considered and the stiffness of bases was considered the same throughout the loading the plastic hinges in all bases would not be developed and structure would theoretically have collapsed as a partial type of collapse by forming a plastic hinge at critical point 4 under the load P.

Although the difficulty in this test did not allow development of the expected collapse mechanism and no actual plastic collapse load for fixed end bases frame was obtained, the method of calculating deflection was quite successful.

6.3.1 Test of Frame BF-2

Frame BF-2 was tested under repeated cyclic loads according to the procedure described in Section 5.3. Resulting modifications of this test frame were incorporated because of the experience in testing BF-1. Longitudinal reinforcing bars were bent without heating. Changes in

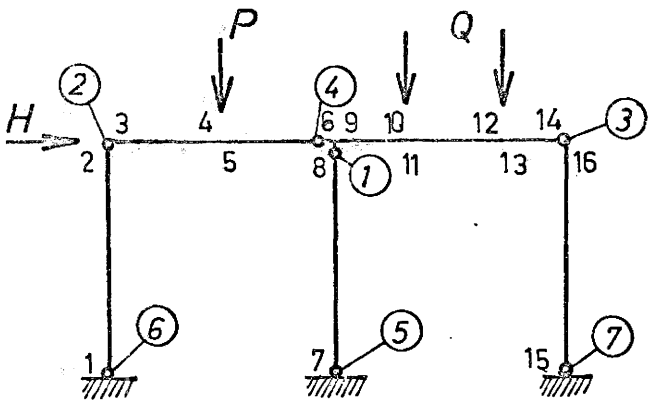

a. From Test Results

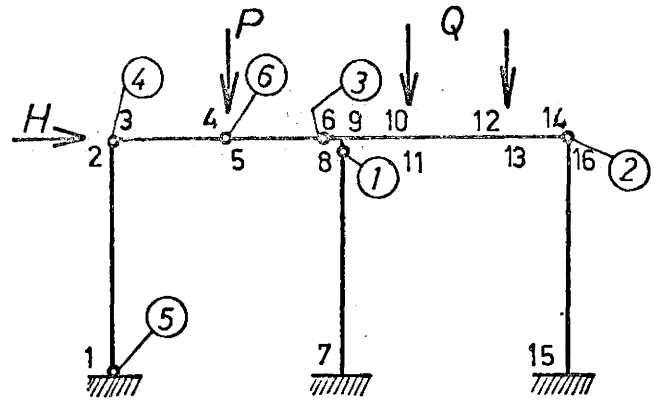

b. From Theoretical Approach

Curvature in the Critical Points under Increasing Loads

LOAD H [KIPS]	CURVATURE IN CRITICAL POINTS $\times 10^4$ [1/INCH]							PL HINGE IN CR. POINTS
	1	2	6	7	8	15	16	
9.735	0.67	6.03	3.32	1.90	7.14	1.23	3.81	2,8
11.5	1.54	7.75	4.31	1.78	13.66	2.03	5.17	2,8,16
13.2	3.58	14.58	5.35	3.94	24.25	2.89	7.45	2,6,8,16
15.0	5.04	33.23	6.58	8.61	38.9	4.37	11.45	1,2,6,7, 8,16

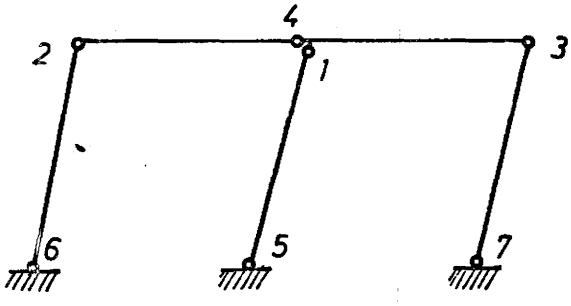

c. Collapse Mechanism Developed During the Test

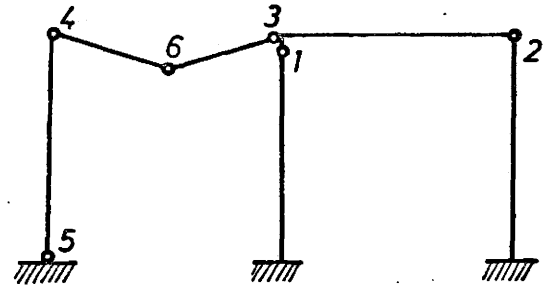

d. Collapse Mechanism Due to the Theoretical Approach

Figure 6.18 Sequence of Plastic Hinge Formations

additional reinforcement of corners was made (as shown in Figure 4.1d) and wideflange steel end bases were welded directly to the one inch thick plate of lower bases. Electrical resistance strain gauges were mounted only on the outside faces of the flanges of steel and bases, which would give an opportunity to check the moments and vertical forces on the ends of the frame columns. The photograph of the base is shown in Figure 6.19.

The program of loading is described in Section 5.3 and was followed during the test. The extreme values of loads were calculated regarding the incremental collapse load theory as described in Section 2.4. For plastic moment M_p equal 312.0 inch-kips it is about 4% less than theoretical value. This change was made due to the safety of the frame with the purpose of avoiding collapse of the frame in the earlier cycles. The half values of loads were applied separately at the beginning of the test to check the system and after a combination of all loads with the same value was applied. When this elastic part of the test was over a repeated cyclic loading took place. The loading program of frame BF-2 is shown in Figure 6.20.

Readings of dial gauges, demac point gauges and electric resistance strain gauges were recorded for the most loading or for the no load state. During the test the demac point gauges and dial gauges performed well, while the electric resistance strain gauges readings were again unsatisfactory.

The most critical section of test frame BF-2 during the test involved the middle corner between the middle column and the second beam, where the stirrup made from a fabricated number four bar broke. Additional outside stirrups were fabricated and substituted for the broken one.

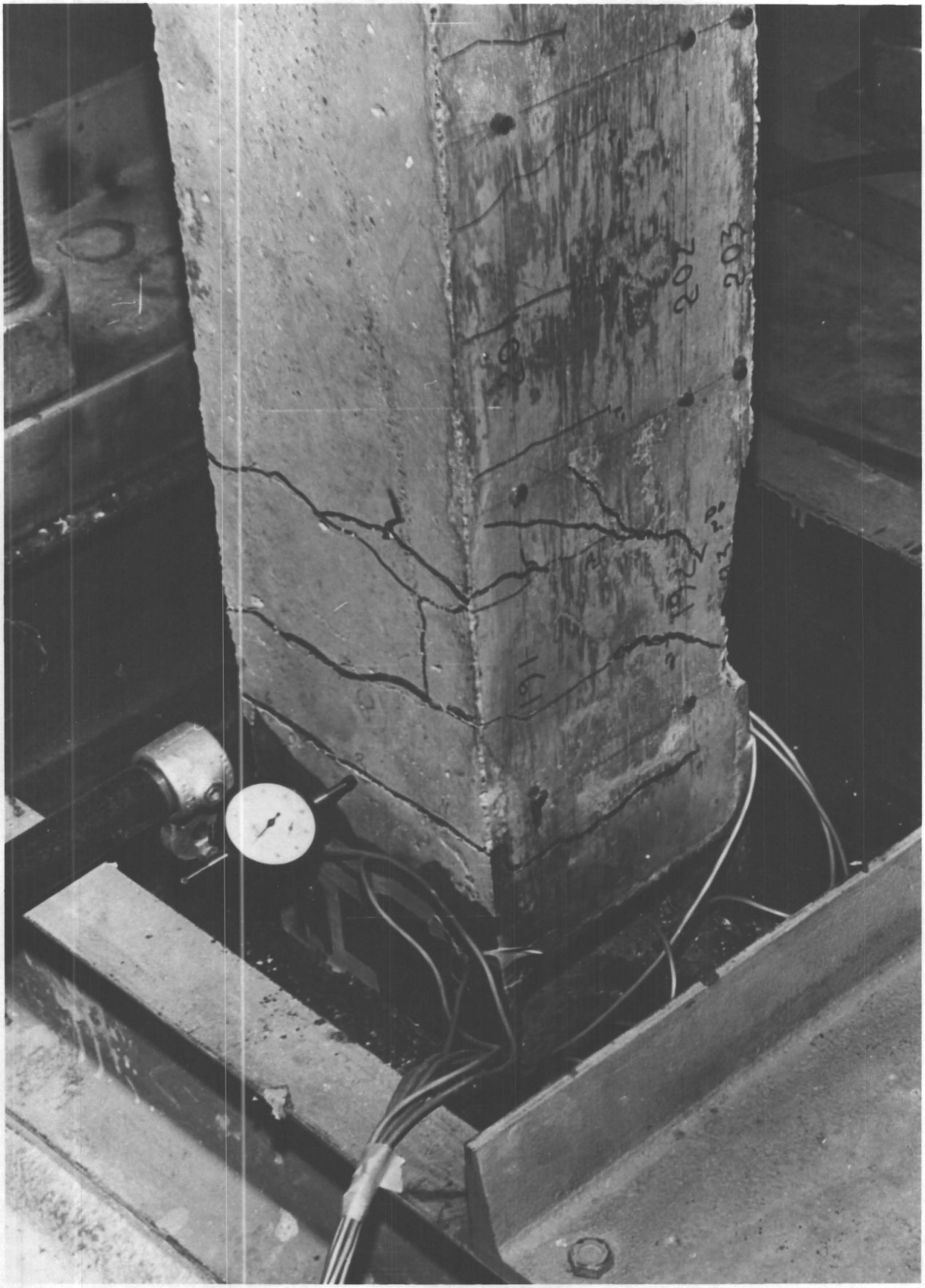

Fig. 6.19 The Middle Base of the Frame BF-2.

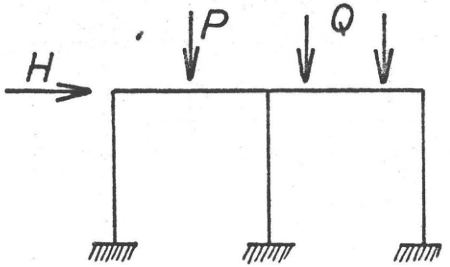

	LOAD H [KIPS]	LOAD P [KIPS]	LOAD Q [KIPS]
ELASTIC LOADING	8.4	5.6	9.8
CYCLIC LOADING	16.8	11.2	19.6

$H = 3W$

$P = 2W$

$Q = 3.5W$

$a = H$

$b = H + P$

$c = H + Q$

$d = H + P + Q$

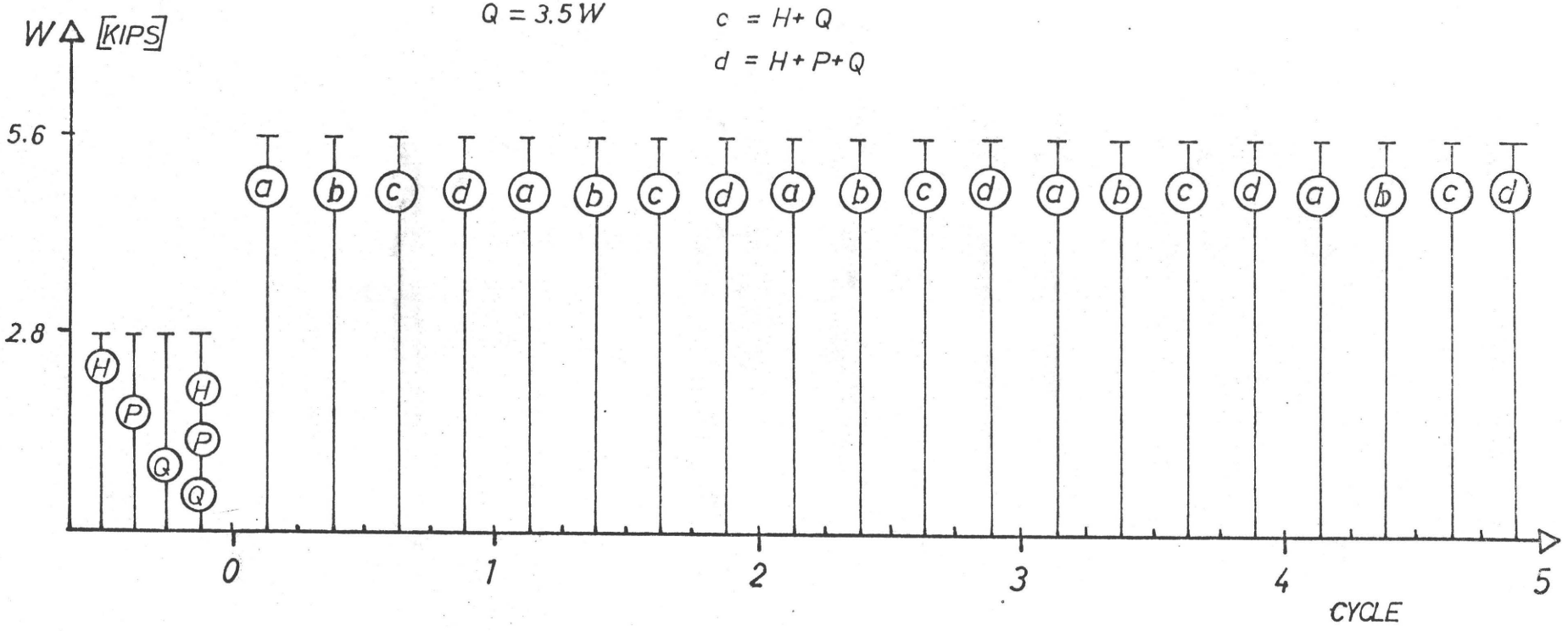

Figure 6.20 Loading Program of Frame BF-2

The photographs in Figure 6.21 and Figure 6.22 show the critical middle corner after the stirrups broke, and photographs of Figure 6.23 and Figure 6.24 show additional outside stirrups of the middle corner. This happened at the beginning of the third cycle when only the horizontal load H was applied.

During the fifth cycle when a combination of all three loads was performed a horizontal deflection kept increasing continuously and spalling of concrete on compression faces of sections in all critical moment areas was observed. The frame was not able to carry any further loading that is therefore at a collapse. The photograph in Figure 6.25 shows the frame BF-2 after the testing procedure was over.

With the exception of electric resistance strain gauges on end bases all instrumentation performed well during the test.

The resulting modifications of this test were changes in the middle corner where a difficulty arose which was described above and the elimination of electric resistance strain gauges because their readings could not be used.

6.3.2 Test Results of Frame BF-2

Deflection readings and strain readings obtained from the test are compared with the predicted values. The frame collapsed after five full cycles of loading.

Because of the sway collapse mechanism the horizontal deflection of the frame was most significant. The horizontal deflection was measured close to the top of columns and was plotted in Figure 6.26. As can be seen, the standard elastic loading caused only negligible permanent horizontal deflection, therefore this part of loading was not considered in theoretical calculations.

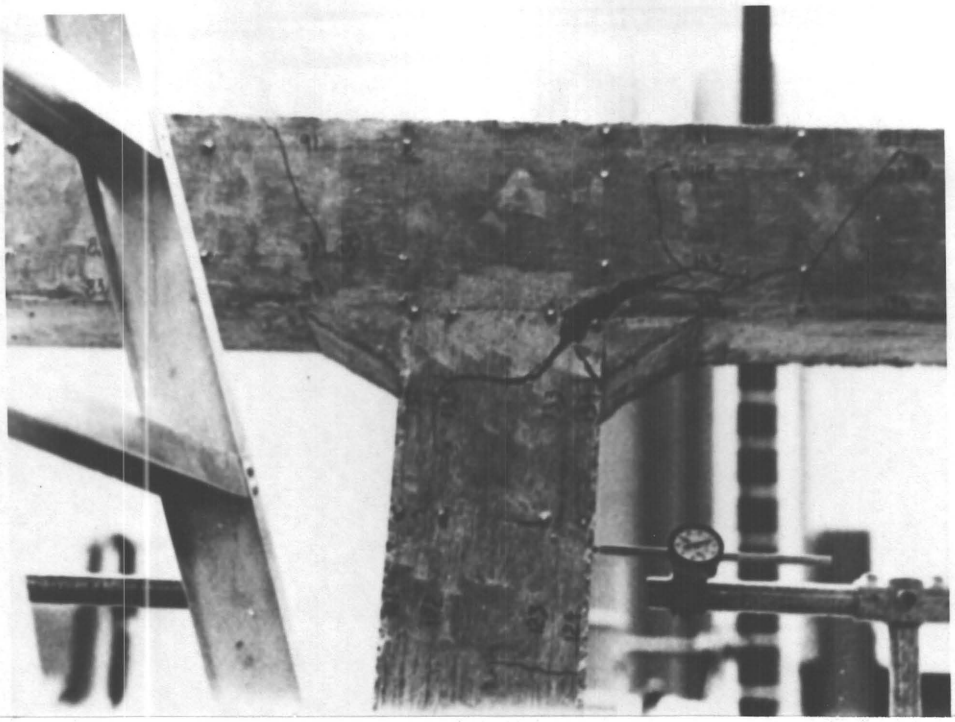

Fig. 6.21 Test of the Frame BF-2, Middle Joint.

Fig. 6.22 Detail of Crack in Middle Joint of Frame BF-2.

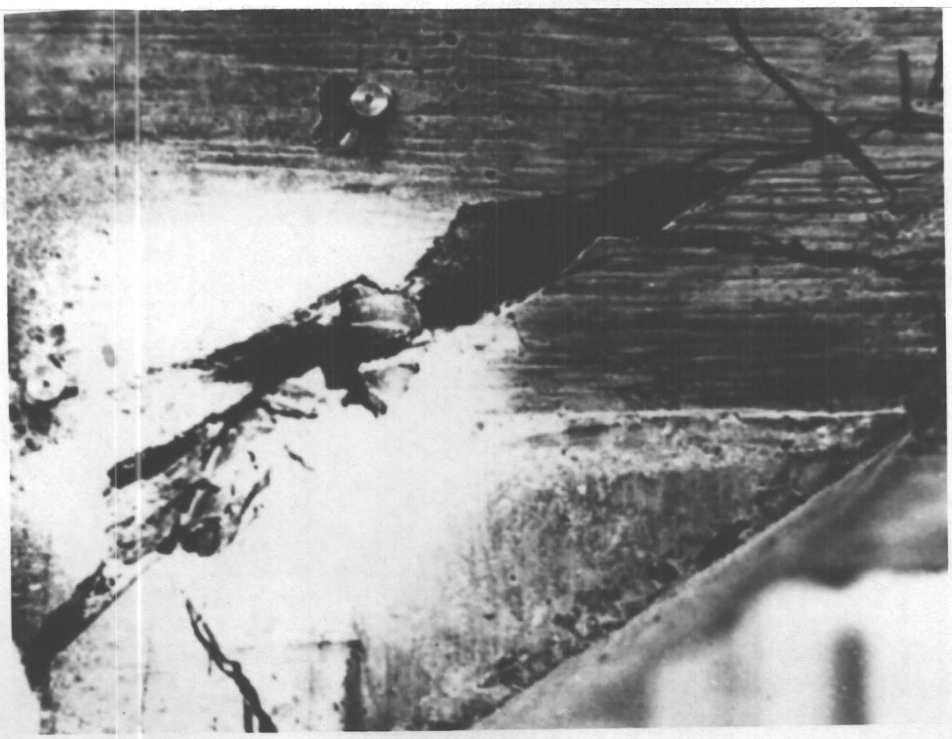

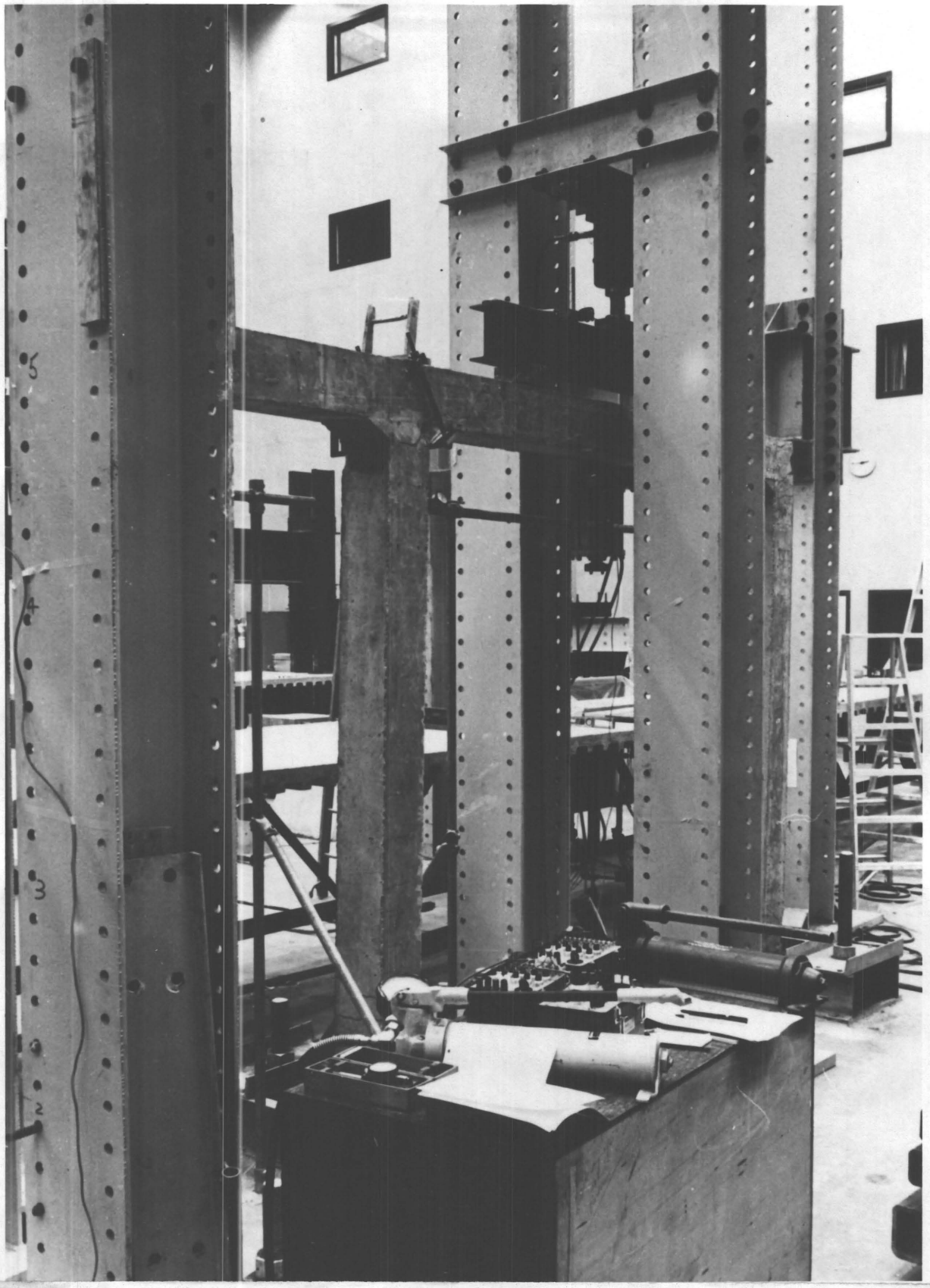

Fig. 6.23 Test of Frame BF-2, Middle Joint, Two-point Load and Test Apparatus.

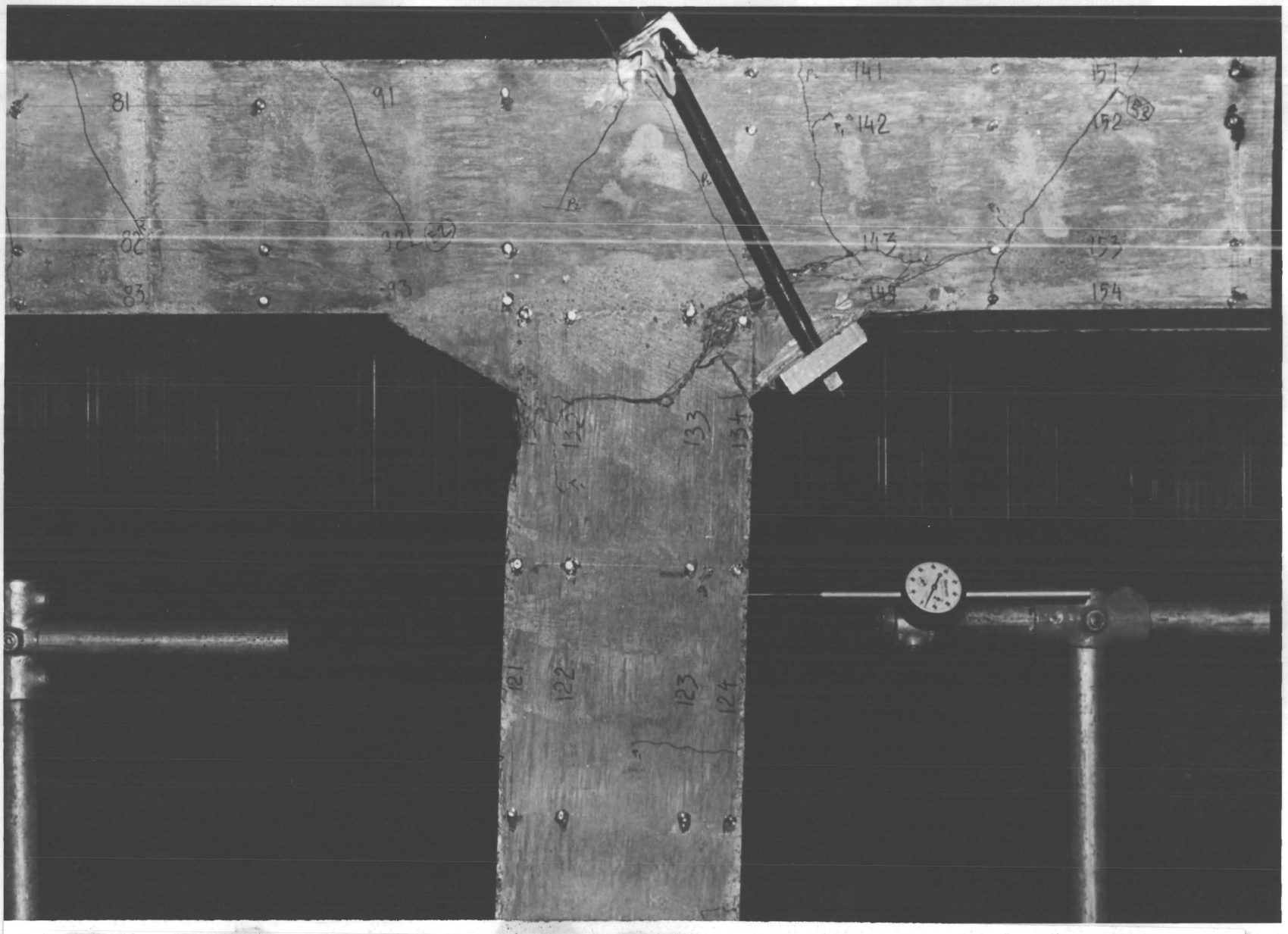

Fig. 6.24 Frame BF-2, Outside Stirrup at Middle Joint.

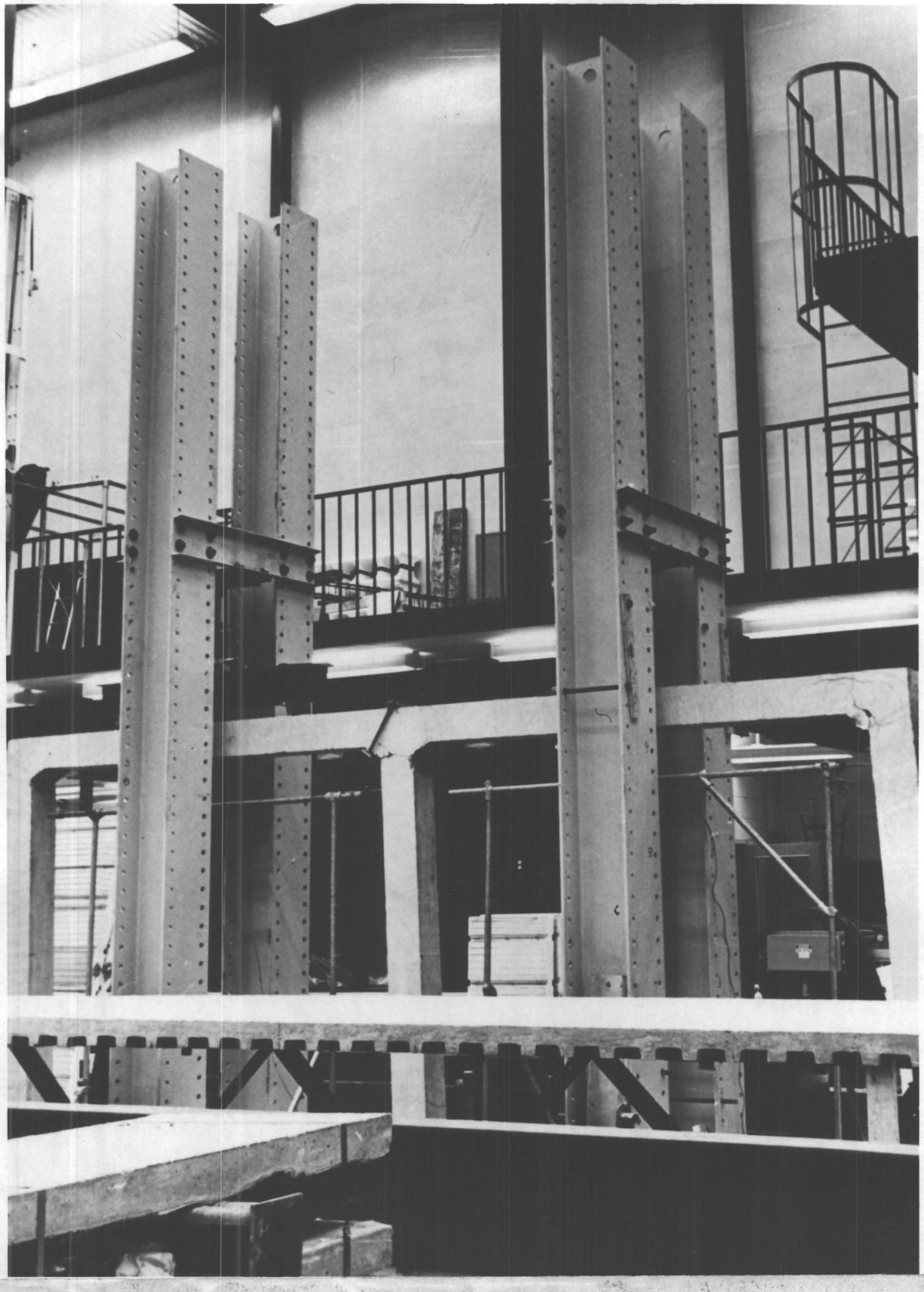

Fig. 6.25 Frame BF-2, After Incremental Collapse.

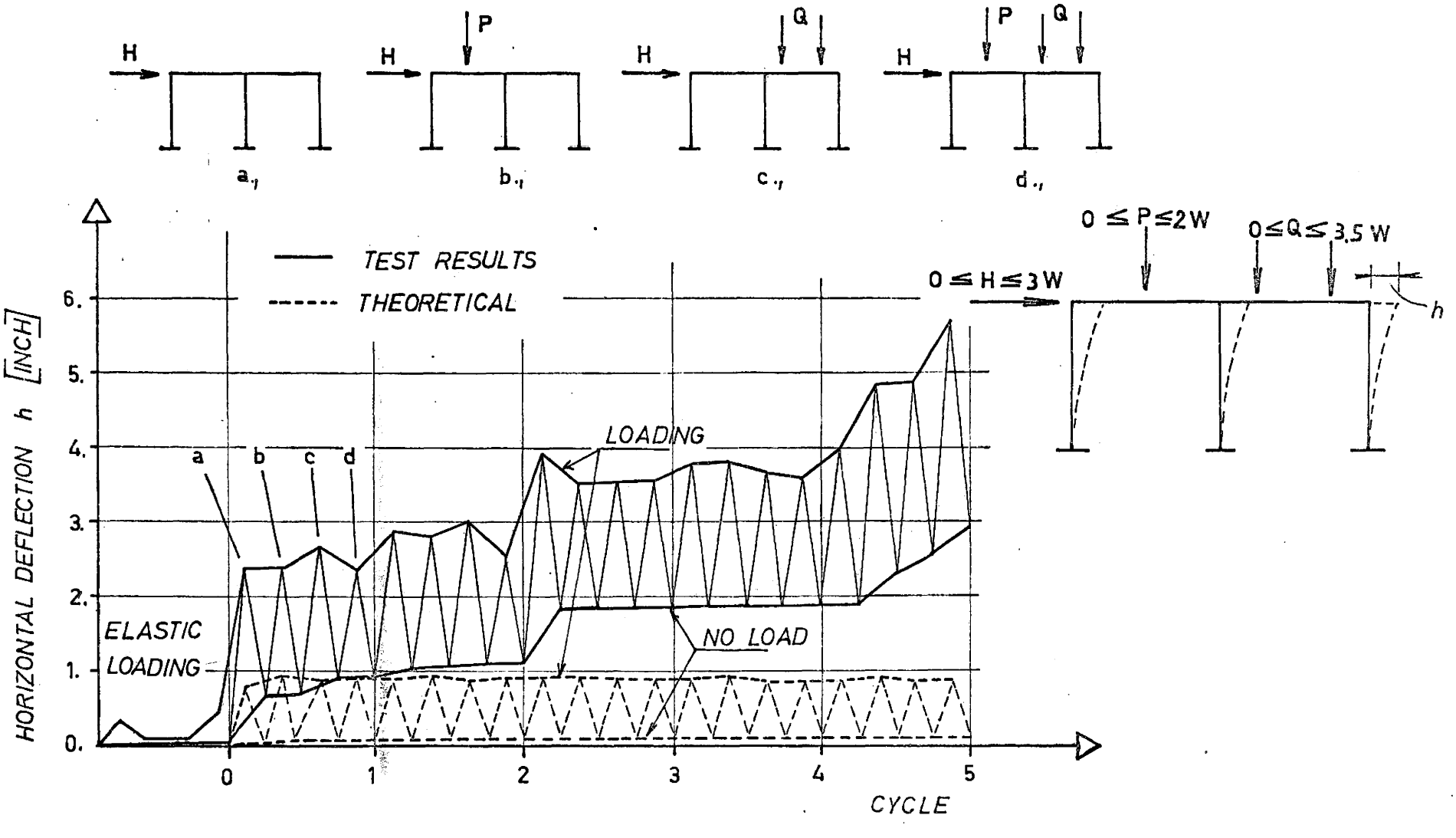

Figure 6.26 Horizontal Deflection of Frame BF-2 During Cyclic Loading

The sudden increase of horizontal deflection in the third cycle could be explained by collapse of the stirrups in the middle corner, as mentioned in the previous section (6.3.1). The broken stirrups were replaced by outside stirrups (see Figure 5.2.4) with the same function as the broken ones. The slope of permanent horizontal deflection assigned as no load line in the Figure 6.26 did not change appreciably after the stirrups were replaced; the frame could be considered undamaged.

In the fifth cycle, when the influence of secondary moments was already significant the permanent horizontal deflection was increasing more rapidly while a full sway collapse mechanism was developed.

In the theoretical approach the matrix method for solving the plane frame was used employing plastic hinges and influence of axial force on moment capacity. Computer programs for this calculations are described in Chapter VII. The effect of secondary moments caused by the deflected shape of frame is not considered in theoretical calculations as well as the effect of loading history on the moment-curvature relationship. Theoretically, the frame would not reach the incremental collapse and would shakedown after the first cycle; the following cycles would provide only elastic changes in the frame. It should be mentioned that the load W_s applied on the frame BF-2 and considered in the calculation of deflection was 4% less than the theoretical incremental collapse load of this frame without considering the influence of axial force on moment capacity (mentioned in the previous Section 6.3.1).

Strain readings obtained from the test are compared with predicted values in Figure 6.27, 28 and 29. Comparisons were made only for critical sections in columns of the frame in position of demac point gauges. Compression strain measured at 3/8 of inch from compression

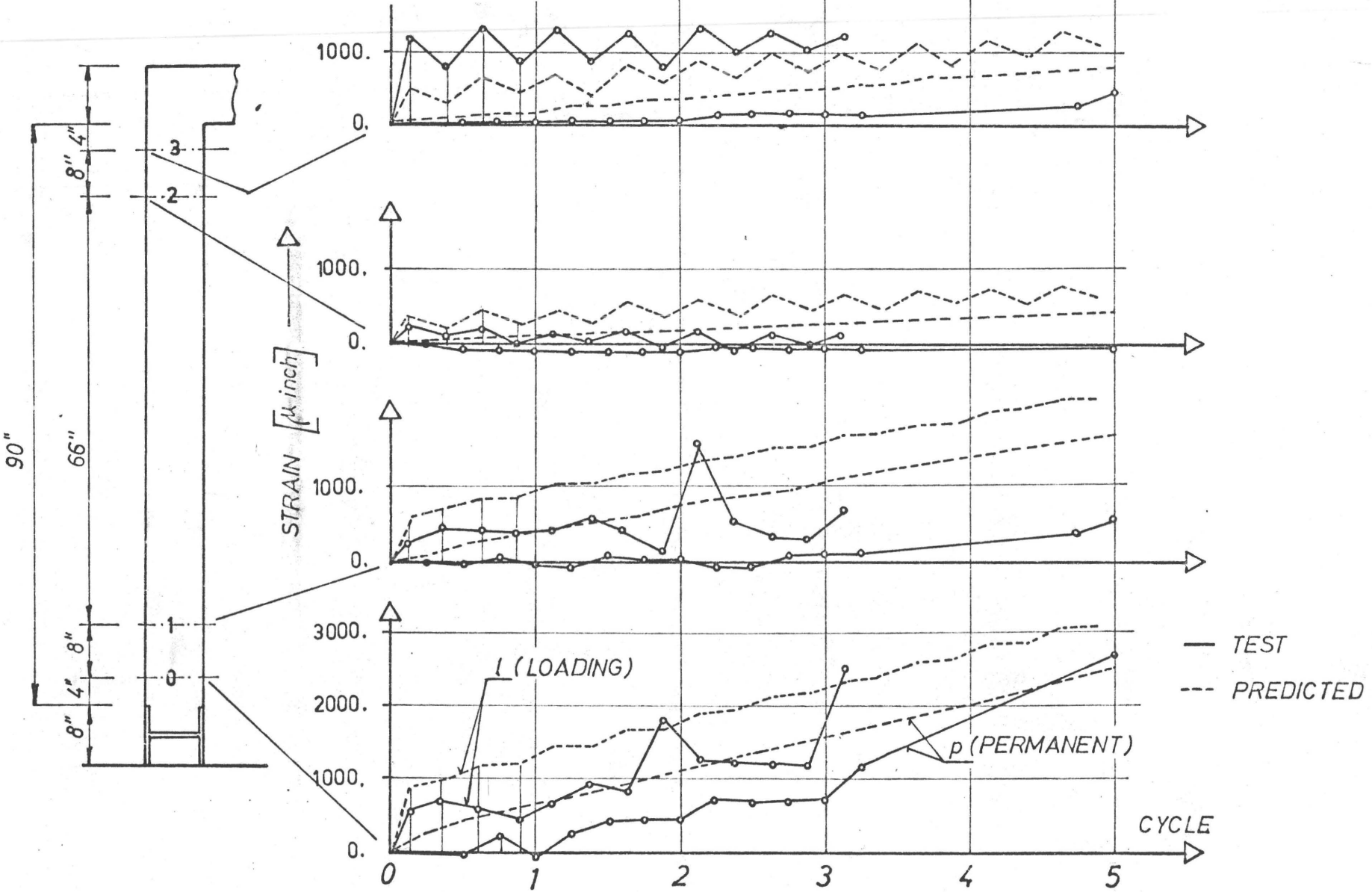

Figure 6.27 Comparison of Strain Reading for Frame BF-2, First Column

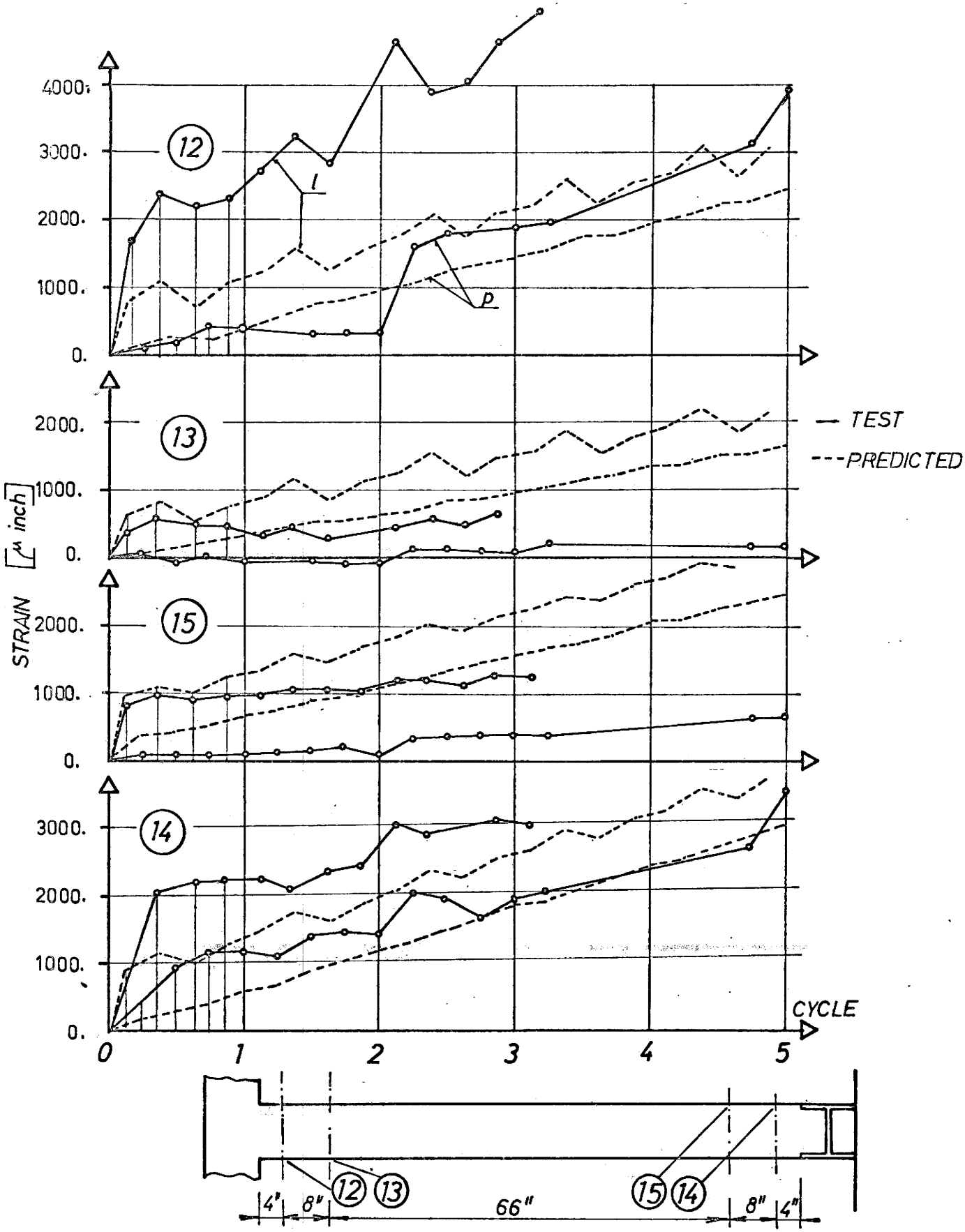

Figure 6.28 Comparison of Strain Reading for Frame BF-2, Second Column

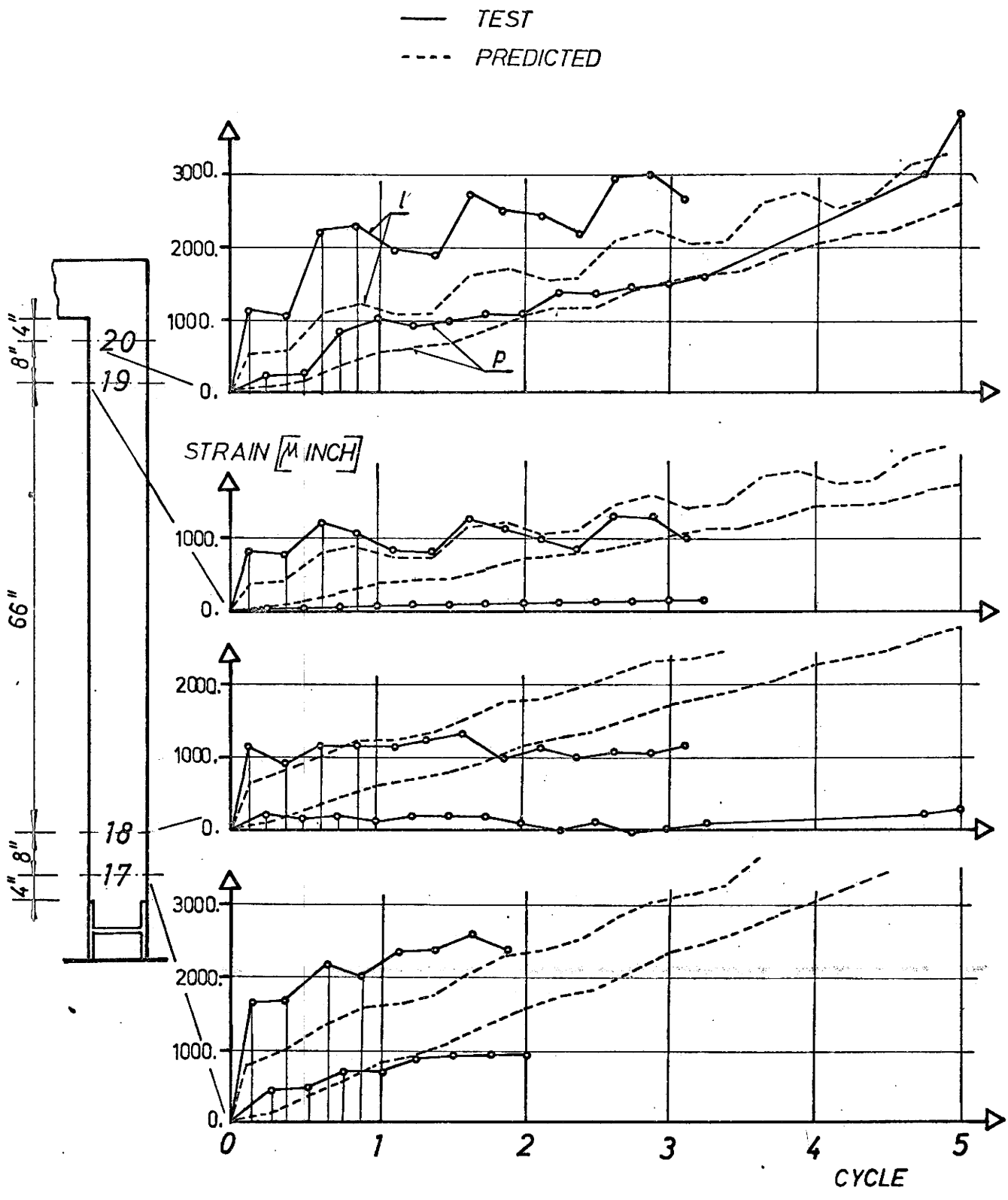

Figure 6.29 Comparison of Strain Reading for Frame BF-2, Third Column

face of the section is compared with predicted values in this position. For calculation of predicted values of strain the loading history of cross-sections is considered. In general, two types of moment-curvature characteristics are involved in this calculation. One, used for loading states, is a moment-curvature relationship already described in Section 2.3. The second type, which is used for unloading states is a linear type resulting from the transform area method. For more details of calculation of predicted values of strain the reader is recommended to see Chapter VII in which the computer program for this calculation is described. Moments and axial forces, used for following the loading history of the cross-section were obtained by the same method as described for predicted values of deflection.

In Figures 6.27-29 the full lines connect the points obtained from the test & the dotted lines represent the predicted values of the strain. In both cases the curves assigned by '1' represent strain values occurring under the loading condition and curves assigned by 'p' represent the permanent strain, when loads were removed.

Although in some gauge zones the differences between predicted and measured values are not too large, the predicted values are not in very good agreement with measured strain generally. There are several reasons for these uncertainties but the main reason was that the matrix method used for calculation of moments did not take into account influence of secondary moments. Furthermore, the breaking of a stirrup which could cause serious change in strain readings could not be traced in the calculations of the theoretical strains.

6.4.1 Test of Frame BF-3

Frame BF-3 was tested under repeated cyclic loading in general the same as frame BF-2. Changes were made in the values of load limits, in stirrup reinforcement at the middle corner, and in the monitoring of deformation behavior.

The influence of axial force on the value of plastic moment was the main reason for the changes in the values of load limits for each stage of a cycle. According to incremental collapse theory as described in Section 3.4 the value of W_s is in direct relationship with the value of the plastic moment. The axial forces which occurred in any of the cross-sections of the frame were approximately in a range between 0.0 and 20.0 kips under applied loads used during the test. The relationship between axial force and plastic moment in the range mentioned above is nearly linear. An increase in axial force increases the moment capacity of the cross-section. This modification stems from theoretical and experimental results of Hiroyuki Aoyama (19) and later was confirmed by frame BF-4.

All combinations of loads were considered and axial forces at the critical sections were arbitrarily specified to observe their significance. Table C in Figure 6.30 indicates their effect theoretically on the shakedown load. Because sway mechanism controls, all the hinge forming sections were on the top or on the bottom of columns. For each load combination a different set of axial forces is applicable. The shakedown load cannot be computed therefore, in the standard manner without involving a history tracing procedure. It appears to be a reasonable assumption however, to assume average axial load values for each load

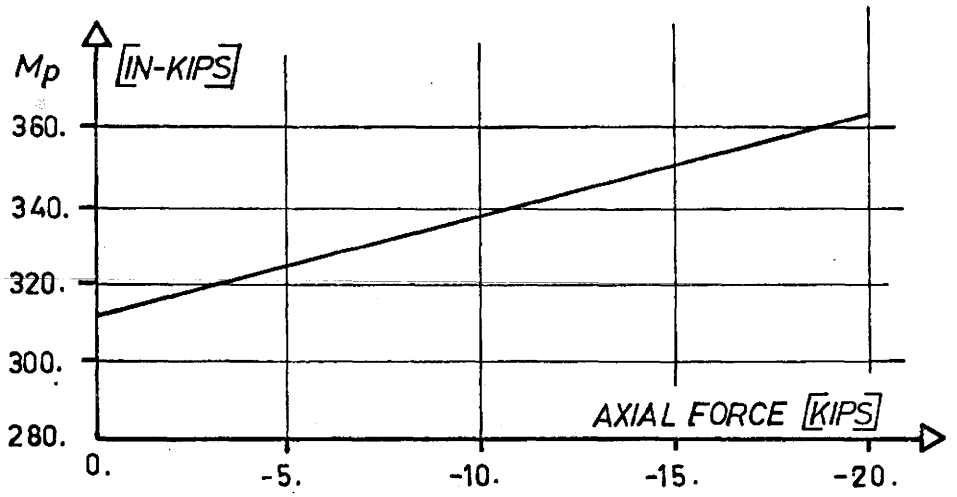

b. Axial Force - M_p Relationship

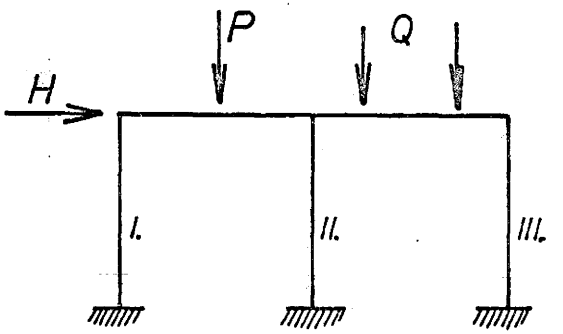

a. Notation of Frame

AXIAL FORCE	Mp	Ws
KIPS	IN KIPS	KIPS
0.	312.	5.81
- 4.	322.	6.0
- 8.	332.	6.18
- 12.	342.	6.37

LOAD COMBINATIO.	AXIAL FORCE IN COLUMN [KIPS]						AVER. AXIAL FORC.	λ
	I.		II.		III.			
	W = 1	W x λ	W = 1	W x λ	W = 1	W x λ		
H	0.58	3.3	0.	0.	-0.58	-3.3	0.	5.8
H + P	-0.34	-2.1	-1.17	-6.17	-0.49	-2.9	-3.7	5.9
H + Q	0.59	3.52	-1.97	-11.8	-2.23	-13.6	-7.3	6.1
H + P + Q	-0.33	-2.1	-3.15	-20.0	-2.13	-13.7	-12.	6.4

Figure 6.30 Approximate Shakedown Values as Determined by Axial Forces

combination and to compute W_s for that case. The procedure is shown in Figure 6.30. The calculation was just approximate and an elastic solution was used for obtaining axial forces.

For example, Figure 6.30 shows a table d, of incremental collapse loads for each of the cases specified. For horizontal load, the average axial force in the three columns is zero. Consequently the appropriate M_p is that which pertains to zero axial force. For a combination of all three loads the average axial force is about -12.0 kips and therefore from Figure 6.30 b, the associated M_p value is 342.0 inch-kips. The shakedown load factor associated with this moment capacity is 6.37 which is about 9.6% higher than for combination 1. The other values in the table are similarly determined.

The testing procedure for frame BF-3 was similar to that of frame BF-2. Individual load cases were based on limits as given by tabulated values of Figure 6.30 d. The load combinations shown in Figure 6.32 and Figure 6.30use as limiting load factors the numbers shown in the second row of the former Figure (6.31 a). A percentage of these load limits appears in Figure 6.31 c and was applied in the actual test to guard against premature failure. The initial step involved elastically loading the frame with each load component increased to half its anticipated maximum. Once confidence was established in the testing procedure and equipment the loads were raised according to Figure 6.31 c to 95% of their individual maximum values.

After the 4th cycle, the load limits attained 97% of full capacity to reduce the time of the test.

The 2% increased load values in the fifth and subsequent cycles resulted in the horizontal deflection being increased more rapidly than

LOADING	a	b		c		d		
LOAD Ws	5.8	6.0		6.0		6.4		
COMBINAT.	H	H	P	H	Q	H	P	Q
FULL LOAD VALUES	17.4	18.	12.	18.	21.	19.2	12.8	22.4
95% OF LOAD	16.5	17.1	11.4	17.1	19.9	18.3	12.2	21.3
97% OF LOAD	16.9	17.5	11.6	17.5	20.4	18.7	12.4	21.7

Note: All Values are in KIPS

a.

ELASTIC LOADING		
H	P	Q
8.	5.7	10.5

b.

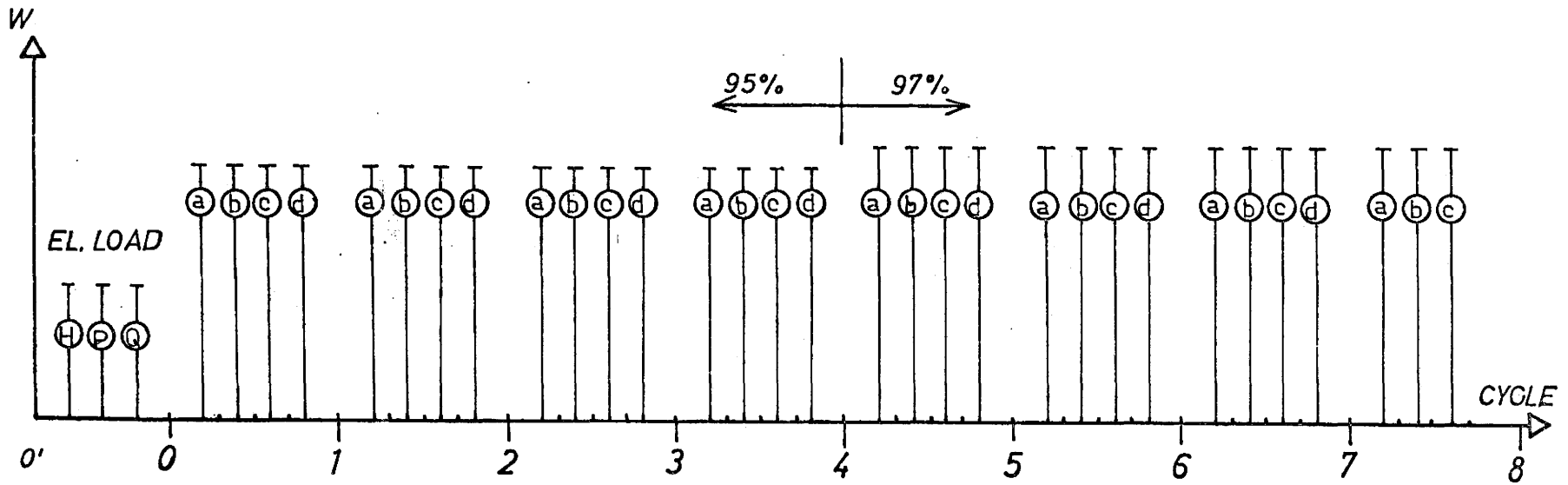

Figure 6.31 Test Procedure for Frame BF-3

in the previous four cycles. Finally, in the eighth cycle under the combination of horizontal load and two point loading in the second beam the horizontal deflection kept increasing continuously while spalling and crushing of concrete on the compression faces of all critical sections were observed. The frame was not able to carry previously attained values of loads, and the sway mechanism was clearly developed. The conclusion to be reached therefore, was that the frame collapsed.

Though the number six bar used as a slanting stirrup in the middle joint did not fail, this corner was still not stiff enough. One of the stirrups in the middle joint made of a number four bar broke during the loading in the eighth cycle. The horizontal deflection of the frame was fairly sensitive to the stiffness of the middle joint. Any wide crack formations or the fracture of a stirrup in the middle joint resulted in a considerable increase in the horizontal deflection. This part of the frame should consequently be considered more carefully since its physical condition deteriorated somewhat.

With the purpose of making the testing procedure faster some less important readings of demac point gauges and dial gauges were omitted.

The load cells, demac point gauges and dial gauges during the test performed well and therefore the test procedure seemed to be quite successful.

6.4.2 The Test Results of Frame BF-3

For the test results a comparison with theory was made for horizontal deflections and strains.

The horizontal deflection versus loading cycle curve is plotted in Figure 6.32. Curves 1 and p drawn by full line were obtained from the results and comprise the envelope of deflection within load limits. Curves 1 and p drawn in Figure 6.32 by dotted line are from theoretical calculation. The top curves 1 were drawn by connecting points corresponding to the deflection under maximum loads, while curves p connect points representing permanent deflections when a no load condition applies. At the beginning of the test some elastic readings were taken and they are represented by curve e in the range from 0' to 0. in Figure 6.32.

As mentioned in the previous section, the first four cycles utilized only 95% of calculated values of loads and 97% starting at the fifth cycle. In the fifth and subsequent cycles not all readings were taken. Dotted lines of the test result curves in the fifth cycle were probably more realistic shapes of curves.

Predicted values of deflection from a computer program were much smaller than those obtained from test as shown in Figure 6.32. There are several reasons for this disagreement, as they are mentioned in connection with test results of frame BF-2. Theoretical calculations were based on the assumption that the structure was made of purely elastic-plastic material with a constant stiffness throughout. In addition, the influence of secondary moments caused by deflection was not included in calculation. This appears to be the main reason for disagreement between theoretical and measured values of deflection.

While the increase in load limits at the fifth cycle did not change the slope of the predicted curves 1 and p significantly, significant changes were observed in the slope of curves 1 and p of the test results. The sensitivity of horizontal deflection on the load limits was much higher in the test than in the theoretical calculation. The increase

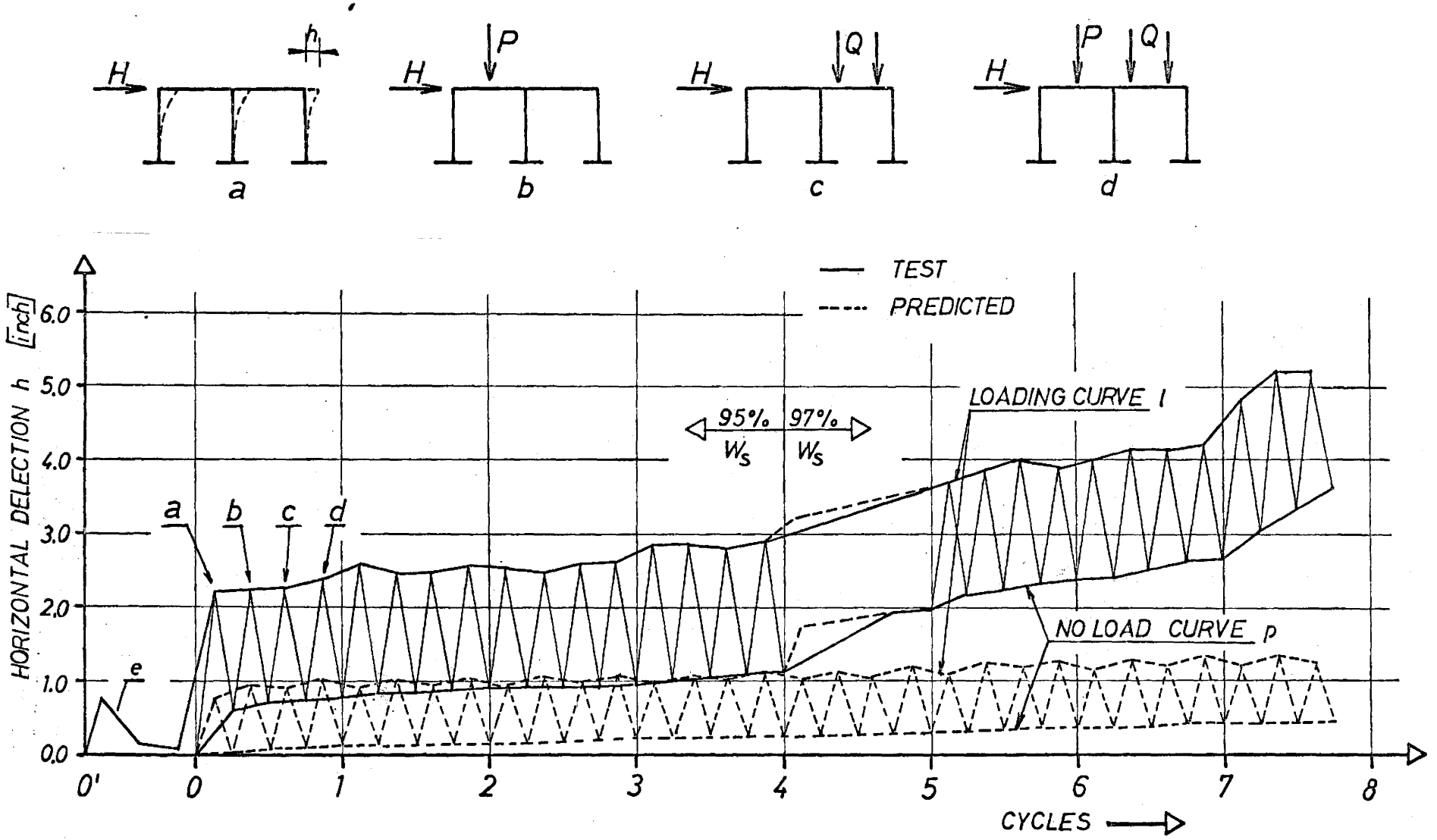

Figure 6.32 Horizontal Deflection Versus Cycle for Frame BF-3

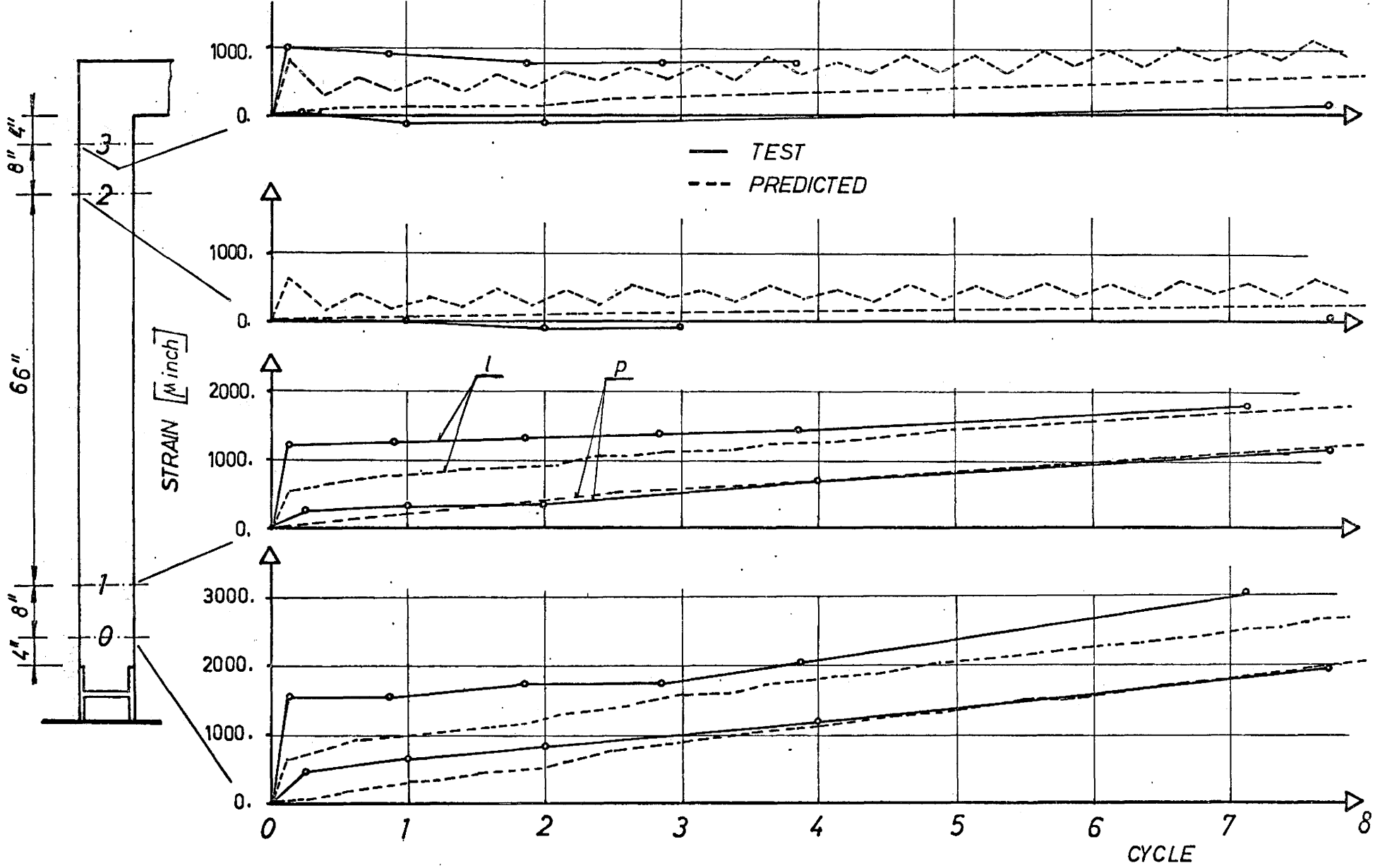

Figure 6.33 Concrete Strains - Theory and Test, Left Hand Column

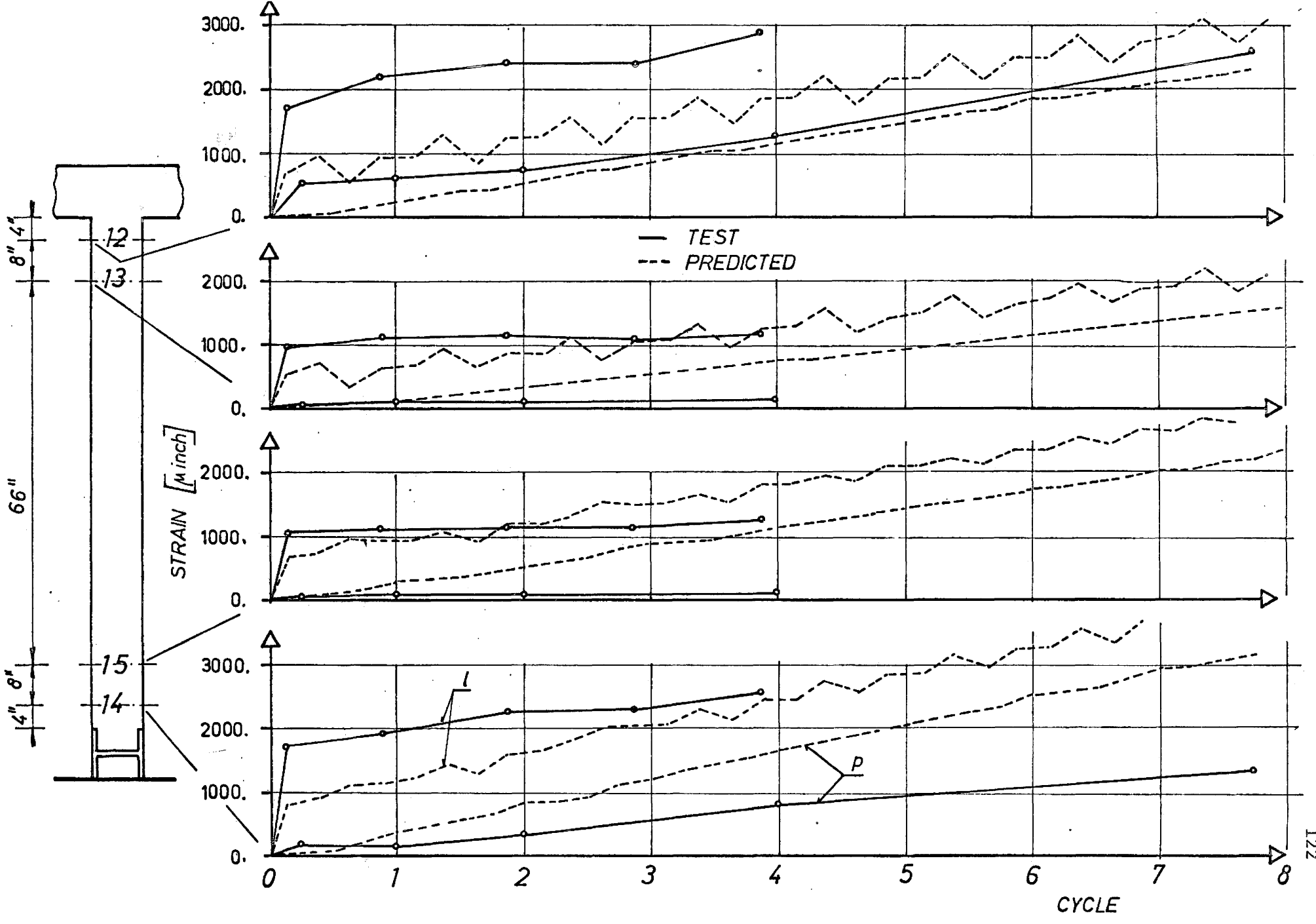

6.34 Concrete Strains - Theory and Test, Middle Column

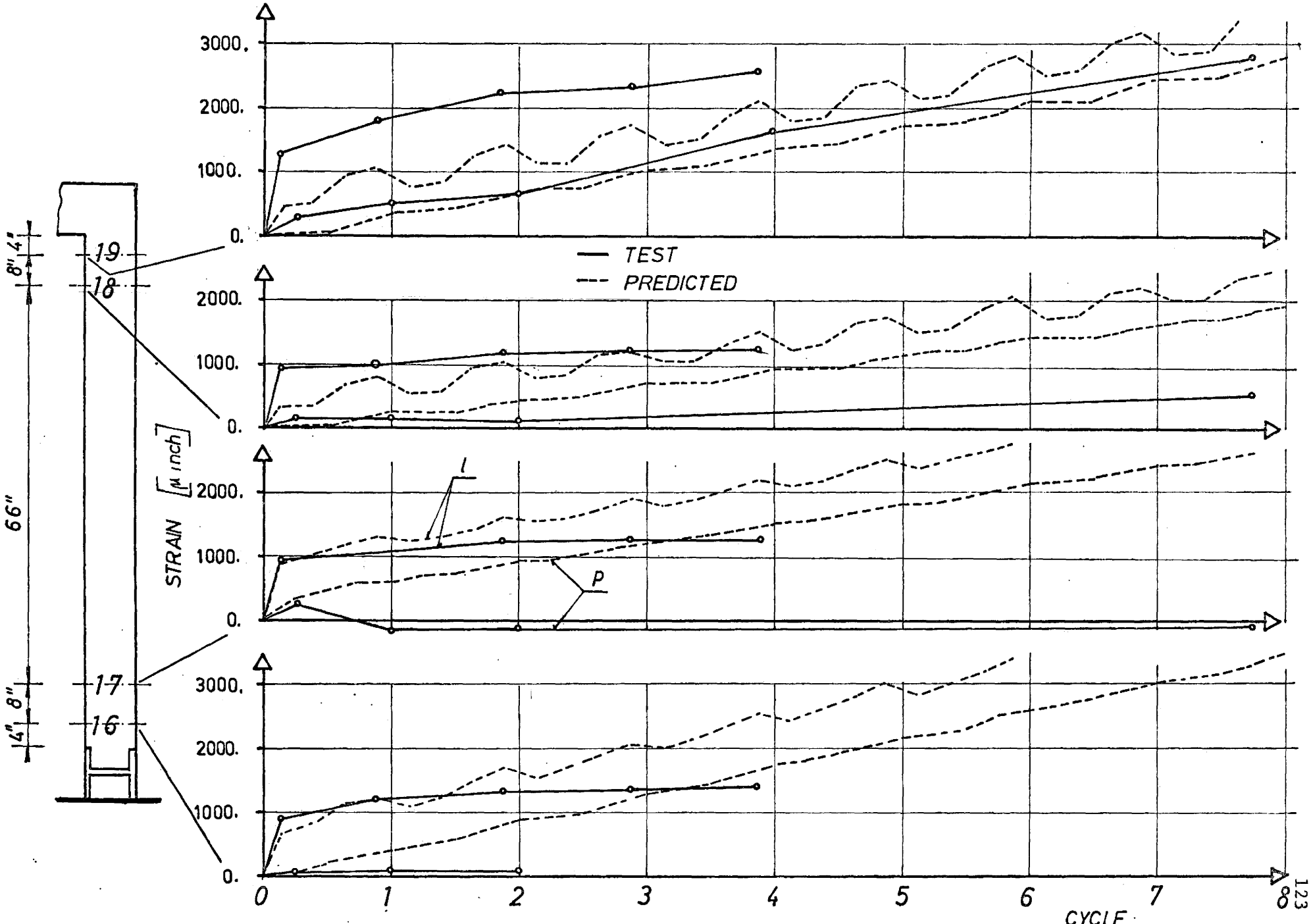

Figure 6.35 Concrete Strain - Theory and Test, Right Hand Column

of loads caused a sudden increase in the permanent deflection, while subsequent loading caused only small increments in comparison. This result is not reflected by theoretical prediction and is likely due to the sensitivity of reinforced concrete frames to variable repeated loading. It seems apparent that standard shakedown analysis is not applicable to such structures unless well-founded modifications can be validated.

In addition to the above high values of horizontal deflection (over 2") it appears to influence secondary moments significantly and accelerates the increase of permanent horizontal deflection almost geometrically.

Strain readings obtained from demac point gauges are compared with predicted strain values in Figure 6.33-35. The method for predicting concrete strains is described in Chapter VII.

7.5.1 Test of Frame BF-4

Frame BF-4 was tested under proportionally increasing loads similar to that of frame BF-1. Comparing the test of these two frames several changes were made in the design of frame BF-4 and to its bases.

The wideflange steel end bases of the concrete columns were welded directly to the one inch thick plate of the lower bases and no electric resistance strain gauges were used. Longitudinal reinforcing bars were welded to the web of the wideflange steel bases as well as to the one inch thick plate of the lower base as shown in Figure 4.4 b by the dotted line.

The cage in the case of frame BF-4 was made of two seperate units forming U and L shaped configurations as shown in Figure 6.36. These two parts were connected at the middle joint by wires and stirrups to form one unit which could be handled by an overhead crane. The composite cage with the middle joint detail is shown in Figure 6.36. Considering moment equilibrium of the middle joint during or near collapse it is clear that the end of the second beam transfers a small moment in comparison to the other members framing together. The joint therefore does not require full moment capacity at the second beam junction to carry the applied load combinations. It was sufficient therefore to reinforce the middle joint in the manner shown.

The test procedure was similar to that of frame BF-1. The loads were increased proportionally up the collapse value of the frame. Dial gauges and demac point gauge readings were recorded after each load increment. A plot of loading procedure including values of loads is shown in Figure 6.37.

The frame collapsed when the value of W reached 8.3 kips. Under this load it was observed that the horizontal deflection increased continuously and crushing and spalling of concrete on the compression faces of critical sections took place.

For proportional loading it is clear that the middle joint as constructed for frame BF-4 behaves well and does not deteriorate the overall carrying capacity. This type of design would not be sufficient for variable repeated loading, however, and needs further study in this regard.

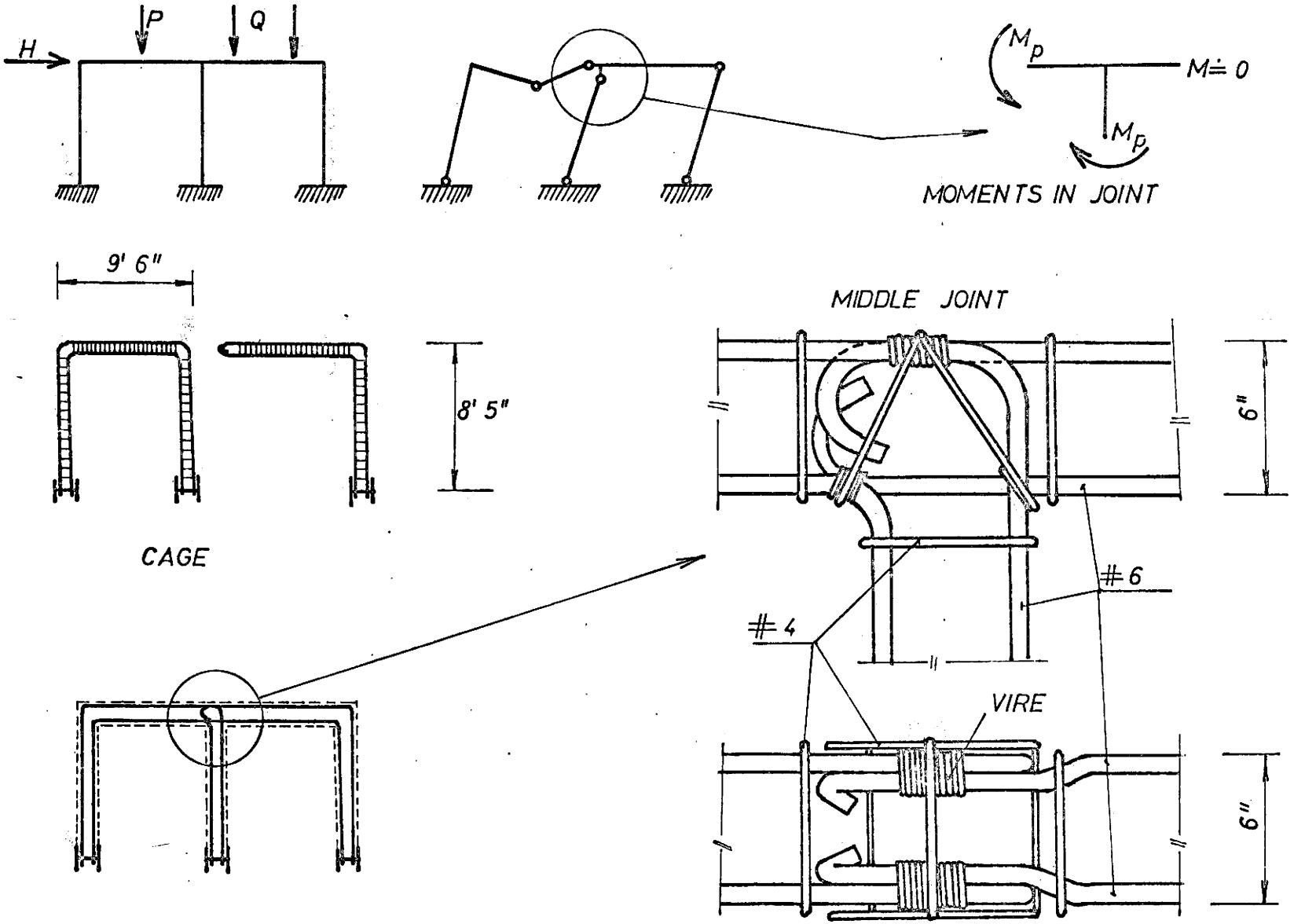

Figure 6.36 Frame BF-4, Middle Joint Detail

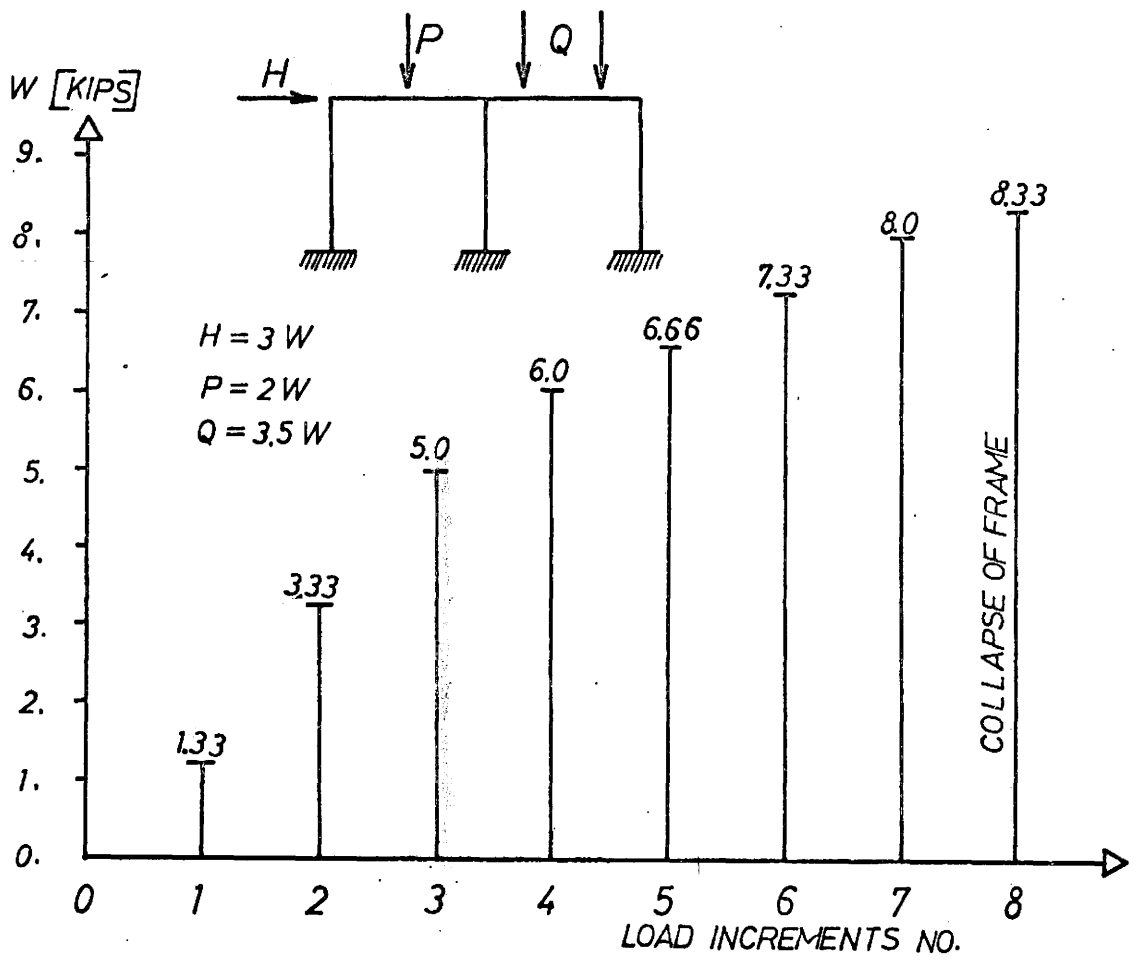

INCRE-MENT	LOADS [KIPS]		
	H	P	Q
1	4.	2.66	4.7
2	10.	6.66	11.65
3	15.	10.	17.5
4	18.	12.	21.
5	20.	13.3	23.3
6	22.	14.6	25.7
7	24.	16.	28.
8	25.	16.6	29.15

Figure 6.37 Loading Program of Frame BF-4

6.5.2 Test Results of Frame BF-4

The horizontal deflection versus horizontal load obtained from the test was plotted and in Figure 6.38 is represented by curve a. The curve b of the figure represents values of predicted theoretical deflection versus horizontal load. The average values of horizontal deflection on the top of the three columns were taken to decrease the error caused by innacuracy in the dial gauge readings.

Though the collapse load of the frame was 10.6% higher than load predicted by the computer program, the horizontal deflection from the test results was in quite good agreement with theory. From both results it is apparent that a plateau region is reached at a horizontal deflection between 1.1 and 1.3 inches. Upon reaching this critical horizontal deflection the increment of horizontal deflection is considerably more sensitive to the increment of loads. After this point the horizontal deflection was increasing much more rapidly until collapse of the frame occured. While the theoretical deflection corresponding to incipient collapse was almost three inches the measured horizontal deflection from the test was about 3.5 inches. This is not considered to be a significant difference because it was not possible to take a reading at precisely the time when the plastic collapse mechanism developed.

The change in the design of the middle joint made for a stiffer connection in comparison to previous frames and this together with the influence of steel strain hardening could be the cause of the higher carrying capacity of the frame. As a result higher curvatures were achieved with the ultimate moment capacity of the section. Strain hardening did not appear to increase the moment capacity of the section significantly and it was not considered in the calculation.

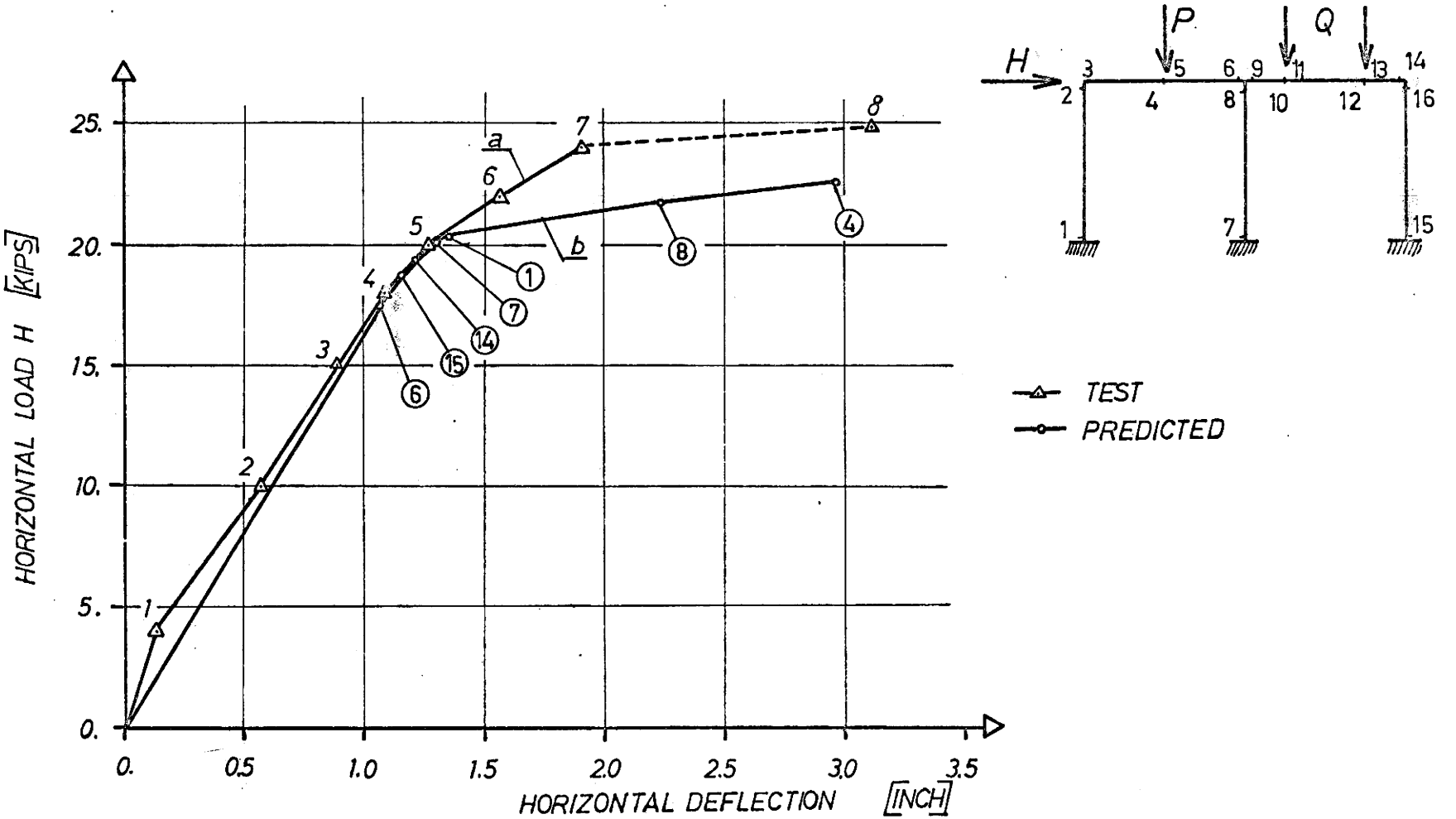

Figure 6.38 BF-4 Horizontal Deflection Versus Horizontal Load

The influence of the joint details plays a more significant role in the carrying capacity of the frame. It is difficult to take this influence into account in determining the carrying capacity and limiting horizontal deflection and therefore this detail was neglected.

There are also differences in the sequence of plastic hinge formation during proportional loading between theoretical calculations and test observations. Referring to Figure 6.38 a, where critical points are assigned numbers 1 to 16 (numbers 2,3 and 4,5 and 10,11 and 12,13 and 14, 16 are always only for one point) the first hinge formed at point 6. This was the same for both the theoretical calculation and test observations (based on strain readings).

Theoretical hinge formation was in the sequence: 6,15,14, 7, 1, 8 and 4. Hinge formation from test was ordered: 6, 16, 8, 15, 7, 1 and 4.

In the theoretical approach the plastic hinge was assumed when the plastic moment capacity was reached while the influence of axial forces was considered. From the test results the strain readings were used for calculating curvature. If the curvature was greater than a critical curvature the plastic hinge was assumed to have formed. This critical curvature was based on the moment-curvature relationship and defined to be that value for which the tangent line at a curvature corresponding to a concrete strain of 0.003 inch/inch intersects the extrapolated linear elastic line at small initial strains. A graphical portrayal of this value is shown in Figure 2.4 and is closely associated with that curvature at which plastic straining in the tension steel starts.

For further details see section 2.3. Though the strain reading could not be taken at the same time as the associated hinge started

to form, the sequence of hinge formation was traced quite readily through critical curvature evaluation.

For the test the first three hinges formed at the tops of the columns or in the beams respectively and later in the bases. In the theoretical approach a hinge formed at the top of one of the columns and was followed by a hinge at one of the bases. Though the base rotations were not significant in terms of plastic collapse load it could cause a change in the sequence of hinge formation. Some flexibility of the bases can be used to explain the hinge formation observed in the experiment. Small rotations of the bases cause a sufficient distribution of bending moments to the top of columns so that higher bending moment are induced there as compared to the rigid base connections.

Bending moments were calculated from strain data and the moment-curvature relationship. For different loading stages the calculated bending moments are plotted in Figure 6.39-40.

A comparison between theoretical and observed bending moments (based on demac point readings) is illustrated in Figure 6.41-45, for proportional loading. Reference is made to horizontal load as the load parameter to be consistent with earlier load-deflection data.

Results of this test confirm the predicted carrying capacity of reinforced concrete frames under proportionally increasing loads and indicates that a somewhat higher capacity can be anticipated than is predicted by conventional rigid plastic analysis or by the somewhat more refined elastic-plastic solution incorporating a hinge formation history, described in Chapter VII as elastic-plastic hinge method.

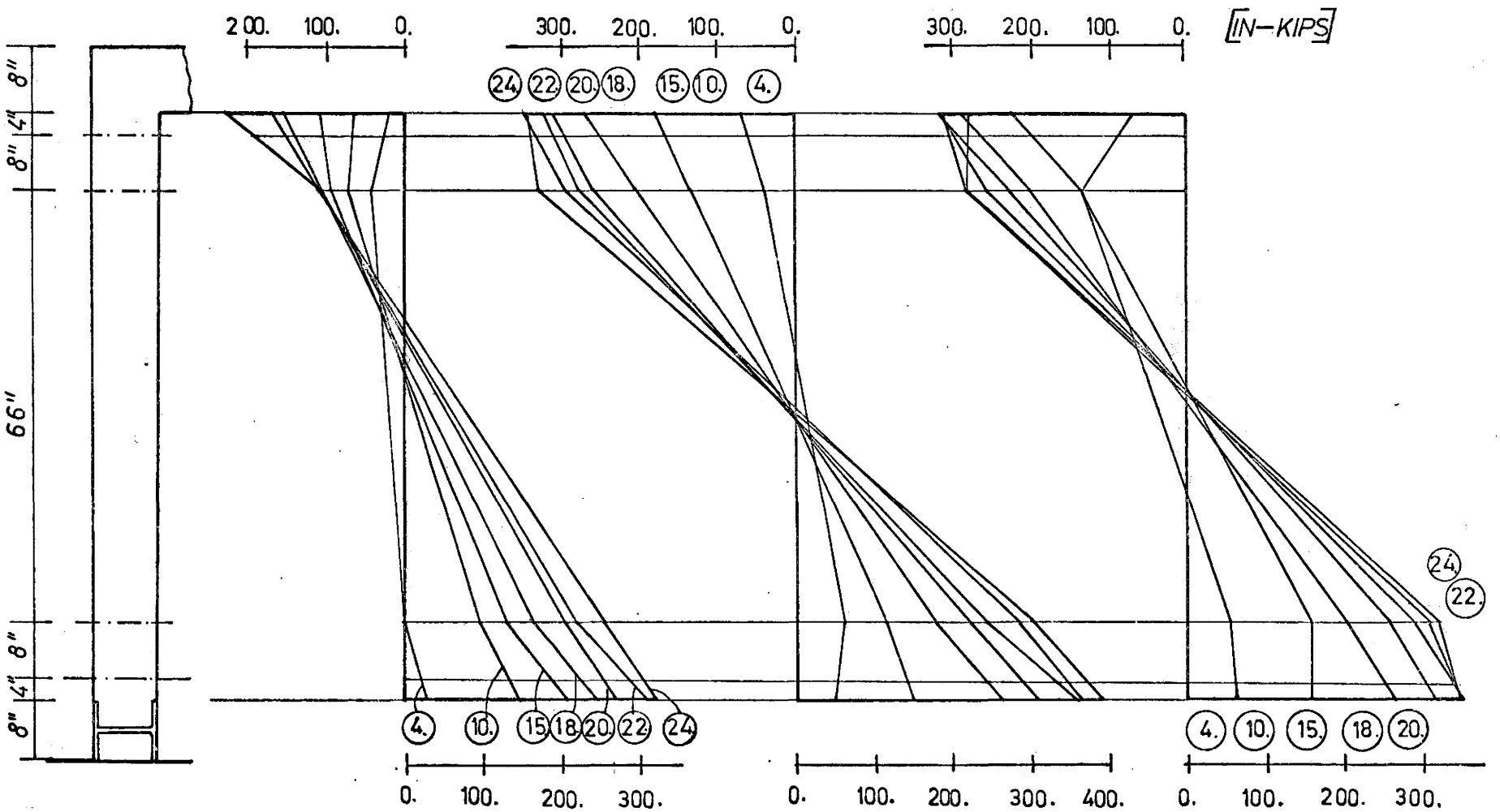

Numbers Refer to Horizontal Load H = 3W

Figure 6.39 BF-4 Columns Moments from Demac Points (for Proportional Loading Case)

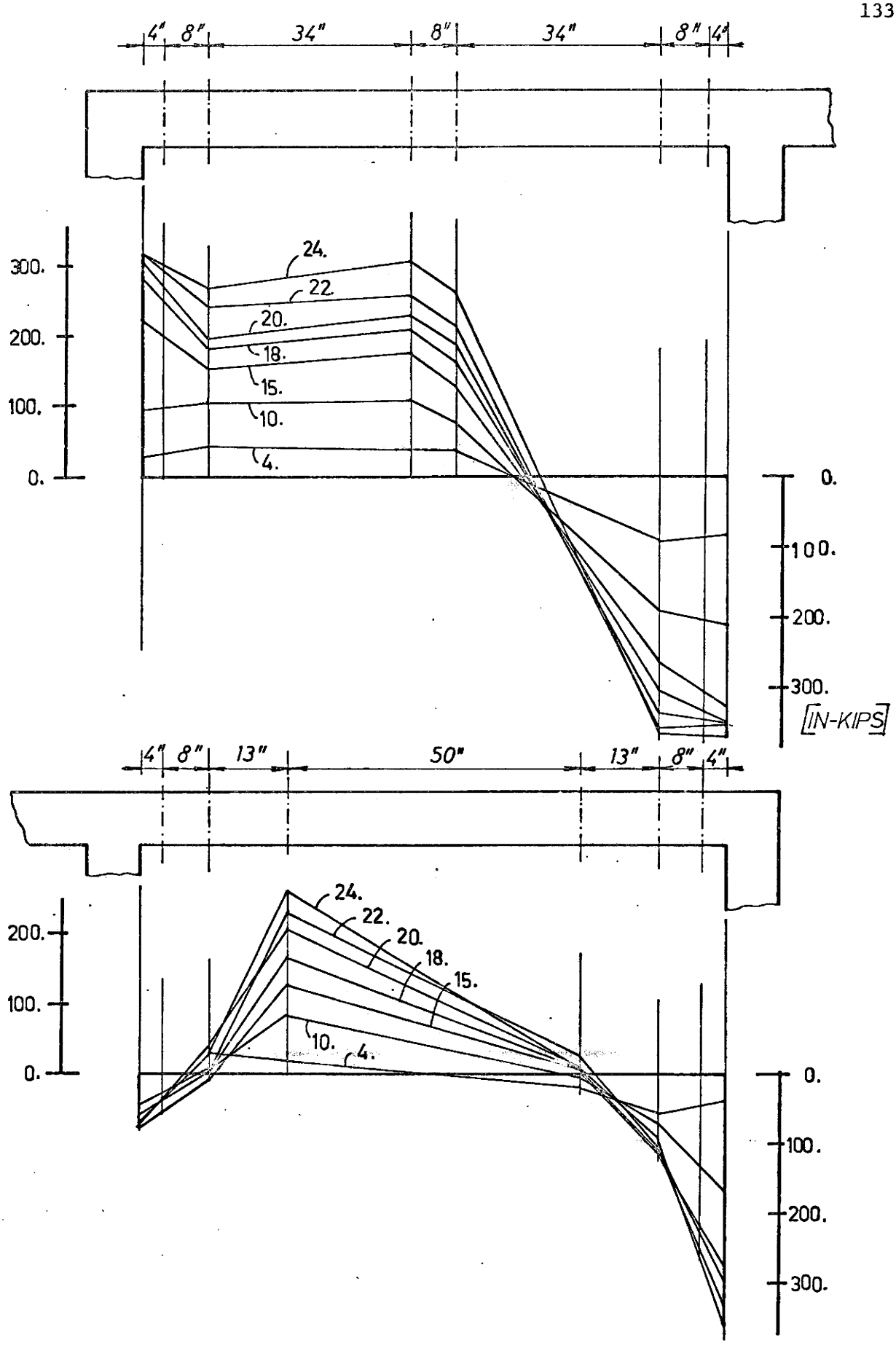

Figure 6.40 BF-4 Beam's Moments from Demac Points

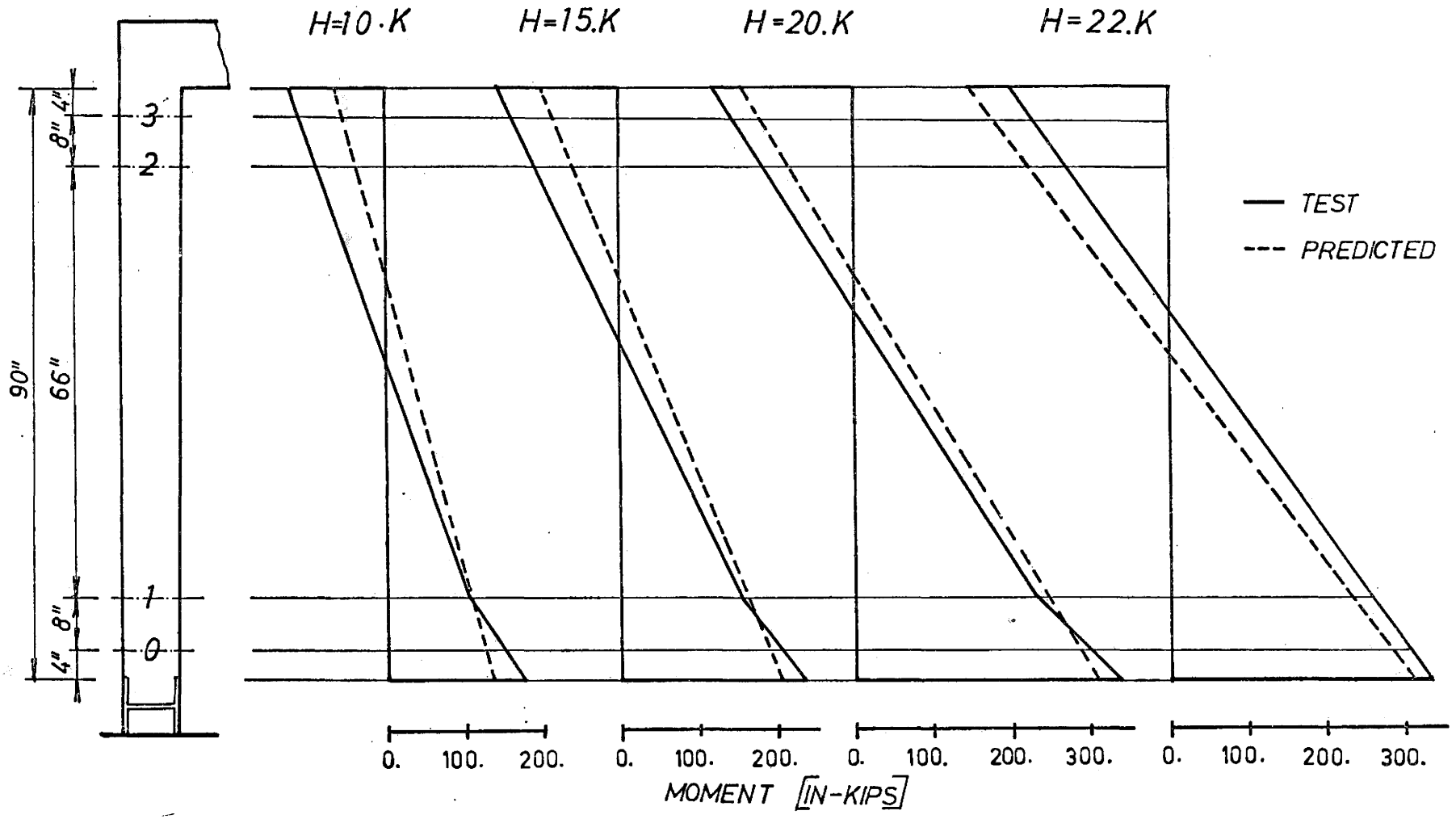

Figure 6.41 Comparison of Bending Moments for Proportional Loading Case BF-4, Left Hand Column

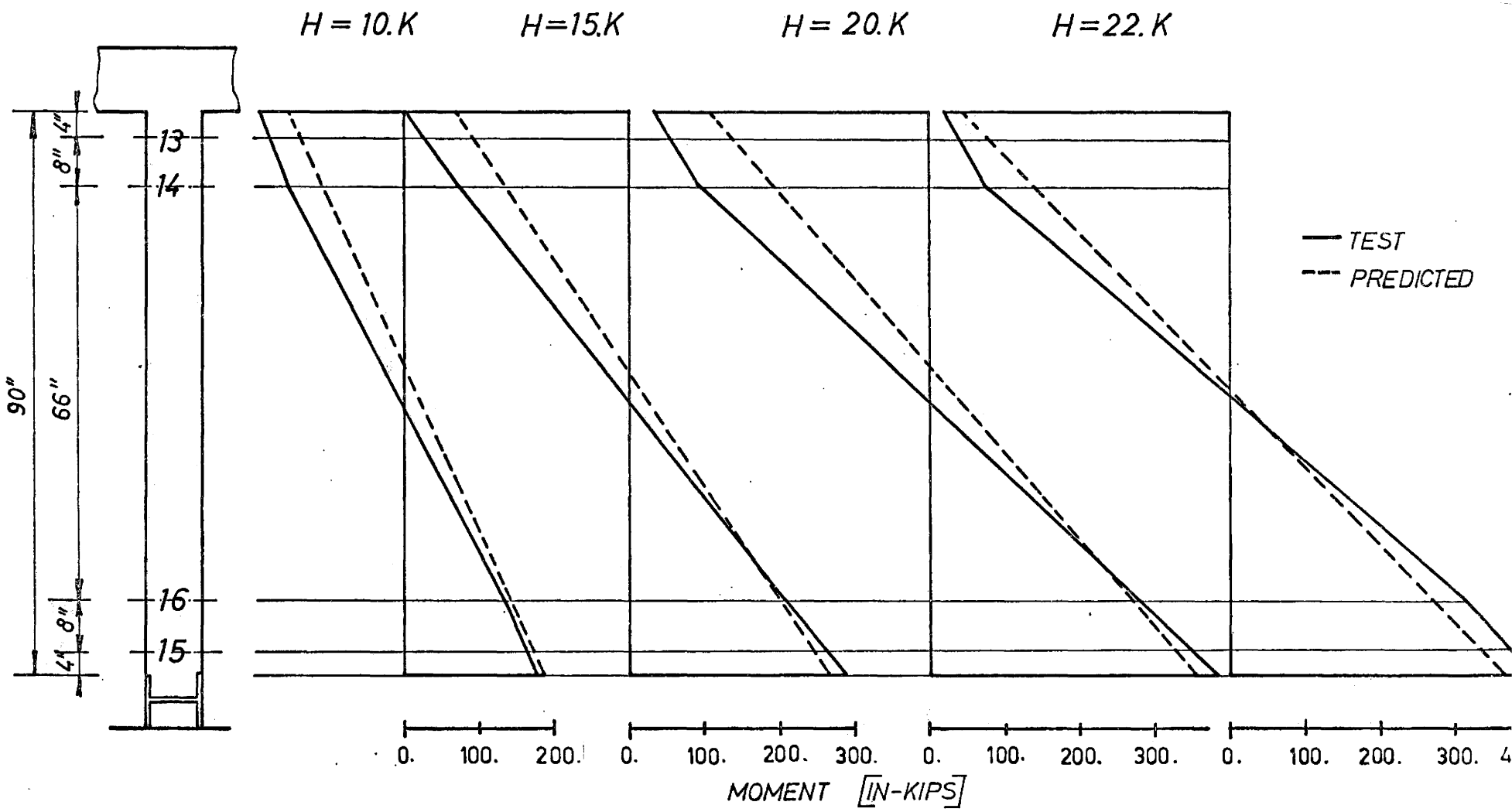

Fibure 6.42 Comparison of Bending Moments for Proportional Loading Case BF-4, Middle Column

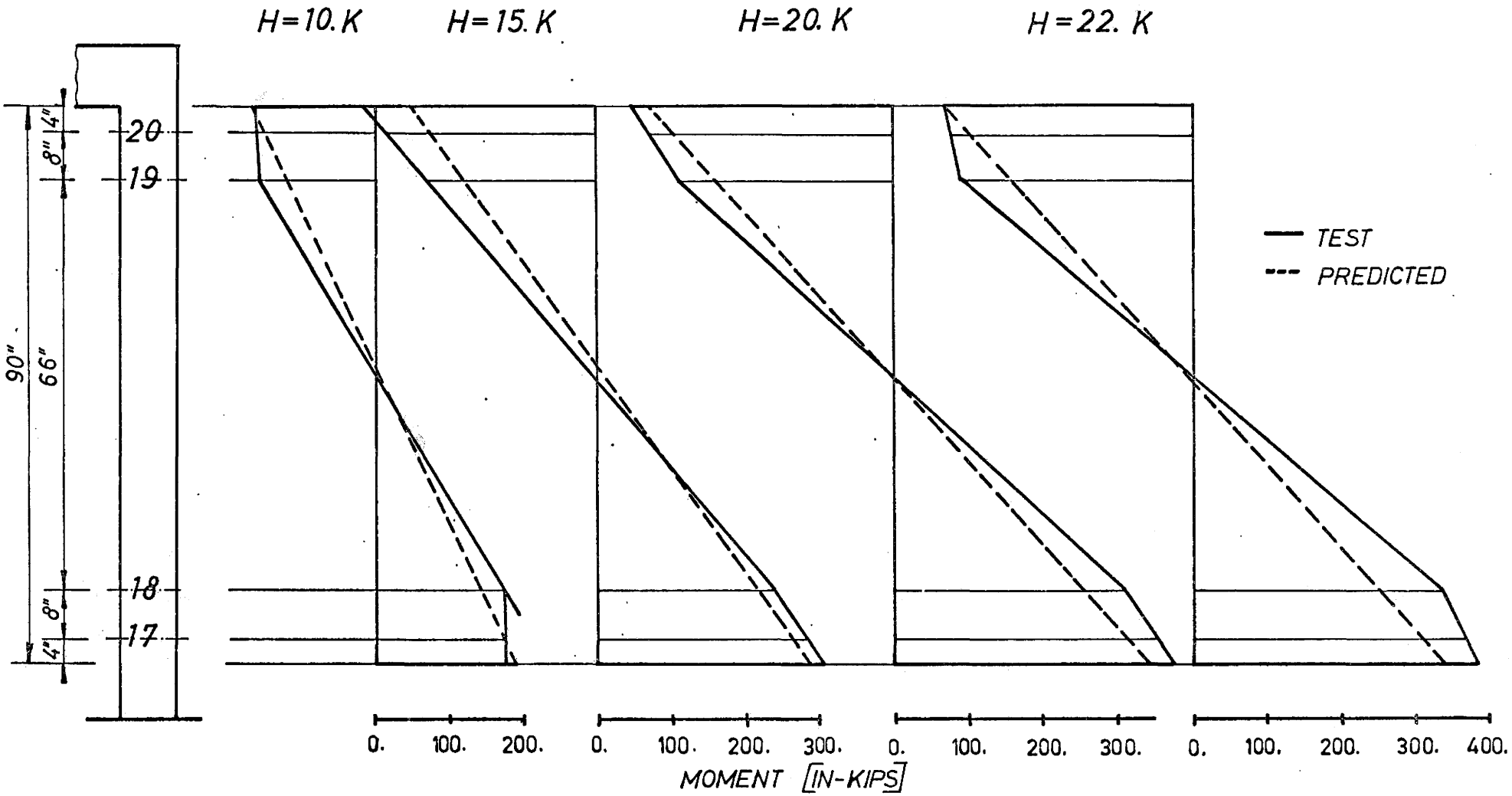

Figure 6.43 Comparison of Bending Moments for Proportional Loading Case BF-4, Right Hand Column

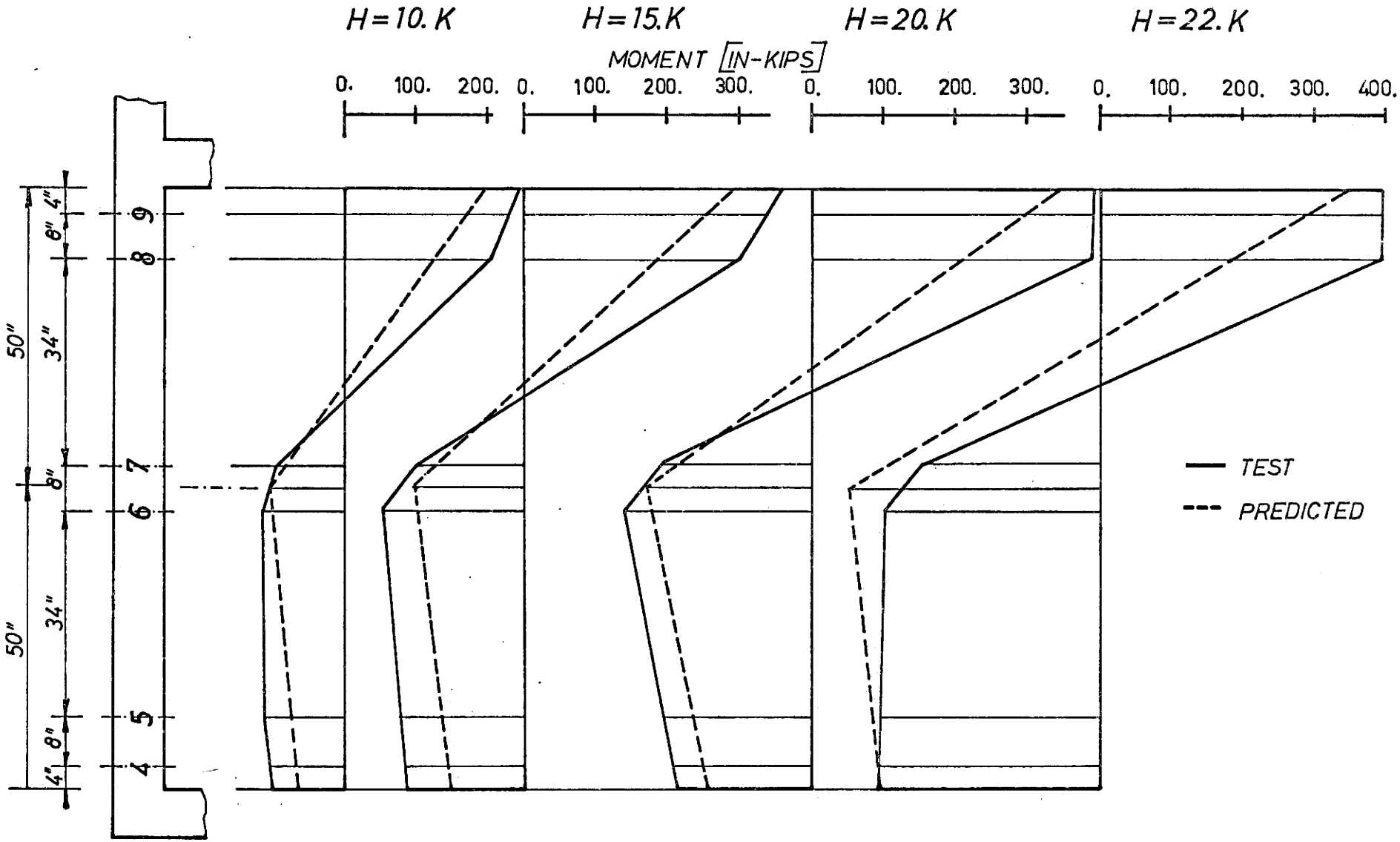

Figure 6.44 Comparison of Bending Moments for Proportional Loading Case BF-4, Left-Hand Beam

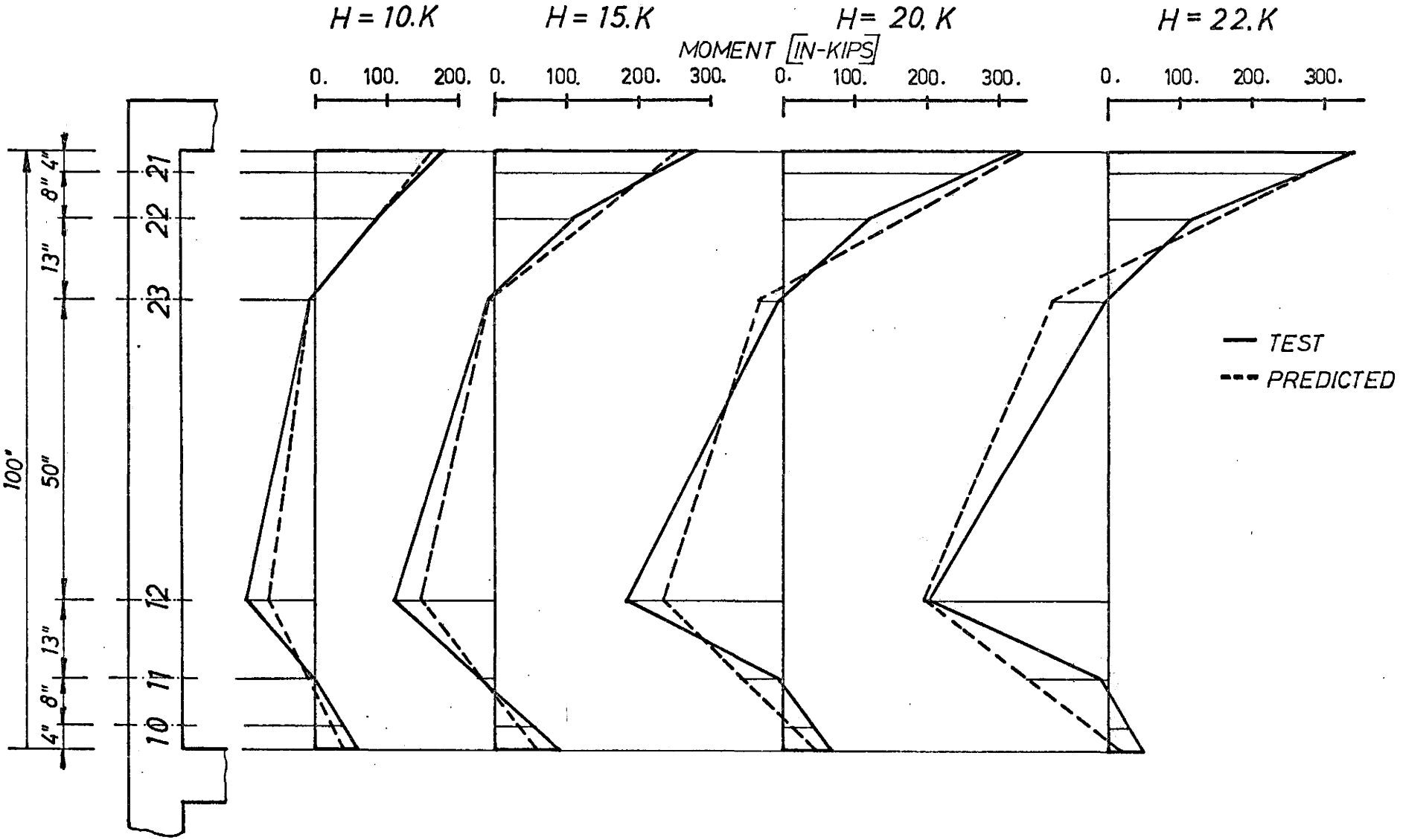

Figure 6.45 Comparison of Bending Moments for Proportional Loading Case, BF-4, Right-Hand Beam

6.6 Discussion of Test Results

Results from the series of tests opened up several interesting questions which need to be discussed.

The size of the models used in this study requires comment. Full-scale models have several advantages. One of the most important ones is close behavior to real structures in terms of material properties, and fabrication. Another advantage is that the errors of inaccuracy in fabrication are reduced and readings of strains and deflection are more accurate. The disadvantages of full-scale models is that fabrication and handling are quite difficult in laboratory conditions. Also the cost is usually much higher than for small-scale models. The latter is significant if some of the tests are unsuccessful due to technical difficulties. This was essentially the case for the test of column C-1 and partly in testing of frame BF-1. A more effective solution would probably have been to test several small-scale models first and then to make a full-scale model. The probability of success would be much higher in such a case. On small-scale models the design of the model, its loading procedure and monitoring methods could be developed, while the prototype model would give more accurate results. Such a process may be balanced, however, by the time to complete such a program.

In all tests deflection was a very important factor. The horizontal deflection was the essential indicator of behavior of the frame. In general, the horizontal deflection reached much higher values in the case of repeated loading than in the case of proportional loading. While for the proportional loading case the horizontal deflection at the time of collapse reached about three inches, the case of repeated loading yielded a horizontal deflection at the time of collapse of about five

inches. Such a deflection is quite important, because the effect of secondary moments becomes significant. Tests showed that under repeated loading the horizontal deflection increased after each repetition of loads. This leads to the following conclusion for the repeated loading case. If values of loads are high enough to cause permanent deflection after each repetition of loading and the increment of deflection does not decrease with subsequent cycles then the collapse of a reinforced concrete frame will occur after a certain number of load repetitions due to "acceleration to collapse" (mentioned in Section 6.4.2). Values of loads for the test conducted are less than or equal to those calculated by the method of plastic analysis for incremental collapse.

Another interesting point is a comparison of deflection between the proportionally loading case and the first load applied of the repeated loading case. While in repeated loading the horizontal deflection under the first load (horizontal load H = 3W) was in both tests (BF-2 and BF-3) about 2.2 - 2.3 inches, proportional loading under the same horizontal load (but also the vertical loads were applied) only about 1.1 of inch as shown in Figure 6.26, 32 and Figure 6.38.

There are several reasons for this significant difference in horizontal deflection. Both frames (BF-2 and BF-3) were designed and fabricated in the same way, while the frame BF-4 (because the frame BF-1 is not included in the comparison) had the middle joint detail altered (see the section 6.5.1 and Figure 6.36) which increased the stiffness of the entire frame. As described in Section 2.3 axial forces play an important role in the moment capacity of the section. For proportional loading case axial forces were high enough (15 - 20 kips) to increase

the plastic moment value of the columns section and caused the frame to remain elastic for higher loads. In the case of repeated loading the first loading included only the horizontal load, the axial forces of the columns not being high enough to increase the plastic moment values significantly. Some plastic hinges developed and this resulted in higher horizontal deflection.

The influence of axial forces on the plastic moment capacity could be explained also by the higher plastic collapse load of the frame under proportional loading. Calculated by the plastic method of analysis by using the plastic moment value 312.0 inch-kips for zero axial force the calculated value of the plastic collapse load was shown to be 6.75 kips (see Section 2.2). By considering the influence of axial forces the plastic moment capacity could reach a value of 360.0 inch-kips and would, therefore, change the value of the calculated plastic collapse load to 7.8 kips. This value is about 15% higher than the case without axial forces. This result is somewhat of a simplification of course because the axial forces varied in each member. The plastic collapse load for the test frame BF-4 was found to be about 8.33 kips which is 24% higher than predicted by method of plastic analysis. By considering the pure elastic-plastic material and also the influence of axial forces on plastic moment capacity the calculated value of plastic collapse load is 7.49 kips (see Figure 6.38). This is still about 10% less than the value obtained from the test.

Two factors were responsible for this error between predicted and test values of plastic collapse load. Firstly, the moment-curvature relationship for reinforced concrete is not precisely an elastic-plastic type as considered in the calculation of predicted values. By following the

results of column C-2 the moment capacity increased with higher curvature, which accounted in part for the increase in the collapse load.

Secondly, the stiffness of the joint connection which was not considered in calculation of predicted values influenced the frame carrying capacity.

A reverse situation was true for repeated loading cases, where the predicted values of shakedown load were higher than values obtained from the tests. The calculation of predicted values was made with and without the influence of axial forces. The effect of secondary moments was not considered which could, because of higher deflection have caused quite a significant reduction in carrying capacity. From both methods (with and without influence of axial forces) the predicted values of load as well as the number of cycles associated with incremental collapse were higher than those from test results. An exception was the horizontal deflection which greatly exceeded predicted values.

What accounted for the differences? This question could be answered by several explanations. There is no doubt that the answer lies somewhere in the method of calculation of predicted values. Incremental collapse load and the number of cycles were calculated by elastic-plastic hinge method as described in Chapter VII, with typical moment-curvature relationships for el-plastic material. This is, as mentioned above, not quite true for reinforced concrete structures. Because of the influence of cracking, the reinforced concrete section does not remain the same during loading, which means that the stiffness of the members varies with loading and loading history. Other factors not included in the calculations were the natural characteristics of

concrete such as shrinkage and creep, which are directly related with time. Even before the tension steel in the reinforced concrete section reached the yield point some permanent deformation had already taken place. Loading and unloading curves for moment-curvature diagrams are the different slopes which is of basic importance in evoluting permanent deflection developed during some stage of repeated loading.

All these effects together with secondary moment influence behavior were not considered in the calculation of the number of cycles and the associated incremental collapse load. The method used for the calculation of predicted values could not include all these effects, therefore, some other method such as an elemental loading history method could be more a realistic approach in terms of accurate prediction.

The calculation for predicted values of strain readings was based on moment-curvature characteristics for repeated loading. A method was developed by using the computer technique and is described in Chapter VII. Though the bases of this method were more realistic, the moments used for calculation were obtained by the same method as mentioned above. This was probably the main reason why the predicted values of the strains were not very close to the measured values.

The conclusion made of these tests could be briefly summarized as follows:

a) for proportional loading of reinforced concrete frames the plastic collapse load is higher than predicted by plastic analysis.
b) for repeated loading of reinforced concrete frames the incremental collapse load is smaller than predicted by plastic analysis. However, it has to be mentioned that no limitation of rotation capacity or of hinge length of plastic hinge were considered in calculation.

Chapter 7

DETAILED CALCULATIONS AND ASSOCIATED COMPUTER PROGRAMS

In this chapter the computer programs used for the calculation of predicted values are described. The basic program for solving the planer frames by the matrix method is not described because the method is generally known and the computer program as used during the graduate course "Matrix Method of Structural Analysis" in 1969, at McMaster University is well documented. This program is still available in the Department. Another basic program for the moment-curvature relationship for under reinforced sections was described by R. Danielsen (23) and the reader is referred for details to his master's thesis which is also available.

7.1 Programs Based on the Matrix Method

As mentioned above the computer program for planer frames using the matrix method was used as the basic program for several types of calculations for predicting the collapse load and deflection of test frames.

Input for the program consists of geometric data for the frame, member properties and of the position and values of loads. Output is in the form of forces including moments and the deformations in the plane of the frame at the ends of members.

Since several seperate problems needed solution the program was successively used for elastic solutions for a frame under different load combinations to obtain a table for calculating the incremental collapse load (see Table 2.2).

The basic program was employed to calculate the plastic collapse of the frame by a step by step calculation for the proportional loading case (elastic-plastic hinge method). The method of calculation is based

on the definition of a plastic hinge, in which any rotation is accompanied by a value of moment which remains constant. To account for the constant requirement at hinges a natural type hinge behavior was permitted in the step by step procedure at those critical points where the moments reached the plastic value. Hinge releases were placed at appropriate locations. All forces and deformations were stored at each step and the influence coefficient K was calculated. By multiplication of all force values F and all deformation values by K and their addition to previous values gave final forces and deformations. By this calculation practically the whole loading history of the frame was traced until the frame developed into a mechanism. The method of calculation can be followed from Figure 7.1.

This program was somewhat altered to take into account the influence of axial forces on plastic moment capacity. Because the relationship between axial force and plastic moment as used in the tests is almost linear, a simple linear relationship was used. An iterative process was used for calculation of the plastic moments as a function of axial forces under increasing loads. The equation for relating axial force and plastic moment capacity used in the program is:

$$M_p = 312.0 - 2.5 \times Fa$$

where M_p is plastic moment in inch-kips and Fa is axial force in kips. The value of plastic moment for zero axial force is 312.0 inch-kips.

The same two programs (with and without the influence of axial force) were extended for tracing, cycle by cycle the response to loading to incremental collapse. Unloading of the frame is represented by loads of opposite sign under purely elastic response. As before all the forces and deformations were added after each loading or unloading.

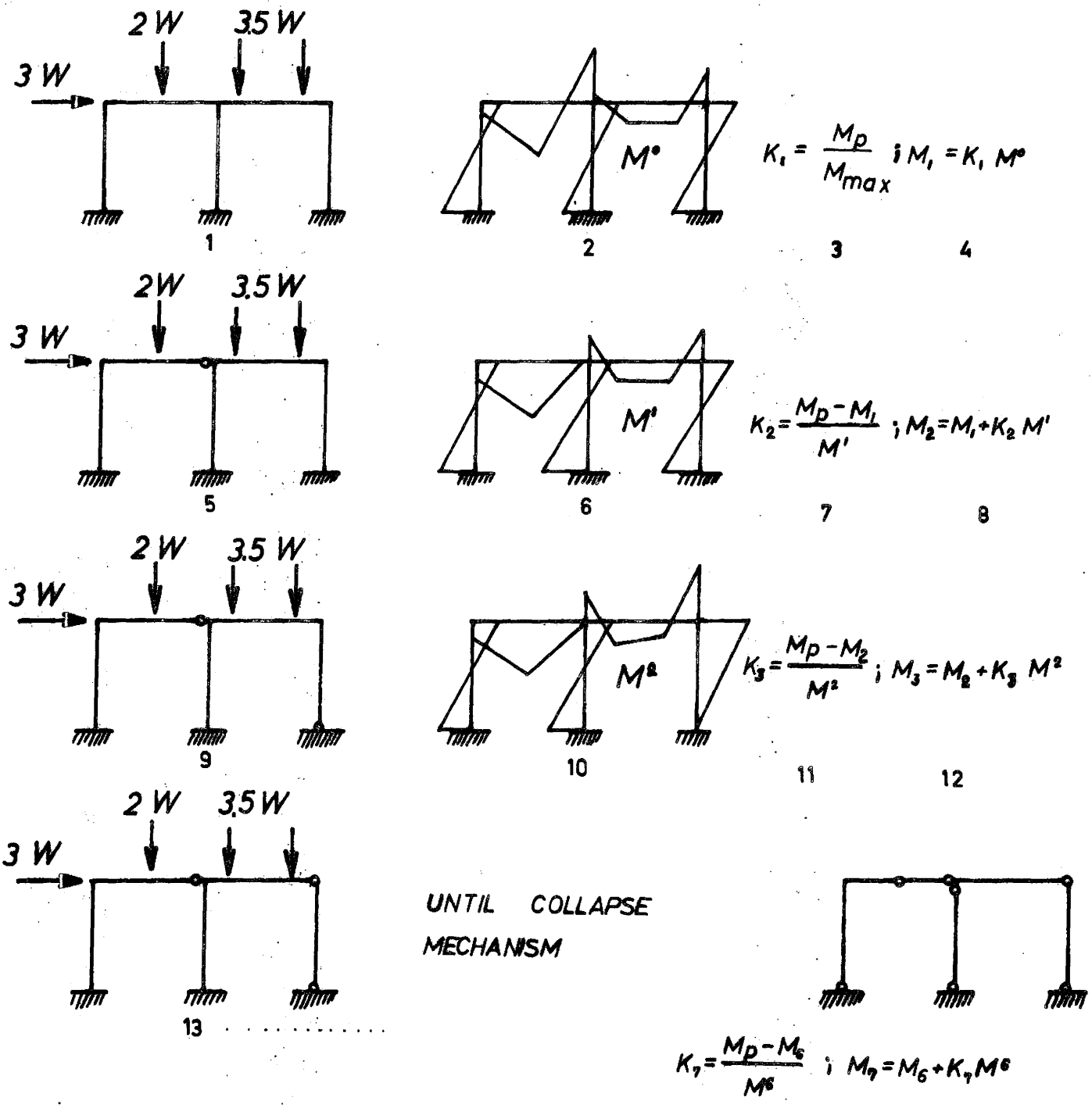

Figure 7.1 Method of Step by Step Calculation Used in Computer Program

For completion flow charts labelled Figure 7.4 and Figure 7.5 are included.

7.2. Programs Based on Moment-curvature Relationship

The moment-curvature relationship program is based on balancing of the equilibrium conditions at a reinforced concrete cross-section. The free body diagram is shown in Figure 6.5. An iterative method was used in assigning position of the neutral axis since the equilibrium condition must be satisfied. For a given concrete strain and axial force only a correct choice for the distance of the neutral axis will satisfy equilibrium requirements. The associated values of curvature are calculated for certain values of strain, starting from a strain of 3000.0 micro-inches and decreasing by small increments to the zero. The program includes influence of shrinkage, axial forces and influence of the tension part of concrete.

The same program with minor changes was used for calculating moment and axial force from the strain data. In this case the inputs into the program was compressive strain and corresponding curvature, while the associated moment and axial force were the outputs.

The above was used as the subprogram for calculating values of strain. The inputs for this program were the moments and axial forces obtained from the incremental collapse load computer program mentioned in the previous section. In the main program the moments were calculated for certain gauge zones by calling subprograms used to predict values of strain readings.

Two of the subprograms worked on the basis of moment-curvature programs as mentioned above. Subroutine XX1 uses a moment-curvature

relationship for an uncracked section including the effects of tensile force in the concrete. Moment and axial force are again the input values while output was curvature and strain. The second subroutine XX2 worked on the same basis except that the cracked section was considered and no effect of tensile capacity of concrete was considered.

The third subroutine XX3 used the method of the transformed area for a reinforced concrete section. While the two first mentioned subprograms were used for calculating strain changes during loading the third was used for calculating strain changes during unloading. Input for this subroutine was the change in moments and axial forces in the section and the position of the neutral axis for a cracked section. By using the transformed area method the stresses and strains were calculated and the latter were added to previous values in the main program.

Due to the loading or unloading the subprograms were called at the required stages.

Typical moment-curvature curves used in the above mentioned subprograms are shown in Figure 7.2 . The point C in Figure 7.2a refers to that point in which cracking of the section occured. The behavior shown in Figure 7.3 is typical of the procedure used in cyclic loading and unloading.

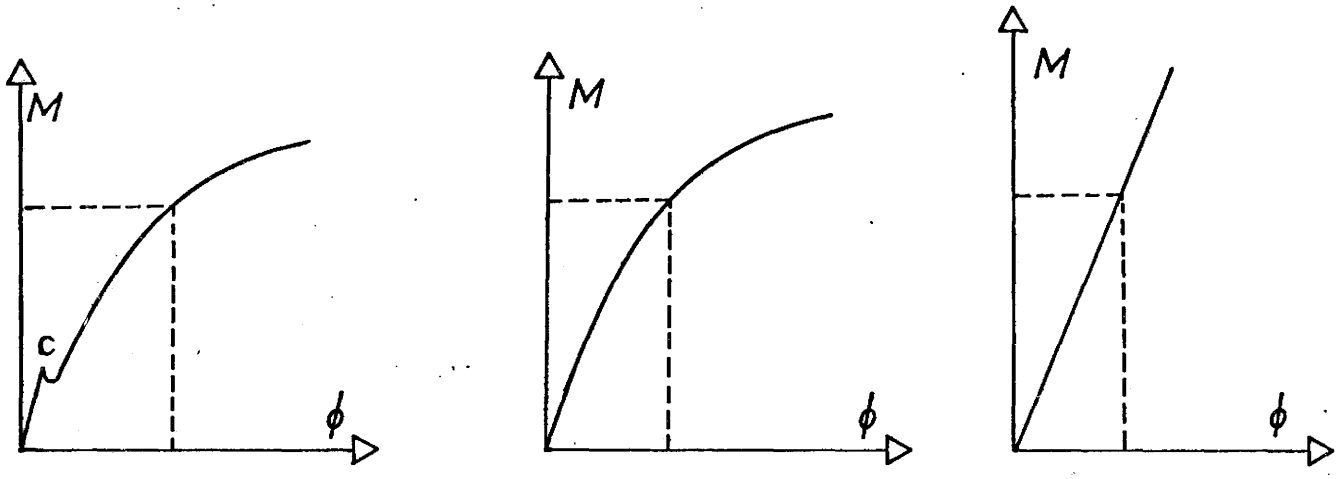

a. Concrete takes Tension

b. Concrete takes Zero Tension

c. Elastic Behavior

Figure 7.2 Typical Moment-Curvature Curves for a. Subroutine XXI, b. Subroutine XX2, c. Subroutine XX3

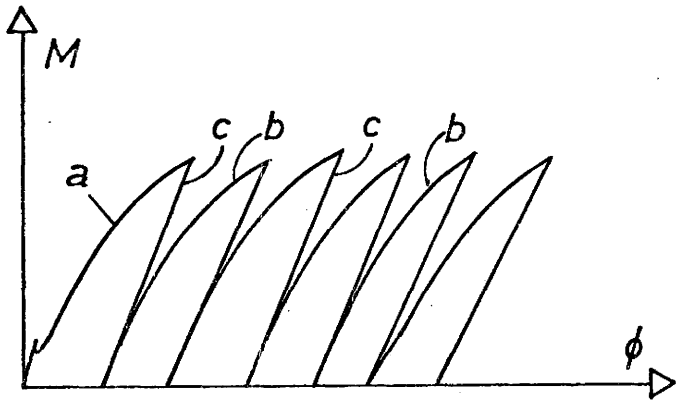

a. from XXi

b. from XX2

c. from XX3

Figure 7.3 Procedure of Calculation for Strain Prediction

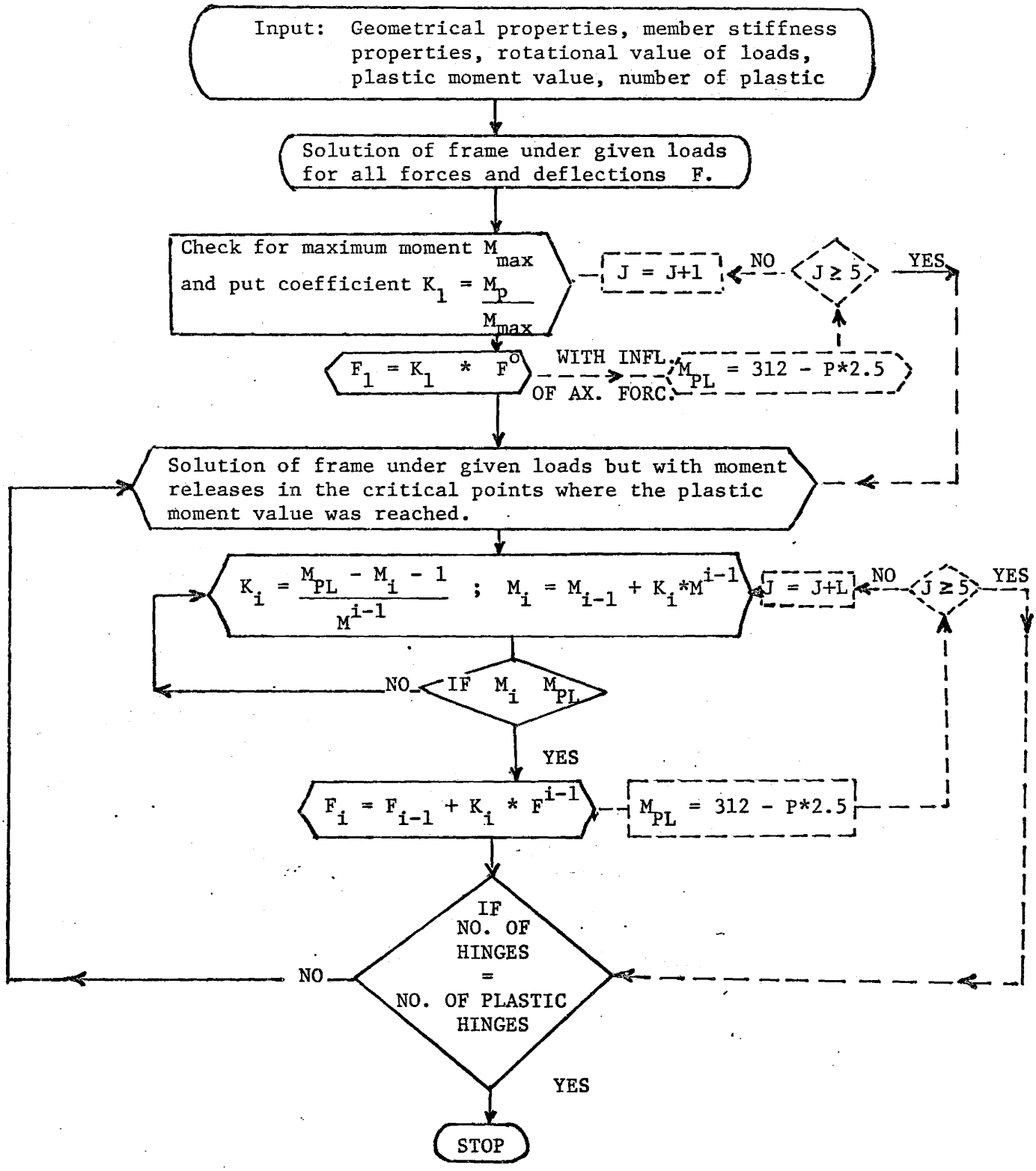

Figure 7.4 FLOW CHART FOR PROPORTIONAL LOADING

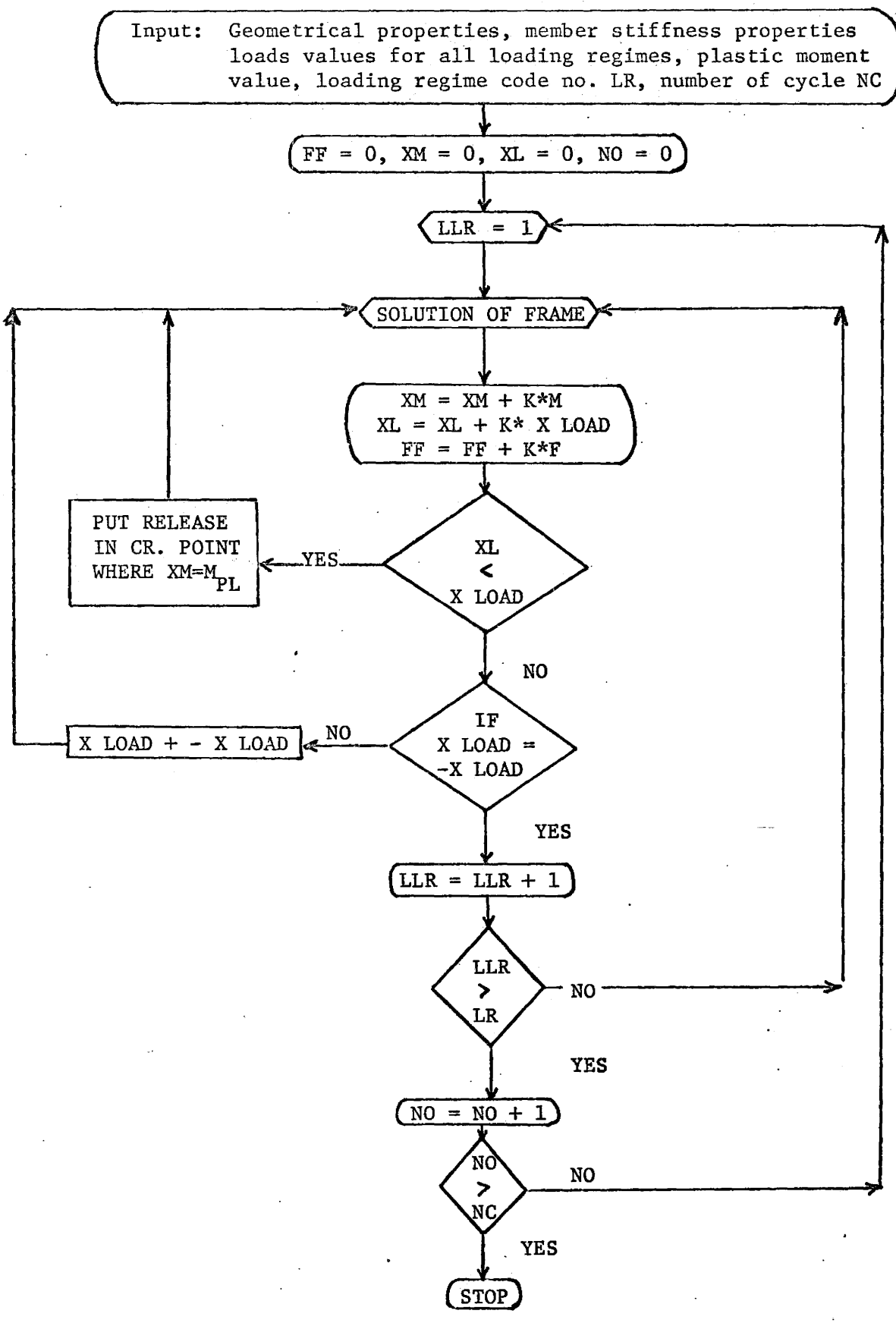

Figure 7.5 FLOW CHART FOR CYCLIC LOADING.

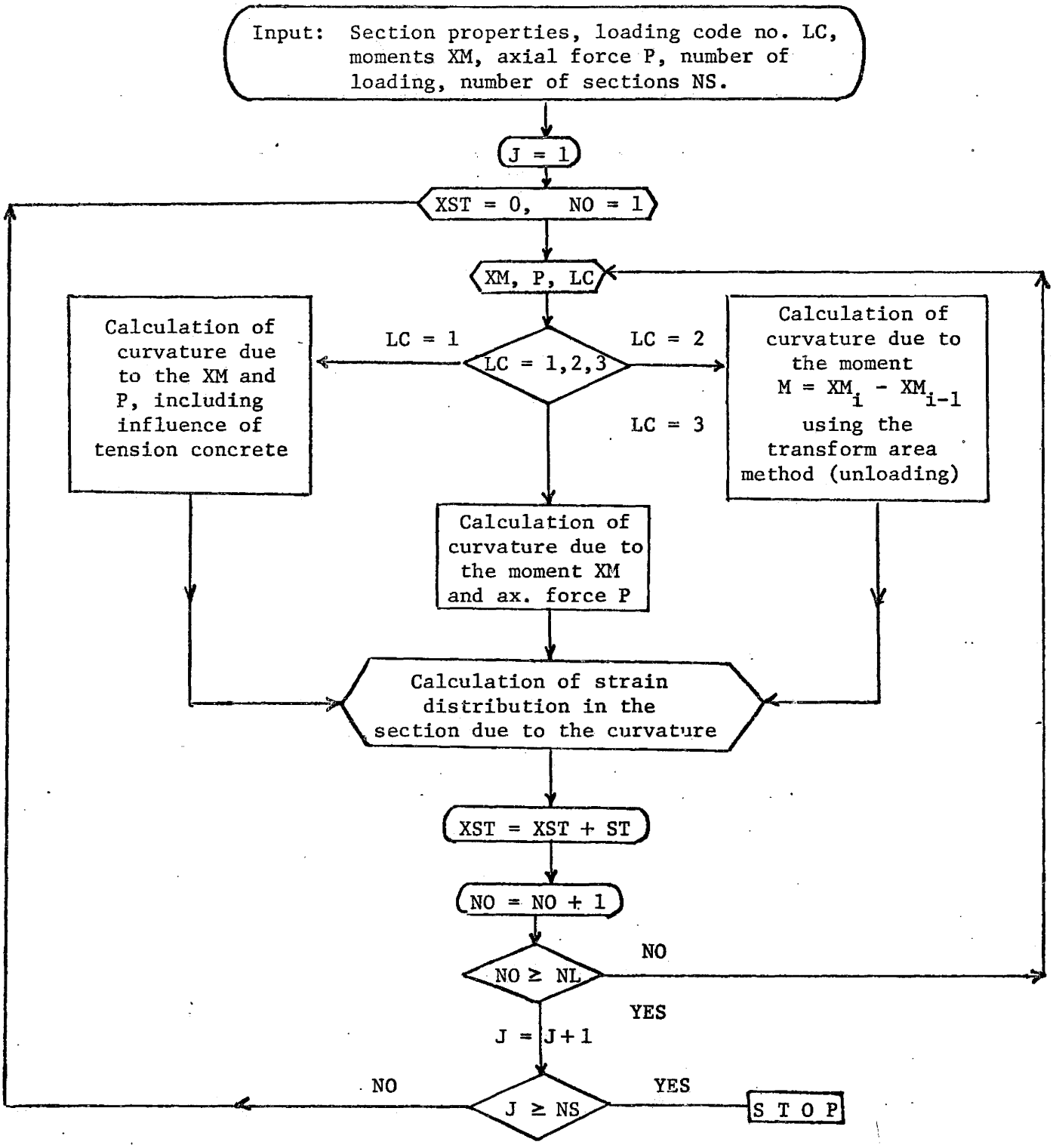

Figure 7.6 FLOW CHART FOR PREDICTED STRAIN VALUES

Chapter 8

CONCLUSIONS

On the basis of the limited experimental results and analytical predictions the following conclusions are made relative to under reinforced structures exhibiting considerable ductility.

The reinforced concrete frame under proportional loading has a carrying capacity which is considerably higher than that obtained by simple plastic collapse load predictions.

In the case of frame BF-4 the collapse load obtained experimentally was approximately 23% higher than predicted by plastic analysis. Even when the influence of axial force on the plastic moment capacity is considered the actual collapse load was still higher by 11%.

The actual incremental collapse load of the reinforced concrete frame considered is near to the value predicted by the simple method of plastic analysis but is more likely to be smaller as evidenced by frames BF-2 and BF-3. The influence of axial force on Mp capacity is not decisive for this case of loading and by taking it into account yields an even higher value for the incremental collapse loads than obtained by the simple theory.

The incremental collapse load for some reinforced concrete structures can be predicted quite accurately by the simple shakedown method of plastic analysis (22). This result does not validate the shakedown theory, however, since a number of compensating factors appear to be responsible. An accurate prediction can only be ascertained by tracing through the loading history on an elemental basis. Since this approach is exceedingly complicated it was not attempted in this work. It is known (24) however, that the stress-strain relation for

concrete under cyclic loading can be an important reason for the incremental collapse load being slightly smaller than that obtained theoretically. Consequently, the ratio of plastic collapse load to incremental collapse load for the reinforced concrete frame studied is somewhat higher than the ratio for the associated steel structure. The ultimate stress of concrete continues to decrease with the number of cycles of loading, while the plastic strain increases. For high concrete stress levels the behavior of reinforced concrete precipitates incremental collapse of the structure at load levels of 65% of the design proportional load limit as compared to 80% for the similar steel structure.

It is recommended therefore, that for proportional loading axial force should be taken into account to determine the collapse load. On the other hand, for variable repeated loading a more accurate prediction for the incremental collapse load is obtained by ignoring axial force effects on the moment capacity since secondary moments are important for such case. The moment capacity increases with axial force up to some critical value. For axial force less than that value, safe preditions of incremental collapse would be forthcoming by neglecting the added moment capacity. Since P-Δ effect (secondary moment) reduces the collapse load, the added moment capacity should be neglected to compensate.

Since the conventional incremental collapse load is associated with a very large number of cycles, the probability of collapse incrementally is likely small unless acceleration to collapse conditions are met. This would not be true for a single storey structure, however. It is more rational to associate a given deflection as being a condition for failure even for structures in which secondary moments are not significant. For such a specified deflection a small finite number of cycles would likely apply and therefore the probability of failure is quite feasible in comparison with failure by proportional loading. For the frames

BF-2 and BF-3 a permanent deflection of three inches is achieved in 5 - 7 cycles. This number is certainly a possibility in considering the lifetime of a structure and especially when the load level is of the order of 85% of the computed proportional limit load.

The behavior of reinforced concrete frames is deeply influenced by the type of joint connection and this is another factor which should be considered in calculation of collapse load.

It must be emphasized that the limited number of tests conducted in this work necessitates confirmation of a number of the conclusions stated above. Sufficient care was taken however, in terms of fabrication and testing procedure that some confidence can be placed in the results nevertheless. The qualitative implications do appear to be valid.

REFERENCES

1.* A. E. H. Love. A Treatise on the Mathematical Theory of Elasticity. Cambridge, 1892.

2.* J. A. Ewing. The Strength of Materials. Cambridge, 1899.

3.* G. Kazinczy. Tests with Fixed-ended Beams. Betonszemble, vol. 2, 1914. Die Weiterentwicklung der Elastizitatstheorie. Technika, Budapest, 1931.

4.* H. Maier-Leibnitz. Test Results, Their Interpretation and Application. Preliminary Publication, Internationale Association for Bridge and Structural Engineering, 2nd Congress, Berlin, 1936.

5.* K. Girkmann. Bemessung fon Rahmentragwerken unter Zugrundel engung eimes ideal-plastishen Stahles. S. B. Akad. Wiss. Wien, 1931.

6.* F. Bleich. Stahlhochbauten, ihre Theorie, Berechnung, und Bauliche Gestaltung, Vol. I, Berlin, 1932.

7. J. F. Baker. A Review of Recent Investigations into the Behavior of Steel Frames in the Plastic Range. Civ, Engrs., 31, 1949. The Steel Skeleton. Vol. II, Cambridge, 1956.

8. H. J. Greenberg and W. Prager. On Limit Design of Beams and Frames. Amer. Soc. Civ. Engrs., 1952.

9. W. Prager. Introduction to Plasticity. Addison Wesley, 1959.

10. M. R. Horne. Fundamental Proposition in the Plastic Theory of Structures. J. Instn. Civ. Engrs., 34, 1950.

11. B. G. Neal. The Plastic Method of Structural Analysis. Great Britain, 1956.

12. L. S. Beedle. Plastic Design of Steel Frames, 1958.

13.** J. E. Coignet, N. de Tedesco. Du calcul des ouvrages en ciment avec ossature metalique. Memoires de la Societe des Ingenieurs de France, 1894.

* Ref. taken from ref. 11

14.** R. M. v. Thullie. Uber die Berechung der Monierplatten. Ing. und Arch., Vereins, 1897.

15. A. L. L. Baker. The Ultimate Load Theory Applied to the Design of Reinforced Concrete Frames. London, 1956.

16. A. H. Mattock. Rotation Capacity of Hinging Regions in Reinforced Concrete Beams. Flexural Mechanics of Reinforced Concrete, 1964.

17. H. A. Sawyer. Design of Concrete Frames for Two Failure Stages. Flexural Mechanics of Reinforced Concrete. Miami, 1964.

18. M. Z. Cohn. Optimum Limit Design for Reinforced Concrete Cintinuous Beams. Inst. of Civil Engineers, Vol. 30, 1965.

19. Hiroyuki, Aoyama. Moment-Curvature Characteristics of Reinforced Concrete Members Subjected to Axial Load and Reversal Bending. Flexural Mechanics of Reinforced Concrete, Miami, 1964.

20. F. Beaufait and R. R. Williams. Experimental Study of Reinforced Concrete Frames Subjected to Alternating Sway Forces. ACI Journal, 1968.

21. G. M. Sabins and R. N. White. Behavior of Reinforced Concrete Frames under Cyclic Loads Using Small Scale Models. ACI Journal, Sept., 1968.

22. K. H. Gerstle and L. G. Tulin. Behavior of Reinforced Concrete Beams Subjected to Cyclical Bending Loads. Revista IMCYC, 1967.

23. R. C. Danielsen. Reinforced Concrete Frame Study under Sustained Loads. Thesis for M. Eng. McMaster University, 1970.

24. B. P. Sinha, K. H. Gertsle, L. G. Tulin. Stress-Strain Relation for Concrete under Cyclical Loading. Journal of the American Concrete Institute, Feb., 1964.

25. Chu-Kia Wang, Ch.G. Salmon. Reinforced Concrete Design, 1969.

** Ref. taken from ref. 15

26. ACI Building Code Requirements for Reinforced Concrete, (ACI 318-63) Chapter 16.

27. J. M. Davies. Collapse & Shakedown Loads of Plane Frames, ASCE Journal of Structural Division, St. 3, June, 1967, p. 35-50.

APPENDIX A1

Uniqueness Theorem of Incremental Collapse

If for a given value of W a corresponding statically admissable distribution of residual bending moment can be found, such that when the maximum and minimum elastic bending moments corresponding to this value of W are added to the residual moment at every cross-section the fully plastic moment is never exceeded, but is attained at a sufficient number of cross-sections to transform the structure into a mechanism if hinges formed at all these cross-sections simultaneously, this value of W must be equal to the incremental collapse load W_s.

B. G. Neal: The plastic method of structural analysis, 1965, p. 298.

APPENDIX A2

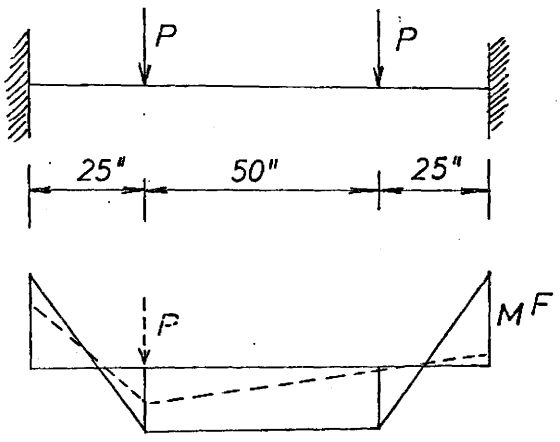

P = 11.36 KIPS

$$M_2 = \frac{11.36 \times 75 \times 25^2}{100^2} = 53.2 \text{ IN-KIPS}$$

$$M_1 = \frac{11.36 \times 75^2 \times 25}{100^2} = 160.0 \text{ IN-KIPS}$$

$$M^F = M_1 + M_2 = 213.2 \text{ IN-KIPS}$$

$$\phi_{1,2} = \frac{\delta}{90} + \frac{90}{3.6\times10^6} \left[2 \times (-300) - (-M_{2,1})\right]$$

$$\phi_{2,1} = \frac{\delta}{90} + \frac{90}{3.6\times10^6} \left[2 \times (-M_{2.1}) - (-300)\right]$$

$$\phi_{2,3} = \frac{v_1}{50} + \frac{50}{3.6\times10^6} \left[2 \times (M_{2,1}) - (-300)\right]$$

$$\phi_{3,2} = \frac{v_1}{50} + \frac{50}{3.6\times10^6} \left[2 \times (-300) - (M_{2,1})\right]$$

$$\phi_{3,4} = \frac{-v_1}{50} + \frac{50}{3.6\times10^6} \left[2 \times (300) - (300)\right]$$

$$\phi_{4,3} = \frac{-v_1}{} + \frac{50}{3.6\times10^6} \left[2 \times (300) - (300)\right]$$

$$\phi_{6,5} = \frac{\delta}{90} + \frac{90}{3.6\times10^6} \left[2 \times (-300) - (-300)\right]$$

$$\phi_{5,6} = \frac{\delta}{90} + \frac{90}{3.6\times10^6} \left[2 \times (-300) - (-300)\right]$$

$$\phi_{6,8} = \frac{v_2}{100} + \frac{100}{3.6x10^6}\left[2 \times (+213.2) - (300 - 213.2)\right]$$

$$\phi_{8,6} = \frac{v_2}{100} + \frac{100}{3.6x10^6}\left[2 \times (300-213.2) - (213.2)\right]$$

$$\phi_{8,7} = \frac{\delta}{90} + \frac{90}{3.6x10^6}\left[2 \times (-300) - (-300)\right]$$

$$\phi_{7,8} = \frac{\delta}{90} + \frac{90}{3.6x10^6}\left[2 \times (-300) - (-300)\right]$$

$M_{2,1}$ = 253 IN-KIPS from elastic solution

$$\psi_1 = -\phi_{1,2} \qquad \psi_2 = \phi_{2,1} - \phi_{2,3} = 0 \qquad \psi_3 = \phi_{3,2} - \phi_{3,4} = 0$$

$$\psi_4 = \phi_{4,3} \qquad \psi_6 = \phi_{6,5} \qquad \psi_5 = -\phi_{5,6}$$

FROM $\psi_3 = 0 = \phi_{3,2} - \phi_{3,4} \rightarrow v_1$

$$\frac{v_1}{50} + \frac{50}{3.6x10^6}\left[2 \times (-300) - (253)\right] + \frac{v}{50} - \frac{50}{3.6x10^6}\left[(600)-(300)\right] = 0$$

$$v = \frac{25x50x1153}{3.6x10^6} = 0.401 \text{ IN}$$

FROM $\psi_2 = \phi_{2,1} - \phi_{2,3} = 0 \rightarrow \delta$

$$\frac{\delta}{90} + \frac{90}{3.6x10^6}\left[2(-253) - (-300)\right] - \frac{0.401}{50} - \frac{50}{3.6x10^6}\left[2 \times (253) - (-300)\right] =$$

$$\frac{\delta}{90} - 0.005 - 0.0083 - 0.01109 = 0$$

$$\delta = 2.19 \text{ IN}$$

CHECK FOR SIGN OF ROTATION:

$$\psi_1 = \frac{2.19}{90} - \frac{90}{3.6\text{x}10^6} \left[-600 + 253\right] = -0.01571$$

$$\psi_4 = \phi_{4,3} = -\frac{0.401}{50} + \frac{50}{3.6\text{x}10^6} \left[600 - 300\right] = -0.00403$$

$$\psi_5 = -\phi_{5,6} = -0.02439 + 2.5\text{x}10^{-5} \ (300) = -0.01689$$

$$\psi_6 = \phi_{6,5} = \frac{2.19}{90} + \frac{90}{3.6\text{x}10^6} \ (-600+300) = +0.01689$$

$$\psi_7 = \phi_{7,8} = 0.02439 + 2.5\text{x}10^{-5} \ (-300) = +0.01689$$

$$\psi_8 = -\phi_{8,7} + \phi_{8,6} = -0.01689 - 0.00943 - 0.0011 = -0.02742$$

$$\psi_{46} = \phi_{6,8} = 0 \quad \rightarrow \quad v_2 = \frac{-3.3396}{3.6} = -0.943 \ \text{IN}$$

APPENDIX A3

STRENGTH OF CONCRETE

Test Model	Strength from Cylinder Tests After		
	7 Days	14 Days	28 Days
C-1	3620	4050	4850
C-2	3680	4090	5020
BF-1	3540	3990	4810
BF-2	3520	3890	4830
BF-3	3910	4200	5300
BF-4	3300	3700	4220

NOTE: Concrete strength is average value obtained from cylinder test is psi.